UNIVERSITY OF THESSALY

SCHOOL OF ENGINEERING

DEPARTMENT OF MECHANICAL ENGINEERING

MEng Thesis

RARE EARTH ELEMENTS AND THEIR APPLICATIONS IN PHOTOCATALYSIS

by

IOANNIS SAKELLARIS

Supervisor

Prof. Panagiotis Tsiakaras

Submitted in partial fulfillment of the requirements for the degree of Bachelor of Science in Mechanical Engineering at the University of Thessaly

Volos, 2025

ΠΑΝΕΠΙΣΤΗΜΙΟ ΘΕΣΣΑΛΙΑΣ

ΠΟΛΥΤΕΧΝΙΚΗ ΣΧΟΛΗ

ΤΜΗΜΑ ΜΗΧΑΝΟΛΟΓΩΝ ΜΗΧΑΝΙΚΩΝ

Διπλωματική Εργασία

ΣΠΑΝΙΕΣ ΓΑΙΕΣ ΚΑΙ ΕΦΑΡΜΟΓΕΣ ΤΟΥΣ ΣΤΗΝ ΦΩΤΟΚΑΤΑΛΥΣΗ

Υπό

ΙΩΑΝΝΗΣ ΣΑΚΕΛΛΑΡΗΣ

Επιβλέπων

Καθ. Παναγιώτης Τσιακάρας

Υπεβλήθη για την εκπλήρωση μέρους των απαιτήσεων για την απόκτηση του Προπτυχιακού Διπλώματος Μηχανολόγων Μηχανικών του Πανεπιστημίου Θεσσαλίας

Βόλος, 2025

Με πλήρη επίγνωση των συνεπειών του νόμου περί πνευματικών δικαιωμάτων, δηλώνω υπεύθυνα ότι η παρούσα εργασία με τίτλο «Σπάνιες Γαίες και Φωτοκατάλυση», αποτελεί προϊόν αυστηρά προσωπικής εργασίας και όλες οι πηγές που έχω χρησιμοποιήσει έχουν δηλωθεί κατάλληλα στις βιβλιογραφικές παραπομπές και αναφορές. Τα σημεία όπου έχω χρησιμοποιήσει ιδέες, κείμενο ή/και πηγές άλλων συγγραφέων, αναφέρονται ευδιάκριτα στο κείμενο με την κατάλληλη παραπομπή και η σχετική αναφορά περιλαμβάνεται στο τμήμα των βιβλιογραφικών αναφορών με πλήρη περιγραφή.

Σημειώνεται ότι οποιοδήποτε εφαρμογή τεχνητής νοημοσύνης χρησιμοποιήθηκε αποκλειστικά και μόνο για την επιμέλεια και τη γλωσσική βελτίωση του κειμένου και **όχι για την παραγωγή ή συγγραφή του περιεχομένου της διπλωματικής**.

In full awareness of the implications of copyright law, I hereby solemnly declare that the present work **"**Rare Earth Elements and Photocatalysis", consists of the result of strictly personal effort. All sources used have been properly cited. Any instances where I have drawn upon the ideas, text, or work of other authors are clearly indicated within the text through appropriate referencing, and the corresponding citations are fully listed in the references.

It is further noted that any use of AI (Artificial Intelligent) apps was applied solely for purposes of editing, and **not for the generation or authorship of the thesis content.**

Approved by the Committee on Final Examination:

Advisor	Dr. Panagiotis Tsiakaras Professor Department of Mechanical Engineering University of Thessaly
Member	Dr. Charalampous George Associate professor Department of Mechanical Engineering University of Thessaly
Member	Dr. Angeliki Brouzgou Assistant professor Department of Energy Systems University of Thessaly

Acknowledgements

I would like to express my deepest gratitude to my undergraduate thesis supervisor, Mr. Panagiotis Tsiakaras, for his valuable guidance, unwavering support, and patience throughout the entire process of this work. His contribution, through insightful comments, knowledge, and advice, was crucial both for the completion of this study and for my academic and personal development.

I would also like to sincerely thank Mr. Georgios Charalambous and Ms. Angeliki Brouzgou, members of the evaluation committee, for the time they devoted, the interest they showed, and their constructive feedback, which significantly contributed to the improvement and completion of this thesis. Their contribution was invaluable not only to the scientific quality of this work but also to my academic growth. Furthermore, I wish to express my gratitude to the University of Thessaly, where I have had the privilege of studying. My years at this institution have provided me with knowledge, experience, and skills that will serve as a valuable guide in both my professional and personal journey.

Finally, I owe a heartfelt thank you to my family-my parents, Evangelia and Thomas, and my siblings, Markisia and Stelios- for their unconditional love, understanding, and support throughout my studies and especially during the preparation of this thesis. Their presence has been a constant source of strength and encouragement at every step of this journey.

Ευχαριστίες

Θα ήθελα να εκφράσω τις πιο θερμές μου ευχαριστίες στον επιβλέποντα της προπτυχιακής μου διπλωματικής εργασίας, κ. Παναγιώτη Τσιακάρα, για την πολύτιμη καθοδήγηση, την αμέριστη στήριξη και την υπομονή που έδειξε σε όλη τη διάρκεια της εκπόνησης της εργασίας μου. Η συμβολή του με τις εύστοχες παρατηρήσεις, τις γνώσεις και τις συμβουλές του υπήρξε καθοριστική τόσο για την ολοκλήρωση της παρούσας μελέτης όσο και για την ακαδημαϊκή και προσωπική μου εξέλιξη.

Θα ήθελα επίσης να ευχαριστήσω θερμά τον κ. Γεώργιο Χαραλάμπους και την κα Αγγελική Μπρούζγου, μέλη της τριμελούς επιτροπής αξιολόγησης, για τον χρόνο που αφιέρωσαν, το ενδιαφέρον που έδειξαν και τις ουσιαστικές παρατηρήσεις τους, οι οποίες συνέβαλαν στη βελτίωση και ολοκλήρωση της παρούσας διπλωματικής εργασίας. Η συμβολή τους υπήρξε πολύτιμη τόσο για την επιστημονική αρτιότητα του έργου όσο και για τη δική μου ακαδημαϊκή πορεία. Επιπλέον, θα ήθελα να εκφράσω την ευγνωμοσύνη μου προς το Πανεπιστήμιο Θεσσαλίας, στο οποίο έχω την τιμή να φοιτώ. Η φοίτηση στο Ίδρυμα αυτό μου προσέφερε γνώσεις, εμπειρίες και εφόδια που θα αποτελέσουν πολύτιμο οδηγό για την επαγγελματική και προσωπική μου πορεία.

Τέλος, ένα μεγάλο ευχαριστώ οφείλω και στην οικογένειά μου, τους γονείς μου Ευαγγελία και Θωμά και στα αδέρφια μου Μαρκησία και Στέλιο, για την αμέριστη αγάπη, κατανόηση και στήριξη που μου παρείχε σε όλη τη διάρκεια των σπουδών μου και ιδιαίτερα κατά την εκπόνηση της παρούσας διπλωματικής εργασίας. Η παρουσία τους υπήρξε για μένα πηγή δύναμης και ενθάρρυνσης σε κάθε βήμα αυτής της πορείας.

Abstract

This thesis focuses on the study of catalysis and modern technologies for energy storage and conversion, with a central emphasis on photocatalysis and its applications. Catalysis represents a fundamental mechanism for accelerating chemical reactions, directly linked to key energy devices such as batteries, fuel cells, and supercapacitors, which are crucial for sustainable energy management.

Special attention is given to photocatalysis, the process of activating semiconducting materials through light irradiation, which finds applications both in environmental remediation and in the production of clean fuels. Photocatalytic water splitting for hydrogen generation is highlighted as one of the most promising approaches, since hydrogen is internationally recognized as a zero-emission energy carrier.

Within this context, the thesis examines the materials employed in photocatalysis, such as metal oxides (e.g., TiO_2, ZnO), composite semiconductors, and nanostructured systems, aiming to improve their efficiency and stability. Particular emphasis is placed on the role of rare earth elements, which, through doping and modification, enhance light absorption in the visible spectrum and reduce electron–hole recombination.

Overall, the study underscores the significance of developing efficient photocatalytic materials and systems as a decisive step toward the green energy transition and the establishment of a sustainable future.

Περίληψη

Η παρούσα διπλωματική εργασία εστιάζει στη μελέτη της κατάλυσης και των σύγχρονων τεχνολογιών αποθήκευσης και μετατροπής ενέργειας, με κεντρικό άξονα τη φωτοκατάλυση και τις εφαρμογές της.

Ιδιαίτερη βαρύτητα δίνεται στη φωτοκατάλυση, δηλαδή τη διαδικασία ενεργοποίησης ημιαγώγιμων υλικών μέσω φωτός, η οποία βρίσκει εφαρμογές τόσο στην περιβαλλοντική απορρύπανση όσο και στην παραγωγή καθαρών καυσίμων. Η φωτοκαταλυτική διάσπαση του νερού για την παραγωγή υδρογόνου αποτελεί ένα από τα πλέον υποσχόμενα πεδία, καθώς το υδρογόνο αναγνωρίζεται διεθνώς ως ενεργειακός φορέας μηδενικών εκπομπών.

Στο πλαίσιο αυτό, εξετάζονται τα υλικά που χρησιμοποιούνται στη φωτοκατάλυση, όπως τα οξείδια μετάλλων (π.χ. TiO_2, ZnO), σύνθετοι ημιαγωγοί και νανοδομημένα συστήματα, με στόχο τη βελτίωση της αποδοτικότητας και της σταθερότητάς τους. Ιδιαίτερη έμφαση δίνεται στη συμβολή των σπανίων γαιών, οι οποίες, μέσω ντόπινγκ και τροποποίησης, ενισχύουν την απορρόφηση στο ορατό φάσμα και περιορίζουν την επανασύνδεση ηλεκτρονίων-οπών.

Συνολικά, η εργασία αναδεικνύει τη σημασία της ανάπτυξης αποδοτικών φωτοκαταλυτικών υλικών και συστημάτων ως καθοριστικό βήμα για την πράσινη ενεργειακή μετάβαση και τη δημιουργία ενός βιώσιμου μέλλοντος.

CONTENTS

LIST OF TABLES

LIST OF FIGURES

Chapter 1

Introduction

The world's energy demands have been steadily rising for the past few decades, with fossil fuels like oil, coal, and natural gas serving as the primary sources. Consequently, issues such as air pollution, global warming, and climate change have become major concerns. Additionally, challenges like fluctuating oil prices, geopolitical tensions, economic instability, and the depletion of oil reserves have highlighted the urgent need to transition toward a more diverse and sustainable global energy system [1].

The 2022 energy crisis, triggered by Russia's invasion of Ukraine, highlighted the ongoing risks of dependence on fossil fuels and reignited national concerns about energy security. The International Energy Agency (IEA, 2023) defines energy security as the continuous availability of energy sources at a reasonable cost [1].

While various aspects of energy security are important, affordability remains a key issue, particularly as concerns over energy poverty continue to grow. Renewable energy is becoming increasingly significant in discussions on energy security. It is reducing reliance on energy imports while also introducing new challenges. In some countries, renewables help stabilize electricity prices, whereas in others, they contribute to price fluctuations. Since energy security is also linked to affordability, price volatility remains a key concern [1].

The swift expansion of renewable energy presents new challenges for energy security, but advanced solutions are already in place. One issue is that the extraction of transition metals is more centralized compared to fossil fuel production. Metals are required only for expanding energy production capacity, not for ongoing energy generation. Therefore, a potential metal shortage would not cause an immediate energy crisis like a disruption in fossil fuel exports would. Additionally, metal resources are distributed across multiple countries and can often be substituted for one another [1].

A central element of decarbonization is the adoption of "green energy" technologies, such as wind turbines and electric vehicles. The 4.1% of energy is generated by wind power (compared to 39% by coal, 27% by natural gas, 19% by nuclear, 7% by hydropower, 1.5% by biomass, 1% by petroleum and gaseous hydrocarbons, and less than 1% by geothermal, solar, and other sources). However, these technologies also introduce new sustainability issues. While the use of green energy helps reduce fossil fuel consumption, it simultaneously raises the demand for permanent magnets that contain significant quantities of rare earth elements (REEs) [2].

The application of rare earth elements (REEs) in these technologies is difficult to replace due to their unique physical and chemical characteristics. According to the IEA, reaching global net-zero emissions

by 2050 would require a sixfold increase in mineral input, with a demand for 3–7 times more REEs by 2040 compared to current levels. Building wind farms and producing electric vehicles typically require 6–9 times more minerals than their fossil fuel-based alternatives. Wind energy generators are widely recognized for producing no air or water pollution, not needing fuel extraction through mining or drilling, and using no water in electricity generation. They also do not produce hazardous or radioactive waste that would need permanent storage. Additionally, wind power is expected to prevent about one-third of global annual carbon emissions by 2050. A 2 MW wind turbine, which contains approximately 350 kg of rare earth elements (REEs), can offset up to 42,000 tons of CO2 equivalent over its lifetime [2].

The green energy industry's leading suppliers of raw materials are China, the US, and Australia, whose production has the greatest environmental impact. Using China as an example, the eco-cost analysis of 19 development pathways for the mining sector of rare earth elements (REEs) has given us net costs for 2015 and 2025 that range from 14.8 to 16 US dollars, respectively [2].

In the long term, diversifying supply sources to meet the current demand for rare earth elements (REEs) from existing technologies- without considering sustainability concerns—essentially shifts environmental issues from one location to another and postpones them into the future, while failing to address the most urgent problems. This emphasizes the need to implement various strategies aimed at increasing the reuse and recycling of REEs (currently less than 1%), reducing material use, promoting substitution, and developing new elimination technologies (such as engines without permanent magnets). These efforts would contribute to the environmentally sustainable development of green energy technologies [2].

Along with materials, catalysts also play an important role. The catalyst can change a lot of molecules and takes part in the process without being consumed [3]. Catalysis offers economical and environmentally friendly ways to convert raw resources into useful compounds. As a result, catalytic processes are now crucial to addressing the global energy and environmental issues that we are currently facing [4].

In Chapter 2, Catalysis, Electrocatalysis and devices for energy conversion and storage will be presented.

In Chapter 3, the basis of photocatalysis will be described. The main applications will also be mentioned.

In Chapter 4, the hydrogen production through photocatalytic water splitting will be examined and materials used in photocatalysis, will be mentioned. Properties and information about rare earths will be analyzed.

Finally, Chapter 5 will outline conclusions and future outlooks for the development of photocatalysis involving rare earth elements, with a focus on practical applications.

Chapter 2

Catalysis, Electrocatalysis and electrochemical devices for energy conversion and storage

2.1 Introduction

The word "catalysis" was first introduced in 1835 by Swedish chemist Berzelius. However, it wasn't until 1894 that a clear definition was provided by Ostwald, who described it as speeding up of a slow chemical reaction through the involvement of an external substance [3].

Catalysis plays a central role in chemical reactions that produce a wide range of synthetic materials and commercial chemical products. In fact, over 80–85% of these products involve the use of at least one catalyst during their manufacturing process. Without catalysts, the production of many everyday items—such as medications, detergents, synthetic fibers, perfumes, fuels, paints, lubricants, and countless other valuable chemical products—would be either impossible or highly impractical [4].

2.2 The Catalyst's work

Catalysts are chemical agents that facilitate the efficient conversion of fine chemicals into valuable products or synthetic materials. They are essential in promoting these chemical transformations by making the processes more effective resulting in lower costs, fewer by-products, reduced energy use, or increased yields of the desired products within shorter reaction times [4].

A catalyst speeds up a reaction by reducing the activation energy required. It does this by binding to the reactant molecule and interacting with it. While the catalyst takes part in the reaction, it isn't consumed in the process and can act on many molecules. As a result, only a small amount of catalyst is needed to bring about the transformation of a large quantity of reactants [3].

By keeping molecules or molecular fragments close together and possibly in a particular relative orientation until the reaction is complete, it polarizes the molecule, which means that it alters the electron distribution in a way that promotes the creation of new bonds. It also facilitates the severing of current ties. Adsorption alone is frequently not the whole picture. The bond strengths and, thus, the distribution of electron densities vary along the reaction path. Low frequency vibrations enable flexible modifications of the local catalyst shape, which support these changes. The flexibility required for energy reduction is provided by the edges, kinks, and corners of crystals or clusters as well as catalyst surfaces with a wide range of imperfections [3].

In addition to their widespread use in traditional chemical processes, catalysts have become increasingly important in addressing major global challenges, such as renewable energy and environmental issues. Developing catalysts that can aid in producing renewable energy and cleaning up the environment is now considered one of the most crucial areas of scientific research. Moreover, with fossil fuel reserves declining, creating catalysts that can efficiently convert CO_2 into fuels and split water to generate hydrogen has become a highly relevant and essential focus in modern research [4].

2.3 Catalyst's requirements

2.3.1 Introduction

Catalysts are available in many ways to suit the wide range of operating conditions, raw materials, and end products involved in different processes. The active metal components can be applied to various types of supports, which are typically highly porous and range in size from fine powders to large pellets. Regardless of the specific setup, achieving high activity and selectivity for the target products is essential [5].

2.3.2 Stability

The stability of a catalyst is crucial, and it is essential to avoid processes like irreversible particle growth or deactivation of active sites. A catalyst's performance and durability are governed by its so-called "DNA," which includes the density, type, and accessibility of its active sites. Notably, the accessibility of these sites is heavily influenced by the pore structure of the support material [5].

A logical and knowledge-driven approach is required to identify potentially stable and active catalysts. Unfortunately, our current microscopic understanding of stability issues is quite poor. In general, powder materials with undefined particle shapes are not well suited for examining catalyst stability because changes in morphology are difficult to recognize, for instance by electron microscopy. High throughput screening methods can be used to find catalysts with high activity and selectivity, possibly based on educated guesses provided by ab initio thermodynamics or scaling relations [6].

The most important characteristic of an industrial catalyst is its long-term stability, particularly in a corrosive reaction environment. Accelerated lifetime testing was created because long-term stability tests take a very long period. The reaction parameters used in these studies, however, are not representative of normal operating settings and may not be important. Thus, long-term stability continues to be a significant obstacle in the creation of novel catalysts as well as in the enhancement of current catalysts [6].

The precise cause of unstable catalysts is frequently unknown; however, it can be linked to the catalyst's sintering, corrosion, reconstruction, evaporation, contamination, or chemical alteration, or a mix of these. However, because the catalyst can also react with the reactants to change its composition and generate a new (metastable) molecule with differing catalytic activity, the problem of chemical transformation is ubiquitous [6].

High-throughput screening can identify catalyst materials with high activity and selectivity, and informed estimates based on ab initio thermodynamics may help with this process. Generally speaking, finding long-term stable catalyst materials is not a good use for this type of screening method. Although theoretical modeling and screening is still in its infancy, it is a viable option. At the moment, the lack of conclusive investigations based on appropriate model experiments significantly restricts the development of theoretical modeling [6].

For stability research, a wide range of model materials are possible, including shape-controlled particles that reveal a distinct surface orientation, nanofibers with a particular morphology but polycrystalline, or ultrathin single-crystalline films supported on different single-crystal substrates [6].

The advantages of ultrathin single-crystalline films made using surface chemical techniques are their great purity and low structural complexity. Although the preparation is difficult, the results are occasionally straightforward and directly comparable to computer modeling. Because single crystalline films are so thin (usually between 2 and 5 nm thick), even slight structural changes can be detected using in situ methods like ambient pressure X-ray photoemission spectroscopy (AP XPS) or surface X-ray diffraction (SXRD). The low specific surface area of this model system, which is usually 1 cm2/g, is its obvious drawback. This makes catalytic testing more difficult and necessitates the use of a batch reactor10,11 or a dedicated flow reactor. In model electrocatalysis, these layer structures are especially helpful for corrosion investigations. For example, the IrO2(110) −RuO2(110)/Ru (0001) model electrode has shown signs of possible induced pitting corrosion under oxygen evolution reaction circumstances. In the hydrogen evolution reaction regime, stability investigations of a 2 nm thick RuO2(110) layer show a mostly homogeneous and partially heterogeneous chemical transformation that results in the synthesis of hydrous RuO2 in association with metallic ruthenium [6].

The active phase is polycrystalline, which provides only limited insight into the microscopic processes on the nanometer level; however, morphological changes due to long-range transport phenomena and chemical bulk transformations of the catalyst material can be easily visualized by scanning electron microscopy (SEM), which is compatible with material screening. By using electrospinning, the morphology of catalyst materials can be shaped in the form of fibers, still exhibiting a high active surface area and thus being applicable in typical flow reactor setups [6].

Even shape-controlled nanoparticles that reveal a single facet orientation can be stabilized by certain materials. For example, CeO_2 and partially $Ce_{1-x}Zr_xO_2$ materials can be used to achieve form control. These model materials' gram-scale fabrication and investigation of structure-sensitive characteristics—that is, the catalyst's stability and activity based on particular surface orientations—are its main advantages. Assuming that the activity is not dominated by the particle's corners and kinks, these tests can be carried out in ab initio modeling. More significantly, high resolution transmission electron microscopy (HRTEM) makes it simple to observe corrosion phenomena and may even be used to detect micro-scale processes [6].

2.3.3 Density of active sites

The activity of a catalyst is largely influenced by the density of active sites, which is determined by the number of particles on the support and the amount of metal loaded. Because industrial reactors are typically size constrained for practical purposes, using a high concentration of active sites (i.e., high metal loading) is often preferred to enhance activity per unit volume. Additionally, the spacing between particles—linked to their local density—can significantly affect the catalyst's stability. For example, increasing the distance between Cu particles significantly improved the stability of methanol catalysts [5].

It should be noted that in the case of solid acids, supported metal nanoparticles, and atomically dispersed catalysts, the active site may potentially be found at a single atom. This last kind of active site is often sometimes referred to as single-atom catalysts, a phrase that is somewhat controversial but describes heterogeneous catalysts with metal atoms that are atomically scattered. However, without other atoms surrounding it, an active site might function considerably differently; depending on the geometrical context, the same "active" atomic site might even be totally inert. Because different classes of catalysts include different types of bonds and length scales, and therefore varied geometries, this fact is externalized differently for each class. Although they are closely related, geometric and electrical impacts on the active site can be distinguished using Brønsted–Evans–Polanyi equations [7].

Distinct particle sizes can reveal distinct aspects of metal catalysts. Similar to Cratty and Granato's "dislocations," it is now generally acknowledged that extremely under-coordinated sites, such steps or kinks, can have significantly more catalytic activity than other sites. Their localized geometry, or the geometric structure of their localized electron density (such as the distinct localization of orbitals protruding from a site), is partly responsible for this [7].

The reactivity of a single Si–O(H)–Al Brønsted acid site or one that is integrated into a particular location within a zeolite's ring can be used to conceptualize geometry for a zeolite. Even while these sites can be constructed from the same basic components, their reactivity will vary

based on factors such zeolite pore size (curvature/lattice strain). The same is true for zeolites' redox sites [7].

2.3.4 Nature of active sites

Catalysis's active sites are incredibly intricate. As scientists, we consequently try to simplify such complicated systems, base new predictions on them, and test their viability through experimentation [7].

The characteristics of active sites significantly influence the surface-specific activity—commonly measured as turnover frequency (TOF)as well as the selectivity of a catalyst. These characteristics are shaped by the nanoparticles' composition, size, and shape. When nanoparticle size is reduced, the number of surface sites per unit mass of metal increases, typically leading to more active catalysts. In structure-sensitive reactions that benefit from particular surface features—such as low-coordination sites at defects, corners, steps, or edges—smaller particle sizes can lead to an improvement in TOF [5].

Metal-based catalysts have drawn a lot of interest because of their high efficiency in a variety of processes, including coupling, oxidation, hydroformylation, and hydrogenation. The researchers have always been motivated to find the best metal-based catalysts that combine high activity and selectivity with exceptional durability. A lot of work has gone into figuring out what characteristics influences catalytic performance. In general, the intrinsic activity and/or selectivity, which are critical for the overall catalytic performance of catalysts, may be significantly impacted by the local fine structure of metal centers. Typically, a particular elementary reaction consists of multiple steps, such as substrate chemical adsorption, surface reaction, and product desorption. According to 18-electron rules or other comparable ideas, the coordination environments of metal centers may control the covalent contact or coordination between metal sites and adsorbates in all of these activities [8].

Surface metal sites may provide a varied binding configuration and strength to reactants, intermediates, and products—all of which are critical determinants influencing reaction pathways and turnover rates—because they usually have different coordination environments. To have a more thorough grasp of the structure-performance relationship and the nature of active sites in metal catalysts, it is first required to understand what the coordination environment is. Coordination number (C.N.) or coordinated bond, electronic structure, steric hindrance of the active metal atoms, and other factors are typically included in the coordination environment of the active center [8].

A minor alteration in the metal nanocrystals' particle size, shape, component, or phase would typically have a noticeable impact on the coordinated surroundings of the active centers, resulting in unique catalytic activity. By adjusting the aforementioned parameters or creating distinct

interfacial sites, the characteristics of the support materials may also clearly affect the fine structure of metal sites in supported metal catalysts. On a fine metal nanoparticle, different metal coordination sites (terrace, edge, kink, or corner sites) will usually present at the atomic level with varying C.N., and their distribution was directly related to the size or form of the nanoparticles. With sizes down to the sub-nano range, the exposed metal atoms would all be weakly coordinated. The main idea underlying size- or shape-dependent catalysis should be that changes in the active center's coordination environment essentially reflect the effects of a catalyst nanoparticle's size or shape on catalytic performance [8].

Furthermore, methods for alloying two or more metals to tailor the active center's catalytic surface environment have also showed promise. Since it is simple to adjust the chemical and physical characteristics of alloy nanoparticles by altering the composition, atomic ordering, and size of the alloyed clusters, more and more work has been focused on creating model nanoalloy catalysts. Apart from the aforementioned, additives are commonly employed to enhance the catalytic performance in a variety of chemical reactions that employ metal nanocatalysts. These additions work well as surface ligands to enhance peripheral steric hindrance and coordinately alter the catalytic surface. By influencing the interaction between substrates and intermediates, each of these adjustable parameters played crucial roles in catalysis [8].

However, gaining a basic understanding of the coordination effect of metal nanomaterials on catalytic performance remains difficult due to the absence of efficient techniques to characterize the intricate surface and interface structures of metal nanoparticles. These difficulties are further compounded by the pressure and material gaps between practical catalysis and surface science. Furthermore, it has been disputed whether the knowledge gathered from model catalyst studies can actually be applied to direct the design of real catalysts because the catalyst would frequently experience a dynamic change in structure under working reaction circumstances [8].

2.3.5 Nature of the metal

A catalyst's stability may also be impacted by the kind of metal or metals and the support material. For example, compared to magnesium oxide (MgO), minuscule silver (Ag) particles adhered much more strongly to reduced cerium oxide (CeO_2). Furthermore, compared to platinum (Pt) particles alone, 4 nm bimetallic platinum-rhodium (PtRh) particles showed higher thermal stability. Given that 2 nm platinum nanoparticles in polymer electrolyte membrane fuel cells were found to be highly unstable while 5 nm particles exhibited nearly no loss of activity, the initial particle size may also be significant [5].

Cu, Au, Pt, Pd, Ru, Ag, Co, and Ni nanoparticles are highlighted. Because they can be used in environmental catalysis, oil refinement, and chemical manufacture, supported metal nanoparticles,

or M-NPs, are of significant scientific and commercial significance. Among the main processes that supported M-NPs catalyze are oxidation and hydrogenation. There are still certain practical concerns with the catalytic activity and deactivation of supported M-NPs, despite the fact that they are better because they are simple to recover and reuse [9].

In recent years, synthetic organic chemistry has made extensive use of metal nanoparticles (M NPs), which are typically referred to as such when their size falls between 1 and 100 nm. Because of their unique characteristics in comparison to their bulk counterparts, nanoparticles (NPs) are of great scientific interest. The characteristics of the materials typically alter at the nanoscale. The size-induced metal–insulator transition (also known as the quantum size effect) is the phenomenon that alters the materials' characteristics. The proportion of atoms at a material's surface increases significantly as its size shrinks in the nanoscale. As a result, the surface-to-volume ratio rises significantly, affecting the material's surface-related characteristics [9].

Generally speaking, NPs' intriguing qualities and beneficial traits include high surface-to-volume ratios, which offer a lot more active sites per unit area than their bulk counterparts, they are more cost-effective because to their higher zeta potential, which prevents nanoclusters from aggregating in solution, potential separation and recyclability, and decreased likelihood of catalyst contamination with the product [9].

Clusters of tens to thousands of transition metal atoms make up transition M-NPs. Their diameters range from one nanometer to hundreds of nanometers. Nevertheless, the most active catalysis is limited to a few nanometers. Therefore, one of the most important aspects of the catalytic processes is the size of the M-NP catalysts. Size and stability in solution are two ways that modern transition M-NPs (1–10 nm in diameter) vary from classical colloids, which are typically [10 nm in diameter]. Modern transition M-NPs with narrow size distributions have attracted a lot of attention in both scientific research and industrial applications because of their unique characteristics, which are based on their naturally high surface-to-volume ratios. Transition M-NPs are recognized for having a number of effective catalyst characteristics [9].

As catalysts, colloidal M-NPs are employed in homogeneous solutions or can be heterogenized with a support like zeolite, silica, alumina, titania, or carbon compounds. Either a powder or a pre-shaped, inexpensive solid with a large surface area that often exhibits minimal catalytic activity on its own can serve as the support [9].

2.3.6 Accessibility of active sites

Catalyst porosity control is necessary for active site accessibility. This is crucial for the mass transfer rate of reactants to and products from the active sites. It influences stability through processes like coke formation and poisoning, activity through diffusion rates, and selectivity

through the magnitude of secondary reactions. Fine powder grains are frequently employed in academia to guarantee good accessibility to the active sites and avoid mass transfer constraints. On the other hand, a catalyst bed of considerable height has a huge decrease in pressure due to tiny grains. As a result, industry frequently uses catalyst support bodies or pellets that are a few millimeters in size [5].

Specific surface locations that enhance a catalyst's activity are referred to as catalytically active spots. When it comes to catalyzing a particular chemical reaction, the surface atoms at active sites are far more active than other surface atoms. To improve our knowledge of catalytic reactions and to direct the development of more effective catalysts, it is essential to identify catalytic sites [10].

Catalysts with porous structures can have several inherent benefits, such as a large specific surface area, which increases the density of surface-active sites, the capacity to transfer reactants and products through their structures efficiently, and improved accessibility of their surface-active sites. Numerous publications have shown that the technique of creating porous structures can also increase the intrinsic activity of catalytic sites or be employed specifically to do so. The pore-making process can produce structural defect sites such corners, edges, voids, and grain boundaries, which can frequently adjust the material's catalytic activity [10].

Additionally, catalytically active nanoclusters and even single metal active sites can be well supported by the porous substrates. Since then, a wide range of porous materials have been investigated for electrocatalysis of the reactions involved in the water and carbon cycles. These materials include metals and alloys, metal oxides (such as oxides of the spinel and perovskite types), monoxide compounds (such as sulfides and nitrides), and carbon-based materials [10].

The most popular techniques for precisely designing the pore architectures of target materials are template-assisted synthetic processes, such as hard and soft templating techniques. Furthermore, a number of adaptable techniques have been developed to create various kinds of porous materials, including dealloying, surfactant-assisted synthesis, and pyrolysis of metal-containing precursors (such as metal–organic frameworks, or MOFs) [10].

Attenuated total reflectance surface-enhanced infrared absorption spectroscopy (ATR-SEIRAS), ambient pressure X-ray photoelectron spectroscopy (APXPS), surface enhanced Raman spectroscopy, surface interrogation scanning electrochemical microscopy (SI-SECM), and scanning tunneling microscopy (STM) are some of the in-situ methods that have been developed recently for monitoring the surfaces and solid/liquid interfaces of catalysts. These cutting-edge methods can improve our understanding of reaction processes and offer crucial direct data about the active locations and adsorbed intermediates on catalyst surfaces [10].

2.4 Types of Catalysis

2.4.1 Introduction

Biological (enzyme) catalysis, homogeneous catalysis, and heterogeneous catalysis are the three types of catalysis. Heterogeneous catalysis was first widely used in commerce, which is consistent with its historical evolution. The newest field is enzymatic catalysis, which has expanded rapidly and found use in numerous commercial applications. In the middle lies homogeneous catalysis, which began with nitrous oxides' activity in the lead chamber process before the effects of heterogeneous catalysts were recognized. According to current estimates, 85% of all chemical reactions are catalyzed, with a roughly 75:25 heterogeneous homogeneous catalysis application ratio [11].

2.4.2 Practical and Mechanistic Views of Heterogeneous and Homogeneous Catalysis

Traditionally, catalysts are classified into two main groups: homogeneous and heterogeneous, depending on the phase the catalyst is in in relation to the catalytic reaction mixtures. Catalysts in the same phase as the reactants are known as homogeneous catalysts. They frequently produce chemo-, regio-, and stereoselective products and are typically soluble organic or organometallic complexes. Heterogeneous catalysts, on the other hand, are solid or insoluble catalysts. Solid catalysts frequently incorporate homogeneous catalysts supported by non-neutral or catalytically active solid support materials like alumina or porous silica. When compared to many of their homogeneous equivalents, these catalysts frequently provide comparatively low reaction yields, despite being readily separated and reusable at the conclusion of processes [3].

It's important to note that homogeneous catalysis avoids many of the major limitations associated with heterogeneous catalysis, such as issues related to pressure differences and limited understanding of complex surface-based processes. One of the main challenges in homogeneous catalysis—namely, separating reactants, catalysts, and products that all exist in the same phase—is made more manageable due to several factors: catalysts can be clearly defined both chemically and spectroscopically, reaction kinetics can be directly linked to each active metal center, and the catalysts themselves can be precisely designed or customized [11].

While homogeneous catalysts dissolve in the reaction medium and thus all catalytic sites are available for reaction, heterogeneous catalysts are insoluble in the medium in which the reaction is occurring, causing reactions of gaseous or liquid reagents to occur at the surface. Heterogeneous and homogeneous catalysts are compared in Table 2.1, which compiles some of the catalysts' characteristics [12].

Table 2.1 Heterogeneous versus homogeneous catalyst comparison [12].

	Heterogeneous	Homogeneous
Catalyst form	Solid, often metal or metal oxide	Metal complex
Mode of use	Fixed bed or slurry	Dissolved in reaction medium
Solvent	Usually not required	Usually required – can be product or byproduct
Selectivity	Usually poor	Can be tuned
Stability	Stable to high temperature	Often decompose < 100°C
Recyclability	Easy	Can be very difficult
Special reactions	Haber process, exhaust clean up etc.	Hydroformylation of alkenes, methanol carbonylation, asymmetric synthesis etc

Heterogeneous catalysts are typically made of metals or metal oxides and often lead to reactions with low selectivity. Since they do not dissolve in the reaction medium, they can often be used in fixed-bed setups, where the reactants flow over them in either liquid or gas form. This allows the catalyst to remain inside the reactor throughout the process. As a result, the catalyst does not need to be separated from the products afterward, simplifying the process. Additionally, it remains consistently exposed to the specific temperature, pressure, and reactant/product environment for which it was optimized. They are highly resistant to heat and pressure, making them suitable for high-temperature processes. However, only the atoms on the surface are involved in catalytic activity [12].

In contrast, homogeneous catalysts are usually metal complexes surrounded by organic ligands. These ligands help dissolve and stabilize the metal center, and they can be adjusted to make the catalyst more selective for producing a specific product. By modifying the ligand's size, shape, and electronic properties, the catalyst can control how the substrate binds, allowing for the formation of just one desired product from many possible outcomes. The separation process can be quite time-consuming and energy-intensive for homogeneous catalysts, which are dissolved in the reaction media that contains the substrates, products, and dissolved gases. In rare instances, where the product is able to evaporate under continuous flow circumstances, in which the substrates are continually added to the reactor and the products are continuously extracted, homogeneous catalytic reactions can be conducted [12].

Homogeneous catalysis offers a far better mechanistic understanding of its microscopic processes ("catalytic cycles") and the potential to influence the steric and electronic properties of these molecularly defined catalysts, even though heterogeneous catalysis has advantages in application (the main mineral oil processing methods use heterogeneous catalysis for good reason).However, 85% of all known catalytic processes are thought to involve heterogeneous catalysis, which dominates the industrial scene [13].

2.4.3 The Rise of Enzyme Catalysis

2.4.3.1 Introduction

Over the course of around 3.5 billion years, enzymes have been developed to catalyze almost all the chemical reactions essential to life. In general, enzymes are exceedingly efficient catalysts that exhibit excellent selectivity and very substantial rate accelerations. But in addition to being excellent catalysts, they have developed to satisfy the specific evolutionary needs of the organisms they live with and the shifting environmental situations they meet. Numerous environmental zones are susceptible to temperature fluctuations, and life (and the constituent enzymes) has changed as global temperatures have changed over the course of geology. Chemical durations for uncatalyzed processes (10^{-3}–10^{16} s) are compressed by enzymes into life-suitable timescales (10^{-3}–10^{5} s) across the biological temperature range (−20°C to +120°C) [14].

2.4.3.2 The function of enzymes

There has been much debate about the exact processes by which enzymes increase their rates at ambient temperatures, and numerous enzymatic mechanisms—such as mutagenesis and kinetic isotope effects (KIEs)have been investigated through experimentation. Enzymes follow the rules of thermodynamics as chemical entities, but because they are big biological molecules, their complexity can mask the intricate mechanisms underlying the remarkable rate increases needed. The situation is further complicated by the relative instability of enzymes, which results from the little difference between the very substantial opposing contributions from enthalpy and entropy of folding [14].

The free-energy profile is usually projected onto a single collective reaction coordinate in enzyme systems, which involve the motions of several atoms. The configuration at the top of the free-energy barrier is known as the transition state [15].

The effects of enzymatic catalysis on the free-energy barrier and the transmission coefficient in relation to the reaction in solution can be examined using basic reaction rate theory. The most significant contributions to enzymatic catalysis are anticipated to come from the reduction of the free-energy barrier rather than from dynamical effects on the transmission coefficient since the transmission coefficient is a prefactor and the free-energy barrier is in the exponential of the overall rate expression [15].

2.4.3.3 Improvements in enzyme function

The quick identification of novel enzyme variations through contemporary bioinformatics and computer modeling-assisted enzyme engineering are significant motivators. Although enzymes' enormous catalytic activity is well known, their stability and expense are sometimes viewed as drawbacks [16].

Table 2.2 below presents some decisions that were solutions to the disadvantages of enzymes.

Table 2.2 Problem descriptions and fixes [16].

Problem statements	Solutions
Enzymes are expensive, not all are available	Recombinant expression in a suitable (microbial) host, either in-house or with specialized enzyme producer company, immobilization to facilitate re-use and cost reduction
Enzymes are unstable	Enzyme engineering via rational design or directed evolution, immobilization to enhance stability
Dependency on expensive cofactors	For NADH, NADPH and more recently also for ATP, efficient recycling systems are available and demonstrated on industrial scale
Development time is too long	Use interdisciplinary teams for planning of best chemical route for integrated enzyme engineering and process development early enough
Process development and down-stream processing are difficult	Numerous examples and concepts for bioreaction engineering are available

2.4.3.4 The contribution of enzymes

However, the benefit of biocatalytic reactions is that they don't require any specific equipment, and they may be used in reactors that are frequently used for chemical synthesis. As a result, they are employed in commercial settings for the manufacture of a variety of target compounds, including alcohols, amines, carboxylic acids, glycosylation, more complex molecules, and, lastly, innovative biocatalytic reactions with the prospect for industrial expanding [16].

2.5 The Band theory and the electronic explanation

2.5.1 The Band Theory

The band theory of solids is a one-electron theory in which an electron moves within a periodic potential that represents the nucleus and the averaged influence of other electrons, following HARTREE'S self-consistent field approach. However, it extends beyond a simple one-electron model, as group theory demonstrates that a perfect semiconductor crystal—with either a single electron in the conduction band or a single vacancy in the valence band—will exhibit energy levels of a similar nature. As long as the interactions between electrons and holes, as well as lattice distortions caused by charges (such as polaron formation), can be ignored, this theory provides a sufficiently accurate approximation [17].

In the early 1930s, Bloch, Brillouin, and Wilson introduced the concept of energy bands in solids, exploring how the presence or absence of energy gaps distinguishes insulators, semiconductors, and metals [17].

If electrons occupy the lowest possible energy states and completely fill certain energy bands while leaving an empty gap above them, the material will be an insulator or a semiconductor, depending on the size of the gap. In contrast, if electrons only partially fill certain bands, with available states directly above them, the material will behave like metal [17].

2.5.2 The s-band and d-band mechanism

The electrical structure of materials substantially determines their surface and the catalytic properties [18].

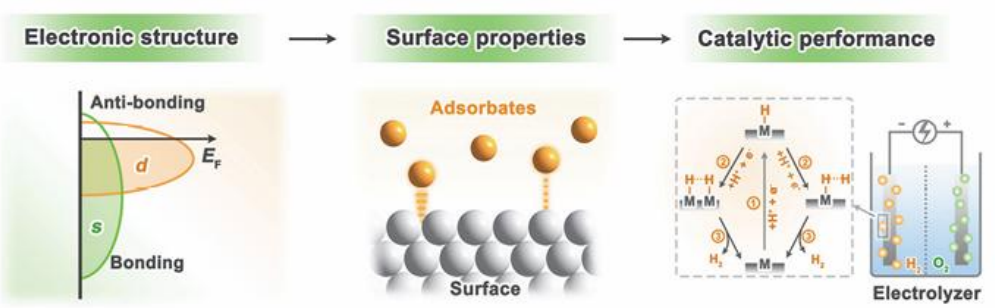

Fig 2.1 Schematic illustration of the hierarchy between surface characteristics, catalytic properties and electronic structure [18].

The state of electronics on transition metal surfaces may be categorized as two types: the s-band and the d-band. The s-band is large overlapping band, whereas the d-band is narrower. When the metal interface reacts with the adsorbed species the s-band initially links to the 2p orbital (Fig 2.2) [18].

The narrow d-band will then couple with the renormalized 2p orbitals to generate bonding and anti-bonding states like those found in molecular orbitals.

The strength of adsorption is closely linked to the d-band since the s-band of most transition metals is essentially the same. The concept served as the basis for Hammer and Norkov's 1995 metal d-band model, which uses d-band analysis to explain the strength of adsorption [18].

The average position of the entire band can be easily and clearly described by the d-band center. Following interaction with the adsorbed species, the anti-bonding orbital will be higher the higher the d-band center. Stronger adsorption results from a comparable decrease in the filling of the antibonding orbital. The d-band center of transition metals steadily decreases as the periodic table advances from top to bottom and from left to right, which weakens adsorption. The gold in the right corner is the «richest» because it has the lowest d-band center and the weakest adsorption energy [18].

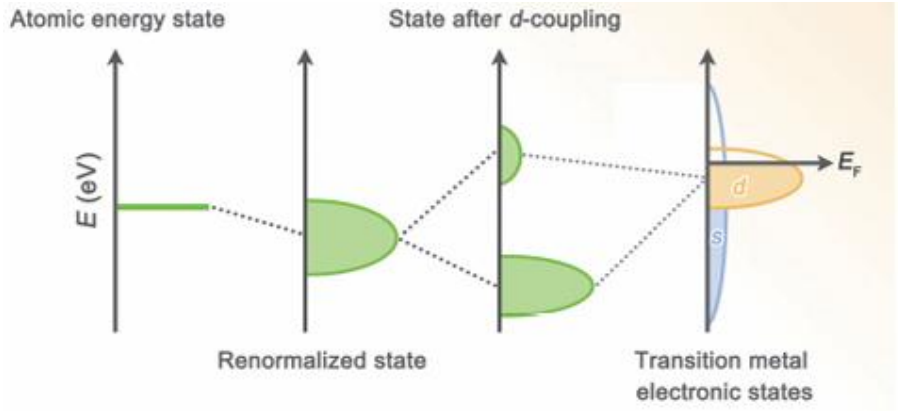

Fig 2.2 Diagrammatic representation of the creation of a chemical connection that links an adsorbate valence state and the s/d states of the transition metal's face [18].

2.6 Electrocatalysis

2.6.1 Introduction

The subject of electrocatalysis is the studying and realization of means for the accelerating of reactions underlying electrochemical methods of energy conversion, as well as searching for new electrode materials. It is the electrocatalysis that provides R&D (Research and Development) in the field of low temperature fuel cells and determines the undoubtedly practical character of the activities in this area of electrochemistry [19].

2.6.2 Kinetics and Surface Effects

The paramount factor influencing the kinetics and mechanism of electrochemical reactions is the adsorption interaction between the reactants/products of the reaction and the electrode (catalyst). The compositional, structural, and dimensional parameters govern the electronic configuration of the active sites on the catalyst, thereby influencing the conditions for adsorption and the kinetic characteristics of the reaction. The activation energy required for a reaction is influenced also by the energy required for medium reorganization, which is dictated by the composition and type of solvent [19].

2.6.3 Revolution in energy production

As the economy rapidly advances, the availability of nonrenewable fossil energy for power generation is diminishing. It is essential to pursue the development of hydrogen, wind, solar energy, and other alternative energy sources to meet and balance energy demands. Additionally, the excessive release of carbon emissions has disrupted the natural carbon equilibrium and harmed the harmonious relationship between humanity and the environment. It is imperative to harness surplus electrical energy from renewable sources like wind and solar power to facilitate effective energy utilization through processes such as the oxygen reduction reaction (ORR), carbon dioxide reduction reaction (CO2RR), oxygen evolution reaction (OER), hydrogen evolution reaction (HER), and nitrogen reduction reaction (NRR), which are fundamental applications of electrocatalysis. Consequently, accelerating the development of electrocatalysts that exhibit high catalytic activity, stability, and selectivity is of utmost importance [20].

2.7 Electrochemical devices

2.7.1 Introduction

Electrochemical techniques provide versatile and efficient approaches for the development of composites derived from conjugated polymers, which may encompass both elemental and compound semiconductors. These polymers are frequently integrated with materials such as metal

oxides (for instance, TiO_2, WO_3, ZnO, NiO, MnO_2), metal chalcogenides (such as CdS, CdTe, CdSe, Bi_2S_3), and carbon-based nanomaterials including nanotubes, graphene, and graphene oxide. The key applications of these composites synthesized through electrochemical methods are highlighted, particularly in fields associated with energy [20],[21].

2.7.2 Solar Cells

The Earth is constantly bathed in an immense amount of energy from the sun. Despite being a typical star, the sun acts as a massive fusion engine that has been active for more than 4 billion years. Solar energy is abundant and freely available, but the concept of utilizing it efficiently is relatively recent. Major improvements in solar power efficiency began with the development of transistors and related semiconductor technologies. Photovoltaic solar power offers several key benefits, making it one of the most promising forms of renewable energy. It produces no pollution, has no moving parts that might fail, needs minimal upkeep or monitoring, and can operate for 20 to 30 years with low operating expenses [22].

Solar power has just two main drawbacks: limited sunlight and the high cost of equipment. The amount of sunlight a place gets can differ significantly based on its geographic location, the time of day, the season, and cloud cover. A solar cell, also known as a photovoltaic cell, is a device that generates electricity directly from light through the photovoltaic effect combination of physical and chemical processes. It falls under the category of photoelectric cells, which are defined by changes in electrical properties like current, voltage, or resistance when exposed to light. These cells form the core components of photovoltaic modules, commonly referred to as solar panels. The term "photovoltaic" applies regardless of whether the light source is natural sunlight or artificial light. In addition to power generation, solar cells can also function as photo detectors, such as infrared sensors, and are used to detect or measure light and electromagnetic radiation close to the visible spectrum [22].

A photovoltaic (PV) cell operates through three main processes: absorbing light to generate electron-hole pairs or excitons, separating the charge carriers with opposite charges, and collecting these carriers separately to form an external circuit. PV cells come in different types, typically named according to the semiconductor material used in their construction. These materials must have specific characteristics to efficiently absorb sunlight. Examples of PV cell types include Amorphous Silicon Solar Cells, Biohybrid Solar Cells, Cadmium Telluride Solar Cells, Concentrated PV Cells, Gallium Arsenide Germanium Solar Cells, Multijunction Solar Cells, Nanocrystal Solar Cells, Photoelectrochemical Cells, and Polymer Solar Cells [22].

A recently identified nanotube structure has the potential to significantly increase the efficiency of next-generation solar cells by transporting electrical charges at a pace 100 million

times faster than previously known. The majority of solar cells nowadays use silicon to absorb light, but because of the material's shortcomings, researchers are looking into using carbon nanotubes, which can enhance existing cells' ability to absorb light. However, because they are hard to organize, these nanotubes have up until now been haphazardly arranged in less-than-ideal configurations. Perovskite is a mineral that can be used to create a new kind of solar panel that has the potential to generate power for homes at a lower cost than previously possible [22].

2.7.3 Fuel Cells

Compared to well-established internal combustion engine (ICE) technologies, fuel cells (FCs) are clean, effective devices that electrochemically convert the chemical energy of fuels like hydrogen, natural gas (NG), methanol, ethanol, and hydrocarbons to electric energy with significantly higher efficiency and significantly lower greenhouse-gas emissions. FCs are therefore thought to be the most promising energy-conversion techniques for the development of sustainable energy [23].

Depending on the type of electrolyte, FC technologies can be divided into high-temperature molten-carbonate fuel cells (MCFCs), solid-oxide fuel cells (SOFCs), low-temperature proton-exchange membrane fuel cells (PEMFCs), alkaline fuel cells (AFCs), and phosphoric acid fuel cells (PAFCs). The characteristics of the electrolytes determine the operating temperatures and ionic-transfer mechanisms of FCs [23]- [46].

The high-quality heat produced by MCFCs and SOFCs can be utilized for internal system usage or as a hot water source, accounts for their high efficiency. The highly corrosive nature of the molten-carbonate, alkaline, and phosphoric acid electrolytes in AFC, PAFC, and MCFC severely restricts their economic viability and competitiveness. In the upcoming energy-conversion technology areas, PEMFCs and SOFCs are thought to be the most competitive and promising [23]-[46].

Operation temperature is an important topic in FC research. The most pressing issue is the expensive cost of the infrastructure required to generate, store, transport, and distribute high-purity H2 (99%), notwithstanding the successful demonstrations of PFSA PEM-based FC cars. Raising the working temperature of PEMFCs to high temperatures of 200–300◦C, or HT-PEMFCs, creates opportunities for the use of different fuels as hydrogen carriers and may lower the cost of hydrogen infrastructure for the use of FCs in the transportation sector. In applications where hauling bulky, heavy H2 bottles is deemed impractical, such as remote communication, unmanned aerial vehicles (UAVs), and soldier-portable electricity, FCs are also beneficial [23]-[46].

The inability of FC technologies to function without system integration is a significant distinction from other electrochemical energy devices. Although FCs can be made on a micrometer or even nanoscale, a functional FC would require a system that orders of magnitude more

complicated and huger. Innovative system integration is necessary for commercial viability, successful use, and market penetration of FC technologies. Therefore, system integration and control are just as crucial to the development of future FC technologies as the FCs themselves. Accelerated commercialization of FC technologies is made possible by compact and dependable system control and integration. In this sense, problems with FC technologies are not just technical and scientific; they are also engineering problems [23]-[46].

2.7.4 Batteries

2.7.4.1 Introduction

An electrochemical battery, which typically consists of two metals joined by an ion exchange membrane or a salt bridge, generates electrical energy from spontaneous redox reactions. The species in one half-chamber of the electrochemical batteries lose electrons to their electrode, while the species in the other half-chamber get electrons from their electrode. To establish ionic contact between two half-chambers with distinct electrolytes and stop the solutions from mixing and producing undesirable side reactions, an ion exchange membrane or salt bridge is used. Paper substrates can be used to create electrochemical batteries in one of two ways: (i) by putting electrodes on the paper, or (ii) by injecting electrolytes into the entire paper or hydrophilic areas that are patterned inside the paper. Because the electrode or electrolyte to be utilized is unstable, explosive, flammable, and/or environmentally harmful, there is a fear that using electrochemical batteries may not be economically or environmentally sustainable [47].

2.7.4.2 Progress and Obstacles in the Integration of Paper-Based Batteries

The first approach uses a flexible paper-based zinc-air battery that has a 0.5 $mAhcm^2$ discharge capacity and an open circuit voltage of roughly 1.2 V. The paper/electrolyte combination has a limited capacity to absorb anode oxidation products before experiencing a decrease in ionic mobility, as seen by the inferior performance of this paper-based battery compared to its counterpart made on a polyethylene naphthalate substrate. Evenly introducing the PPy through the cellulose fibers is a clear way to enhance performance. With only 6% capacity loss over 100 subsequent charge and discharge cycles, the cellulose-PPy conductive paper-like battery could be charged with currents as high as 600 $mAcm^2$ [47].

However, the direct integration of paper-based batteries into multilayer paper-based electronics for simple system integrations has been made possible by the techniques for patterning microfluidic channels in paper. A more useful galvanic cell was created by Phillips et al. as an inexpensive power source, particularly in environments with limited resources. Direct integration

of the Ag–Al galvanic cells into the microfluidic channels allowed for a direct connection between the device's analytical function and power source [47].

Direct fluorescent readings of the assay zone were made possible by a UV LED inside the pa perbased device that was powered by a battery. They also demonstrated how several of these batteries' cells may be coupled predictably in parallel or series to achieve the required power levels. They could only be used for one-time diagnostic checks, though, because their operating lifetime was only 15 minutes. Furthermore, there are still significant obstacles to overcome to increase battery stability and recycle the heavy and noble metals used [47].

The 2 most important types of batteries are the Lithium-ion and the Lead-acid.

2.7.4.3 Lithium-ion battery

Since its initial commercial development by Sony in the early 1990s, Li-ion batteries have seen tremendous advancements. Demands for EVs, smart grids, and portable electronics have largely fueled their success, displacing other battery types based on different chemistries, like Ni–Cd and NiMH cells. Due to continuous cost and performance improvements, Li-ion battery deployment is anticipated to increase rapidly soon, positioning them to dominate the energy storage market. With an energy efficiency of 200–250 watt-hours per kilogram and a cost of $250 per kilowatt-hour, Li-ion batteries are more costly than fossil fuels like gasoline and diesel. Furthermore, throughout a battery's whole lifecycle, issues including safety, dependability, and state of health (SoH) must be addressed [48].

Lithium ions are transported between the anode and the cathode by an electrically insulating, ion-conductive electrolyte. Because of (i) their inherent qualities, notably their substantial surface roughness and porous structure for enhancing power generation, and (ii) their mechanical flexibility to completely actualize flexible electronics, paper or paper-like Li-ion batteries have also been investigated. They often have far higher power and current densities than other kinds of paper-based batteries that are used to power high-power devices. These batteries have a long lifespan and can be recharged [47].

2.7.4.4 Lead-acid battery

Gaston Planté created the first lead-acid battery in 1859, and it is now one of the earliest chemical systems that can store electrical energy. Many uses have been discovered over the past 160 years, and they are still widely used today, such as backup power or automobile batteries. The lead-acid battery is a secondary cell that generates lead (II) sulfate (IV) from lead (IV) oxide (on the positive electrode) and metallic lead (on the negative electrode) during a discharge [49].

The primary benefits of this kind of battery are its inexpensive cost, straightforward and well-known technology, nearly 100% recycling efficiency, extended operation under floating charge

conditions, and minimal self-discharge. Compared to modern battery types, the drawbacks include low specific energy, a large mass, a limited number of full charge/discharge cycles, and the requirement to be stored in a charged state [49].

Nowadays, most casings and separators are made of plastics like polypropylene and polyethylene. Now, most plates have the lead alloy current collector and active mass (positive or negative) adhered to them. This paste goes through the electrochemical processes of lead oxidation or reduction while the battery is running. The progress of lead-acid battery technology is, however, still continuous, and it can be enhanced in many ways [49].

2.7.5 Supercapacitors

In recent years, supercapacitors—energy storage devices based on electrochemical processes—have garnered a lot of interest. In terms of charge/discharge rate, power density, safety, and environmental effect, supercapacitors are usually better than batteries. They are potential energy storage technology that is especially well-suited for storing and delivering large amounts of energy quickly, such as during regenerative breaking and vehicle acceleration. Their favorable performances such as their high-power density, high temperature tolerance, and exceptional cyclability—is functionally responsible for these phenomena [48].

With two electrodes, an electrolyte, and a separator that electrically isolates the two electrodes, supercapacitors are designed and manufactured similarly to batteries. Electrostatic supercapacitors accumulate pure physical charges at the electrode/electrolyte contact, while faradaic super capacitors store charges directly during charging and discharging [47].

Recently, there has been increased interest in the idea of paper-based supercapacitors, mostly because of the potential for producing thin, flexible, inexpensive, and lightweight devices. "Paper-like" supercapacitors, like Li-ion batteries, are more frequently used than commercially available paper because cellulose reinforcement of the nanocomposites would significantly increase the Young's modulus, reduce elongation at break, increase tensile strength, and improve electron/ion transfer rates [47].

Carbon nanotubes (CNTs) and graphenes are two examples of extremely conductive carbon-based nanomaterials/nanocomposites that are mostly employed for "paper-like" supercapacitors. Nanocomposite papers can incorporate all the fundamental supercapacitor components. The electrolyte and carbon nanotube (CNT) electrode were aligned, and nanoporous cellulose paper was used to embed them. The calculated specific capacitance of this paper-based supercapacitor produced a higher working voltage (2.3 V) demonstrating good capacitive performance. At room temperature, a power density of 1.5kWkg 1 was achieved, which is equivalent to and within the stated ranges of flexible devices and commercial supercapacitors [47].

They produced an energy density of 32.7 W h kg $^{-1}$, an improved cell voltage of 1.8 V, and an 86% capacitance retention after 10,000 continuous charge/discharge cycles. The effective operation of a photoelectrochemical lab-on-paper device using a paper-based super capacitor for the measurement of adenosine triphosphate (ATP) in human serum samples is an excellent example of a supercapacitor application [47].

2.7.6 Electrochemical Sensors

A chemical sensor is a tool that transforms chemical data into a signal that can be used analytically. This data can range from the concentration of a single sample component to a full composition analysis. A chemical sensor's usefulness is in providing precise, up-to-date information about the chemical makeup of its environment. Such a gadget should ideally be able to react continuously and reversibly without affecting the sample. These devices use a transduction element coated with a chemical or biological identifying layer. The electrical signal generated by the interaction between the target analyte and the recognition layer is where the analytical data in electrochemical sensors is extracted [50].

Maintaining a high level of specificity for the target analyte in the presence of possibly interfering with chemical species is one of the fundamental needs for sensors to prevent false-positive results. The transducer, which transforms the signal produced by the receptor–analyte interaction into a readable value, is another essential part of sensors [50]-[66].

The two primary functional components of a chemical sensor are a physicochemical transducer and a receptor. Depending on the sensitivity or selectivity requirements, the analyte's nature, and the sample matrix's characteristics, a variety of electrochemical devices can be used for environmental monitoring. Amperometric, potentiometric, impedimetric, photoelectrochemical, and electrogenerated chemiluminescence are some of the classifications for electrochemical sensors [50]-[66].

An advancement in biological research is the use of electrochemical sensors. Furthermore, the industry will benefit from improvements in processing time, sensitivity, and selectivity. A variety of selected targets can be analyzed quickly, accurately, and nondestructively using electrochemical technologies. To improve sensitivity, functional peptides, aptamers, and nanomaterials (such as metal nanoparticles, gold nanoparticles, graphene, graphene derivatives, and carbon nanotubes) have been employed. During the electrochemical measurement, a measurable read signal is produced when the target interacts with a certain probe or composite [50]-[66].

2.7.7 Electrolysis and Electrolyzers

2.7.7.1 Water electrolysis

Water electrolysis is an electrochemical process that uses energy to break water molecules into hydrogen and dissolved oxygen. Redox (reduction-oxidation) chemical processes are

specifically involved in this electrochemical process. One anode will produce electrons (oxidation), while the cathode will consume them (reduction). Whether the electrolyte is alkaline or acidic will determine the reactions that take place at each electrode. The general response of water electrolysis, independent of the kind of electrolyte, can be expressed as follows [67]- [81]:

$$2H_2O_{(l)} \rightarrow 2H_{2(g)} + O_{2(g)} \quad (1)$$

So, the same amount of hydrogen and half as much oxygen are created for every two moles of water.

At temperatures below 2250 ◦C, water electrolysis does not happen on its own. Additional energy must be provided for it in the form of heat and electricity. The difference in enthalpy between reactants and products is known as the enthalpy of reaction. This reads per mole of water (ΔH in [kJ mol 1]) when the products hydrogen and oxygen are created in the gas phase [67]- [81]:

$$\Delta H = \Delta G + T\Delta S \quad (2)$$

Thermodynamically, the reaction of Equation (1) requires the application of at least 1.229 V [67]- [81].

The principles of water electrolysis can be used to make large-scale electrolyzers to manufacture hydrogen on an industrial scale. Two commercially available and industrially established low-temperature water electrolysis technologies—alkaline and PEM—are used to accomplish this. Only a few commercial items of the third low-temperature electrolysis method, AEM, are currently on the market [67]- [81].

2.7.7.2 Alkaline Electrolyzer

The most advanced electrolysis technology is alkaline electrolyzers. The electrodes are separated by a porous separator after being submerged in an alkaline solution (potassium or sodium hydroxide) with a typical concentration of 30 weight percent. The electrodes are usually composed of nickel or coated with Raney nickel as a catalyst at the cathode. The electrodes' mesh design makes it easier to remove bubbles [67]- [81].

The separator helps to keep the hydrogen and oxygen gases apart, preventing the formation of a hazardous combination of them. Originally constructed of toxic asbestos, it is now made of materials like a mixture of zirconium dioxide and polysulfone sold under the brand name Zirfon^{TM}. However, for the reaction to occur, this separator needs to permit the movement of OH ions. The addition of this separator raises the ionic resistance of the cell and makes it easier for bubbles to adhere to it, which increases the electrical resistance that the bubbles produce. Bubbles will form in any space that separates the electrodes from the separator. The gap will affect the ohmic losses by influencing the way bubbles assemble and producing vacant spaces where no reaction takes place. Because the ions must travel greater distances to reach the electrodes, the freely floating bubbles affect the electrolyte's conductivity. The electrodes can alternatively be positioned in the zero-gap configuration to get around this issue. In this case, the electrodes and separator are in direct touch. While this aids in lowering the

resistance brought on by bubbles, it also presents additional difficulties for the separator, which must be carefully designed to prevent gas crossover [67]- [81].

To generate 1 kilogram of hydrogen, alkaline technology uses 47–66 kWh of power. This corresponds to 50–68% in percentage terms (for the lower heating value of hydrogen, LHV = 33.33 kWh/kg) [67]- [81].

2.7.7.3 (PEM) Electrolyzer

When a solid membrane took the role of the fuel cells' liquid electrolyte during the Gemini space program, alkaline technology advanced. The solid electrolyte in this new technology makes it easier to adopt the zero-gap setup. A thin polymer membrane that permits ion conduction makes up the solid electrolyte. The term Polymer Electrolyte Membrane (PEM) comes from this. This technology is also known as solid polymer electrolyte or proton exchange membrane. One of the most well-known membrane materials is Nafion^{TM}, which was created by DuPont [67]- [81].

The membrane becomes extremely acidic due to the presence of H^+ ions, which can damage the electrodes and catalyst layers that come into contact with it. Using strong but frequently rare materials, like platinum and ruthenium, in the electrodes and catalysts is the way to stop corrosion, but it comes at a high cost [67]- [81].

The thickness of the membrane is another characteristic. Design decisions must be made for thicknesses ranging from 50 to 300 μm. On the one hand, the resistance of this component is correlated with the thickness of the membrane. The resistance decreases with membrane thickness. However, to prevent gas crossover and enhance safety and Faraday efficiency, a larger membrane is required if a high-pressure operation is desired. The reaction is aided by the introduction of an intermediate (catalyst) layer. The final layer in this stack is a gas diffusion layer, which is compressed to create a single unit known as a membrane-electrode assembly, or MEA. In addition to allowing water to enter the cathode and making gas extraction easier, the gas diffusion layer gives the catalysts strength, permits compression, transfers heat, and shields them from fluid fluxes [67]- [81].

This method and the alkaline have comparable efficiency (50–68% with respect to the LHV) for industrial size units (about 1 MW). The wider operating spectrum of PEM technology is its advantage. PEM can operate as low as 5%, but alkaline technology has a minimum operating limit of 20% of its nominal capacity. PEM, on the other hand, can function over the nominal capacity, something that alkaline electrolyzers cannot do. PEM's capacity to function at greater current densities up to 2 A/m^2 is another benefit. Better generation of hydrogen is the result of this [67]- [81].

2.7.7.4 (AEM) Electrolyzer

Utilizing the benefits of PEM electrolysis, anion-exchange membrane (AEM) electrolysis is a new technology that functions in alkaline environments. AEM does not require rare elements like

platinum or iridium because of the alkaline atmosphere. Like the PEM, the AEM electrolyzer is constructed with a membrane positioned between two electrodes. The membrane maintains the separation of the product gases (oxygen and hydrogen) while permitting the movement of hydroxyl ions (OH^-) [67]- [81].

The separator is where the alkaline technique differs. This material is porous in the AEL, but the membrane is not in the AEM. Only the OH^- ions are permitted to conduct across the membrane; in the porous separator, these ions pass through the material's pores. As with PEM, pure, demineralized water can be fed into the AEM electrolyzer. The low availability of hydroxyl ions in the membrane, however, results in poor system performance and can cause electrode degradation if fed only to the anode. As in AEL, a solution is created by adding an electrolyte, like KOH. It is possible to lower the electrolyte concentration, which is normally 30% wt in AEL, to 3–10% wt [67]- [81].

AEM is still a young technology having issues with mechanical, chemical, and thermal stability that eventually affect durability. Materials for electrocatalysts, membrane design, and membrane-electrode assembly (MEA) construction are also being studied. Commercial products based on AEM are currently available, albeit they are still in the development stage. Examples of these include the electrolyzers made by HydroLite and Enapter. AEM includes features of both alkaline and PEM, however it is still less efficient than any of them (67%, based on LHV for a unit size of a few kW). Similar to alkaline technology, it can function with a maximum current density of 2 A/m^2, which is the same as a PEM, but it cannot go over the nominal capacity [67]- [81].

2.7.7.5 Vital generation of hydrogen

The creation of hydrogen using electricity has gained attention as the world strives for net-zero emissions by 2050. The International Energy Agency (IEA) has identified this gas as being crucial to energy transition and has included it in its roadmap for Net Zero Emissions. Steam Methane Reforming (SMR), which involves heating coal or natural gas with water vapor at high temperatures and pressures over nickel-alumina catalysts, currently produces most of the hydrogen generated worldwide. CO and hydrogen gas are the end products. This procedure uses a lot of CO (gray hydrogen). Therefore, if this approach is to be employed, considerable effort must be made to use carbon sequestration (blue hydrogen) to reduce the carbon footprint of gray hydrogen [67]- [81].

Water electrolysis is a superior substitute. There will be no CO_2 emissions from the hydrogen produced if the electricity used for electrolysis is generated using renewable energy (green hydrogen). Only 2% of the hydrogen produced worldwide now comes from electrolysis; the majority is a byproduct of the chlor-alkali process. Water electrolysis accounts for only 0.1% of all hydrogen production out of all the procedures that primarily aim to produce it because the technique

is still more expensive. In addition, the quantity of electricity required to convert grey to green hydrogen is massive, easily approaching the Terawatt-hour range [67]- [81].

The hydrogen that is generated will be utilized as a raw material to make ammonia. This emphasizes how crucial it is to produce hydrogen from renewable resources soon. The fact that major oil-producing nations are also investing in hydrogen further supports this. One of the world's top oil producers, Saudi Arabia, recently launched a $5 billion scheme to generate all its hydrogen from renewable resources. By 2030, it is anticipated that the cost of hydrogen produced by this project will be less than that of production methods based on fossil fuels, which contribute to the annual emission of 830 million tons of CO_2 [67]- [81].

Chapter 3

Photocatalysis basics and applications

3.1 Introduction

Since it is the foundation of all the most significant cycles (such the hydrologic cycle) and processes that enable the presence of highly evolved forms of life on the Earth´s surface, the astounding amount of electromagnetic energy that the Sun sends to our globe is the true fuel of the planet [82].

An estimated 6000 GW of primary energy is consumed by all people worldwide, which is 7500 times less than the amount of energy that reaches the planet. The photosynthetic process, which transforms light that reaches the surface into chemicals, is the foundation for the evolution of higher species and has helped define the general makeup of the atmosphere [82].

The concept of conducting a photochemical reaction with the aid of a substance capable of catalyzing the process was first introduced in the early 20th century by Plotnikow in 1910 and later by Landau between 1912 and 1913. Around the 1920s, initial attempts were also made to replicate natural photosynthesis. These efforts aimed to produce organic compounds, such as formaldehyde and carbohydrates, through photochemical reactions involving carbon dioxide and water, as well as organic nitrogen compounds through photoactivated reactions between carbon dioxide and inorganic nitrogen sources like nitrate or ammonia [82].

The photocatalytic characteristics of oxides were not identified and explored until the 1940s, primarily with the practical objective of enhancing the longevity of paints, paper products, and fabrics that incorporated titanium dioxide or other white semiconductor materials as pigments. Within this scope, the light-induced oxidative potential of certain semiconductors—such as zinc oxide (ZnO), antimony trioxide (Sb_2O_3), and titanium dioxide (TiO_2)—was examined, and the possible emergence of reactive compounds like hydrogen peroxide (H_2O_2) was detected [82].

3.2 Photocatalytic Phenomenon

The fundamental process of photocatalysis involves exposing a semiconductor to ultraviolet (UV) or visible light, which initiates a series of chemical reactions [83]. After each catalytic cycle, the photocatalyst must restore its original chemical composition and properties [82]. Consequently, two processes occur: oxidation and reduction. When the semiconductor absorbs light with energy

equal to or greater than its band gap, electrons are excited from the valence band (VB) to the conduction band (CB), creating electron–hole pairs. As the electron moves to the conduction band, it leaves behind a hole in the valence band—together, they form what's known as a photogenerated or photoinduced electron–hole (e/h) pair. As shown in Fig. 3.1, this mechanism begins with the generation of these charge carriers, followed by their separation and movement toward the surface of the photocatalyst, where redox reactions occur at active catalytic sites [83].

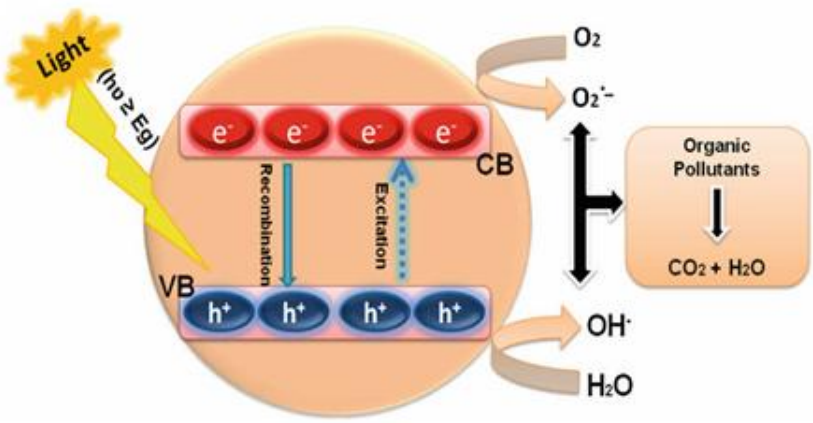

Fig.3.1 Core principle of the photocatalytic mechanism [83].

The following equations represent the overall photocatalytic mechanism [83]:

$$\text{Photocatalyst} + h\nu \rightarrow \text{photocatalyst}\ (e^{-}(CB) + h^{+}(VB)) \quad (3)$$

$$H_2O + h^{+}(VB) \rightarrow OH\cdot + H^{+} \quad (4)$$

$$O_2 + e^{-}(CB) \rightarrow O_2^{-} \quad (5)$$

$$O_2^{-}\cdot + H^{+} \rightleftarrows HOO\cdot \quad (6)$$

$$2HOO\cdot \rightarrow H_2O_2 + O_2 \quad (7)$$

$$H_2O_2 \rightarrow 2OH \quad (8)$$

$$OH\cdot + \text{organic pollutants} \rightarrow CO_2 + H_2O \quad (9)$$

3.3 Influence of Various Factors on Photocatalytic Performance

The speed of oxidation reactions and the efficiency of photocatalytic processes can be influenced by several factors, such as temperature, pH, light intensity, the amount of catalyst, and the concentration of wastewater. The effects of these different operating parameters are discussed in the following sections [84].

3.3.1 The structure of the catalyst

A catalyst's physical structure directly influences its photocatalytic performance. The substantial surface area of nano photocatalysts enables numerous pollutants to react at once,

rendering them more effective than bulk particles. The catalyst's configuration, dimensions, and appearance all play a role in the degradation rate of wastewater pollutants. Smaller nanoparticles break down pollutants more effectively due to their greater surface area and active spots. As a case in point, the photocatalytic breakdown of methylene orange dye is better demonstrated by diverse ZnO forms, including nano spindles, nanoflowers, and nano-rods [84].

3.3.2 Temperature

Temperature is another crucial factor that significantly affects the breakdown of pollutants and photocatalytic performance. While most photocatalytic reactions occur at room temperature, studies indicate that the activation energy rises when the temperature drops below 0°C due to a reduced desorption rate of the final products. Conversely, as the temperature exceeds 80°C, the adsorption of reactants becomes a limiting factor. Increased temperature caused the nanorods to grow longer and narrower, which expanded their surface area and absorption rate. In this context, photooxidation at low pH (pH = 3) led to hydroperoxide formation, and fragmentation at a low temperature (0°C) amplified the microplastic's surface area [84].

3.3.3 Impact of pH levels

The pH of the medium or environment is a crucial aspect that can influence photocatalytic activity. Since some reactions are pH-sensitive, the ideal pH can differ based on the specific photocatalyst and the substances reacting. The pH of the solution affects the extent of ionization, clumping, the oxidation potential of the photocatalyst's band, and the presence of pollutants. Another key factor impacted by pH in photocatalysis is the surface charge. The point of zero charge (PZC) is the pH where the surface charge is entirely balanced. Studies have shown that increasing the pH enhanced $BiVO_4$'s efficiency in breaking down phenol through photocatalysis. Enhanced photocatalytic activity has been linked to smaller band gaps, less electron-hole pair recombination, increased solar light absorption, and changed shapes [84].

3.3.4 Amount of the catalyst

Research indicates that the catalyst concentration in a photocatalytic reaction influences the speed at which dyes break down. To boost the dye photodegradation percentage in a heterogeneous photocatalytic process, increasing the photocatalyst amount is an option. More catalysts in the photocatalytic process leads to more active sites, which promotes the creation of more reactive radicals during photodegradation [84].

3.4 Heterogeneous Photocatalysis fields

Over the past forty years, the field of heterogeneous photocatalysis has grown significantly, particularly with advancements connected to energy and environmental applications. This process

involves enhancing the speed of a photoreaction by a catalyst (which is not in the same phase as the reactant) [85].

The light-exiting photocatalysts produce electrons and holes, as seen in Figure 3.2. This scheme can be used for a variety of purposes, such as the selective organic synthesis of high-value products, energy production toward CO_2 reduction, water splitting, alcohol reforming reactions, and the degradation of undesirable chemicals, pollutants, and pathogenic organisms. The electrons and holes at the surface can start a reductive and an oxidative reaction pathway, respectively. Furthermore, the most popular photocatalysts are TiO_2-based materials and TiO_2-based photocatalytic processes [86] because they offer resilience, abundance, and strong photoactivity for both disinfection and degradation at low cost [87].

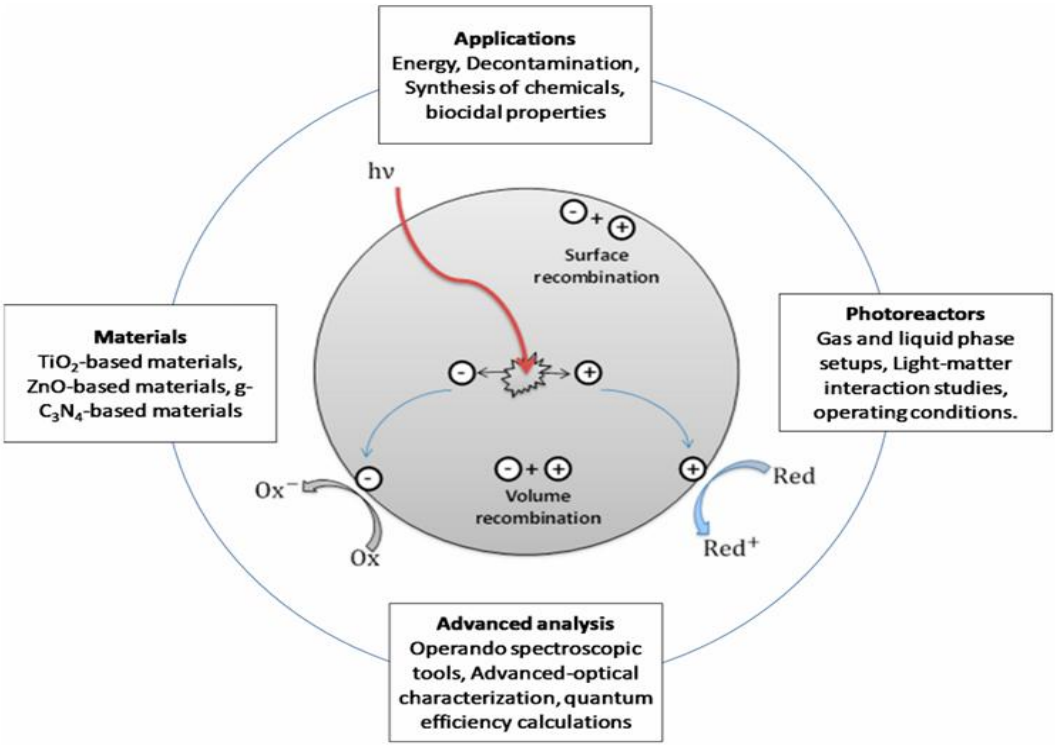

Fig 3.2. Diagrammatic representation of a semiconductor's photo-activation and major reaction stages, as well as the primary areas of unresolved research in the field of heterogenous photocatalysis [86].

The use of heterogeneous photocatalysis for synthetic applications is less common. This finding illustrates a widespread lack of confidence in heterogeneous photocatalysis's ability to synthesize pertinent commercial chemicals. Although useful intermediates, naturally occurring chemicals, and raw materials have been produced in good to exceptional yields, corresponding improvements in process engineering are still needed [87].

3.5 Homogeneous photocatalysis

Homogeneous catalysis refers to a catalytic process where both the reactants and the catalyst exist in the same phase, typically the liquid phase. In recent years, a more specific definition has

gained popularity, limiting homogeneous catalysts to systems involving (organo)metallic complexes as catalysts. Technically, organometallic compounds are defined by the presence of a metal–carbon bond, though not all catalysts discussed necessarily meet this criterion. For convenience, this narrower term will be used here, but it's important to remember that many valuable homogeneous catalytic reactions involve catalysts that are not (organo)metallic complexes [88],[89].

Examples of such systems or catalysts include general acid-base catalysis, as seen in ester hydrolysis; Lewis acids, which are commonly employed in Diels-Alder reactions; and organic catalysts, such as thiazolium ions involved in Cannizzaro reactions. Other notable examples are porphyrin complexes, which play a role in epoxidation and hydroxylation reactions; enzymatic processes; and coordination complexes that facilitate polyester condensation [88].

Ligands play a crucial role in homogeneous photocatalysis involving metal complexes. By altering the ligands surrounding a single metal center, it's possible to produce different products from the same substrate. This is illustrated in Figure 3.3, which shows the range of products that can be derived from butadiene using different nickel catalysts [88],[89].

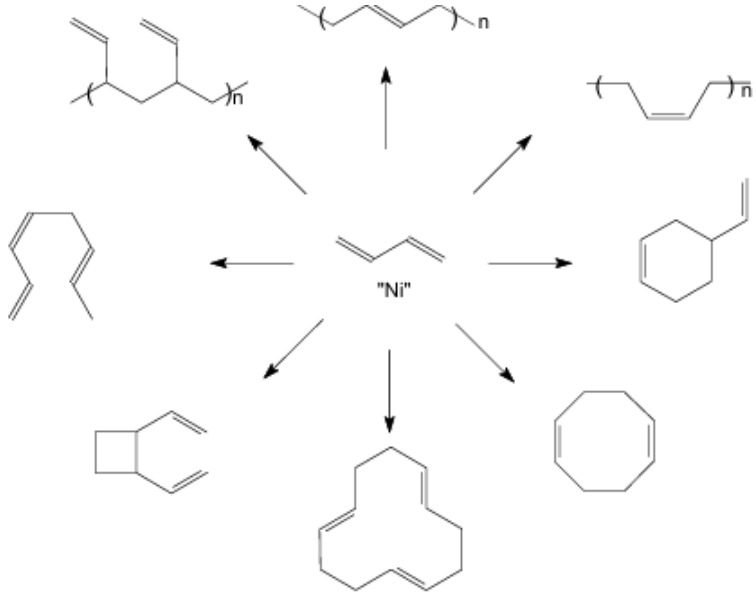

Fig.3.3 Impact of valence states and ligands on selectivity in the butadiene process catalyzed by nickel [88].

Photochemistry and homogeneous complex catalysis are connected by photoinduced catalytic processes brought on by the photogeneration of coordinatively unsaturated species (Fig. 3.4). The benefits of photocatalytic reaction pathways are highlighted by the photochemical activation of catalyst precursors, which takes place at a very moderate reaction temperature and pressure. From a mechanistic perspective, the photochemical production of catalysts and the identification of their structures provide new avenues for a deeper comprehension of the

fundamental stages of intricate catalytic cycles. Electron-transfer methods using reducible or oxidizable sacrificial ligands like azide or oxalate and dithiooxalate are one method for the photogeneration of coordinatively unsaturated molecules that act as catalysts [89].

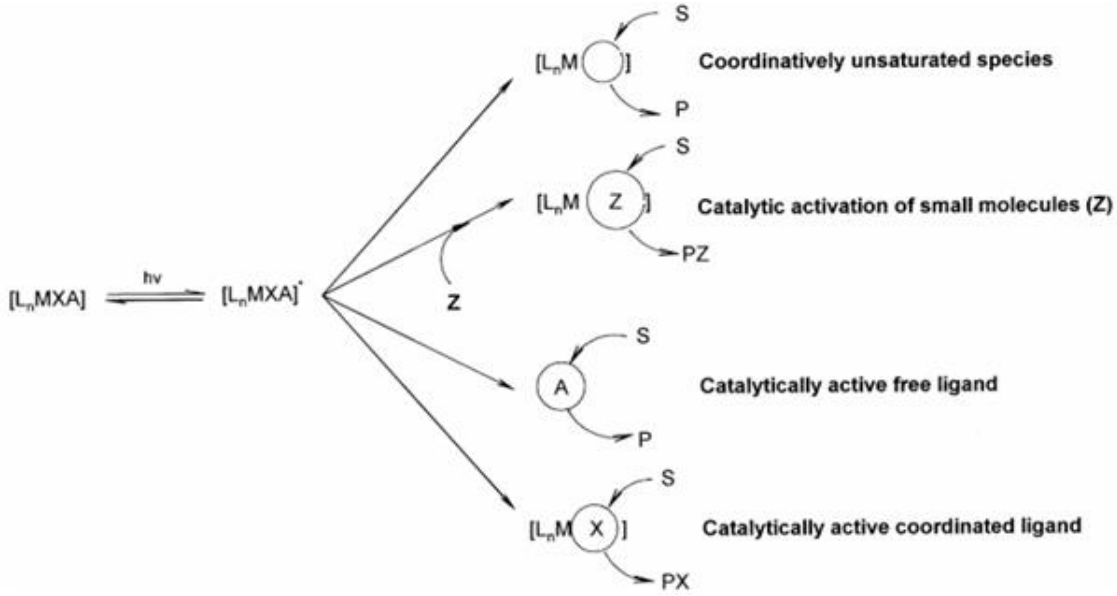

Fig.3.4. An overview of how light-sensitive transition metal complexes of organometallic compounds ([LnMX(A)]) cause substrates (S) to be photo catalytically activated, producing products (P, PX and PZ respectively) [89].

3.6 Types of photocatalysis

I offer four groups of reactions in Figure 3.5 to classify current photocatalysis techniques. The most effective photocatalysis is seen in the first category (Fig.3.5. a), organic photosynthesis. The process, an inventive outcome of billions of years, has been the origin of our energy. The main byproduct of these processes are carbohydrates [90].

A version of this reaction is depicted in figure 3.5.b, where microalgae perform reactions comparable to those in plants but synthesis unique compounds such as H_2 or other useful chemicals (e.g. ethanol, butanol, glycerol, and isoprene) [90].

There are several different types of artificial photosynthesis systems available. An intrinsically low-cost system is produced when the reduction and oxidation reactions are not purposefully segregated (Fig 3.5.c). Keep in mind that responses involving both homogeneous and heterogeneous catalysts into this group. Physically separating the sites of oxidation and reduction is another tactic [90].

Figure 3.5.d displays the wired version of the previous tactic. However, in this case, the wire is not necessary. Back-to-back wireless setups belong to the same category additionally. One of the main differences between **Figure 3.5.c and 3.5.d** examines if there is sufficient physical distance (more than a few hundred feet) between the reduction and oxidation sites [90].

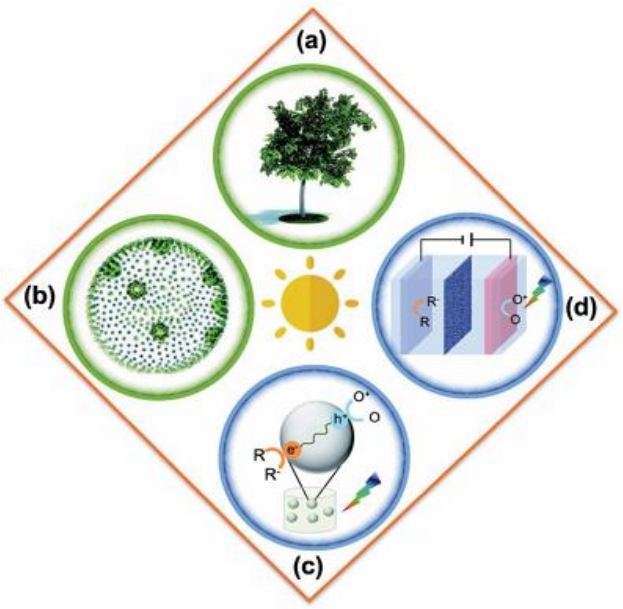

Fig.3.5 Categories of photocatalytic processes. a) Natural photosynthesis by plants, b) photosynthesis by microalgae, c) nanoparticles photocatalysis, d) photo electrocatalysis [90].

3.7 The applications of photocatalysis

3.7.1 Introduction

People's need for resources has significantly increased because of the growth of industry and the improvement of living standards, leading to energy crises. The primary energy sources in the world today are still fossil fuels including coal, oil and natural gas. Most of them are predicted to run out in the twenty-first century due to the ongoing growth of industrialization. Furthermore, using fossil fuels contributes to increasingly severe air and water pollution, which endangers people's lives and health [91].

Photocatalytic technology has emerged as a popular study area in recent years due to its demonstrated potential as an inexpensive, sustainable, and environmentally benign technology [91]. Some of its applications are presented below.

3.7.2 Water Treatment

Organic contaminants, heavy metals, inorganic compounds, and several other complex substances have been found in surface, ground, sewage, and drinking water resources over the past few decades because of population development and fast industrialization. The Unites Nations´2020 World Water Development Report states that modifications to the water cycle will also endanger human health, food security, energy generation, economic growth, and poverty alleviation, so putting the attainment of sustainable development goals in grave danger. As a result, it is crucial to create sophisticated, eco-friendly, affordable, and highly effective wastewater reclamation methods [92].

Electrodialysis, membrane filtration, precipitation, adsorption, electrochemical reduction, and electro deionization are among the various technologies used in wastewater decontamination. These procedures typically use a lot of energy and can become more complex when pollutants are transferred between diverse fluids, wastes, and byproducts produced during wastewater treatment [92].

Heterogeneous photocatalysis has been extensively researched and used since 1972 in several fields, including N_2 fixation, CO_2 reduction, water splitting, and water/air purification (Figure 3.6). Mild temperatures, a straightforward procedure, and green technology allow photocatalysis to oxidize or convert inorganic pollutants to innocuous compounds while breaking down organic contaminants in wastewater into water, carbon dioxide, or other tiny molecules [92].

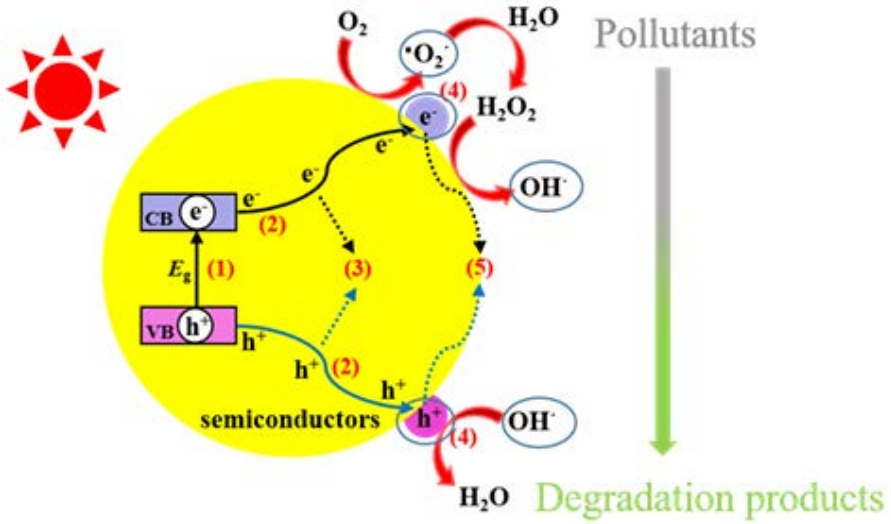

Fig.3.6 The role of heterogeneous catalysts in photocatalytic applications [92].

The high rate of electron/hole recombination considerably reduces the photocatalytic activity of single photocatalysts. Researchers are paying more attention to the subject of enhancing photocatalytic activity by preventing their recombination. Numerous modification techniques have been created to solve the shortcomings. Complexion can be somewhat avoided by metal doping and morphology control, and the incorporation of plasma excitonic elements and up conversion effects into photocatalysis materials significantly increases light absorption and utilization, which has significant ramifications for the creation of new, effective photocatalysts with broad-spectrum absorption capabilities. In addition to these methods, further methods have been investigated and documented in the fields of biphasic semiconductors and the use of photocatalytic effects in the design of external circuits, both of which can significantly enhance photocatalytic performance [92].

Additionally, because deactivated photocatalysts are unstable, the catalyst is prone to self-etching in photocatalysis. The creation of heterojunction structures, doping, defect synthesis, and the restoration of effective photocatalytic performance by the oxidative reduction of deactivated photocatalysts for recycling have all been extensively investigated [92].

3.7.3 Removal of Trace Metals

Wastewater from a variety of human endeavors and businesses, such as plating and electrolysis, pesticides, batteries, rayon production, mining, metal rinsing, textile production, tanning, papermaking, petrochemical processing, and electrolysis, might contain heavy metals. Serious health problems, including harm to essential organs including the liver, heart, brain, and kidneys, are common in people exposed to heavy metals. Mercury (Hg), chromium (Cr), and arsenic (As) are the three most prevalent metal ions in contaminated water [93], whose removal procedures I present below.

3.7.3.1 Chromium Removal

Studies on the photocatalytic reduction of heavy metals like chromium (VI) have generally shown an increase in the rate of chromium (VI) photocatalytic reduction in the presence of organics in natural and wastewaters. Converting Cr (VI) to Cr (III) has been the focus of recent research due to the higher toxicity of Cr (VI) ions in comparison to Cr (III) ions. When exposed to ultraviolet (UV) or visible light, photocatalytic nanoparticles, including zinc oxide (ZnO), tungsten trioxide (WO_3), and titanium dioxide (TiO_2), go through a chemical reaction known as photoelectrons. While electrons, e^-, power the oxidation of Cr (VI) to Cr (III), positive holes, H^+ drive the reduction of Cr (VI) to Cr (III) [93].

3.7.3.2 Arsenic Removal

The two oxyanions that are most found in natural waters are asenate (As(V)) and arsenite (As (III)). As(V) in the form of H_2AsO_4 or $HAsO_4$ prevails in oxidizing and alkaline environments, while trivalent non-ionized arsenite, H_3AsO_3, predominates in reducing environments, such as aquifers with a pH close to neutral. Compared to arsenite, arsenate is less toxic and more stable. These water contaminants are eliminated using heterogeneous photocatalysis. The hydroxyl radical (HO• radical), which produces electron-hole pairs (e^-H^+) that can reduce and oxidize molecules, is produced when the gap in semiconductors is stimulated. As (III) is changed into As(V) by TiO_2 when the oxygen is present. Photon efficiency is reduced by this material's significant e^-H^+ pair recombination rate. To address this issue, scientists have created new materials by either (i) doping TiO_2 with nonmetal or transition metal ions or (ii) incorporating other semiconductor oxides such as CuO, ZrO_2, Fe_2O_3, MnO_2, GaO_2, SnO_2, and WO_3. Since they employ mild oxidants and have the potential to replace traditional high energy treatment methods, photocatalytic oxidation processed-which combines UV light with nanoparticles such as Fe_2O_3, TiO_2, and ZnO-have been extensively reported [93].

3.7.3.3 Mercury Removal

There are many different contaminants in chimney gas from coal-fired power plants, and the effects of these contaminants on the environment are getting worse. The main pollutants, like SOx, NOx, and hazardous particles, as well as the contaminants that contain trace amounts of heavy metals, like mercury (Hg^0), are getting even worse. Crucially, photocatalytic oxidation technology may be used to efficiently

remove Hg^0 in its gaseous state. Oxidation has been accomplished with success using photocatalytic technology. Photocatalytic performance is limited by a high recombination rate of photogenerated electron-hole pairs, a significant band gap that restricts the excitation of the pure semiconductor to the UV, and a poor electron transfer rate. Mercury gas was extracted using $BiOIO_3$ photocatalysts exposed to UV and LED light. The crystal structure and form of BiOIO3 were determined by the pH of the precursor. Only in acidic settings could $BiOIO_3$ products develop. After exposing a $BiOIO_3$ nanosheet sample to UV light for 25 minutes and LED light for 100 minutes, almost all Hg0 was eliminated [93].

3.7.4 Organic Degradation

Different kinds of bacteria and other microorganisms, which can break down organic contaminants through regular cellular responses, are usually the foundation of biological degradation technologies. For the removal of organic materials from wastewater, physio-chemical methods such as reverse osmosis, Fenton reagent, nanofiltration, hydrogen peroxide, electrochemical breakdown, ozonation, flotation, coagulation, chemical oxidation, and adsorption demonstrate satisfactory results. These technologies have advantages of low energy usage, inexpensive investment, and simple maintenance. Some disadvantages of these treatment techniques include the fact that they can only turn the non-biodegradable component into sludge, which creates a secondary waste product that must be recycled or disposed of in a costly way [94].

The advanced oxidation process (AOP), which was initially proposed in the 1980s, has shown itself to be a successful wastewater treatment technique. The in-situ production of strong hydroxyl radicals (OH) and other reactive oxygen species (ROS) in sufficient to attempt to destroy the refractory hazardous chemical pollutants in a non-selective and efficient manner is referred to as "advanced." Furthermore, by producing extremely reactive radicals, AOPs like Fenton reactions, sulfate radical-based AOPs, sonochemical oxidation, electrochemical oxidation reactions, and photocatalytic oxidation can fully mineralize the hazardous organic pollutants, turning them into tiny molecules like CO2 and H2O and less sludge [94].

It is important to note that there are two types of ROS generation: photochemical and non-photochemical. The energy of photons is harvested to create various active radicals in photochemical processes like the photo-Fenton process, ultraviolet (UV-photolysis), microwave irradiation-included photocatalysis, gamma radiation-included photocatalysis, visible light-assisted photocatalysis, and UV-light-assisted photocatalysis. Heterogeneous photocatalysis using semiconductors has emerged as one of the most effective and sustainable methods for mineralizing different kinds of organic contaminants in wastewater [94].

This method offers several benefits, including environmental protection, total pollution degradation, no secondary pollution, green technology (visible light harvesting), and repeated usage without degrading catalyst capacity [94].

3.7.5 Elimination of Inorganic Substances

Carbon monoxide, sulfur oxides, nitrogen oxides, and hydrogen sulfide are a few significant inorganic gas pollutants that need to be treated in both indoor and outdoor air. While there is research on the removal of volatile organic compounds (VOCs) from the air, this is not the case for inorganic contaminants. The use of photocatalytic oxidation to reduce air pollutants, such as nitrogen oxides, ought to be economical. TiO2 is again the most extensively employed photocatalyst in photocatalytic oxidation because of its comparatively low cost, non-toxicity, and chemically stable nature [95].

Table 3.1 provides an overview of current research on the use of photocatalytic oxidation to remove inorganic contaminants [95].

Table 3.1 Overview of research on the oxidation of inorganic compounds utilizing TiO_2-based photocatalysts [95].

Order	Catalysis	Modification	Optical property (nm)	BET (g/m^2)	Target (ppm)	M.W (g/M)	Avarage wavelength (m)	Catalyst dose (g)	Gas Retention Time (h)	Lamp power (W)	Total Reactor Volume (L)	Initial pollutant concentration (ppm)	Initial pollutant concentration (mg/L)	Age conversion degradation (%)	Final pollutant concentration (mg/L)	Flow rate (L/h)
1	$RuO_2/TiO_2/Pt$	Combination of $RuO_2/TiO_2/Pt$	365	65	CO	28.01	3.65E-07	0.35	5.8	300	0.02186	470	0.53844	100	0.0000	0.0038
2	TiO_2	Cobalt imidazole complex with functionalized GO supported on a TiO_2 film	400	205.8	NOx	30	4.00E-07	1.029	2	8	N. A.	1	0.00123	51	0.0006	N. A.
3	TiO_2	Cobalt imidazole complex with functionalized GO supported on a TiO_2 film	400	205.8	CO	28.01	4.00E-07	1.029	2	8	N. A.	50	0.05728	46	0.0309	N. A.
4	WO_3/TiO_2	Using two photocatalysts with each other (WO_3/TiO_2)	365	17.7	H2S	34.1	3.65E-07	N. A.	0.31	8	0.12826	N. A.	N. A.	100	N. A.	0.4137
5	TiO2	TiO_2 coted on Polyamide nanofiber materials	365	2.1	NOx	30	3.65E-07	5	N. A.	300	N. A.	1	0.00123	41.6	0.0007	N. A.
6	Cryptomelane-type manganese oxide	No modification	365	137	O3	48	3.65E-07	N. A.	N. A.	N. A.	N. A.	40	0.07853	80	0.0157	N. A.
7	Fe0.1%T-c	Fe/TiO_2 catalysts with 0.11% Fe	420–700	105.4	NOx	30	5.60E-07	0.05	0.0015	500	12.3	0.4	0.00049	38	0.0003	8200.0000
8	Fe0.1%T-h	Fe/TiO_2 catalysts with 0.11% Fe	420–700	197.3	NOx	30	5.60E-07	0.05	0.0015	500	12.3	0.4	0.00049	20	0.0004	8200.0000
9	Fe0.1%T-i	Fe/TiO_2 catalysts with 0.12% Fe	420–700	68.3	NOx	30	5.60E-07	0.05	0.0015	500	12.3	0.4	0.00049	9	0.0004	8200.0000
10	T-0	Pure titania nanotubes	365	376.5	NO2	46	3.65E-07	0.11	4	N. A.	N. A.	0.019	0.00004	54	0.0000	N. A.
11	Mo/T-H	Molybdenum-doped titania nanotubes (ammonium molybdate tetrahydrate added at the same time as the TiO2 precursor)	365	403.3	NO2	46	3.65E-07	0.11	4	N. A.	N. A.	0.019	0.00004	56	0.0000	N. A.
12	Mo/T-P	Molybdenum-doped titania nanotubes (ammonium molybdate tetrahydrate added during the acid washing process)	365	387.2	NO2	46	3.65E-07	0.11	4	N. A.	N. A.	0.019	0.00004	25	0.0000	N. A.
13	Mo/T-I	Molybdenum-doped titania nanotubes (ammonium molybdate tetrahydrate impregnated to TNTs before calcination)	365	333.3	NO2	46	3.65E-07	0.11	4	N. A.	N. A.	0.019	0.00004	27	0.0000	N. A.
14	T-0	Pure titania nanotubes	365	376.5	CO2	44.01	3.65E-07	0.1	4	N. A.	N. A.	N. A.	N. A.	0	N. A.	N. A.
15	Mo/T-H	Molybdenum-doped titania nanotubes (ammonium molybdate tetrahydrate added at the same time as the TiO2 precursor)	366	403.3	CO2	44.01	3.65E-07	0.1	4	N. A.	N. A.	N. A.	N. A.	0	N. A.	N. A.
16	Mo/T-P	Molybdenum-doped titania nanotubes (ammonium molybdate tetrahydrate added during the acid washing process)	367	387.2	CO2	44.01	3.65E-07	0.1	4	N. A.	N. A.	N. A.	N. A.	N. A.	N. A.	N. A.
17	Mo/T-I	Molybdenum-doped titania nanotubes (ammonium molybdate tetrahydrate impregnated to TNTs before calcination)	368	333.3	CO2	44.01	3.65E-07	0.1	4	N. A.	N. A.	N. A.	N. A.	N. A.	N. A.	N. A.
18	TiO_2	Pt-doped TiO_2	420	108	NOx	30	4.20E-07	0.05	0.000375	500	0.0045	40	0.04908	54	0.0226	12.0000
19	TiO_2	Pt-doped TiO_2	365	108	NOx	30	3.65E-07	0.05	0.000375	125	0.0045	40	0.04908	N.A.	N. A.	12.0000
20	$Au/CeO_2–TiO_2$	Au/Ce/Ti of 0.004:0.1:1	365	63.6	NO	30.01	3.65E-07	0.2	0.075	32	18	0.5	0.00061	85	0.0001	240.0000
21	Au/CeO2–TiO_2	Au/Ce/Ti of 0.004:0.1:2	420	64.6	NO	30.01	4.20E-07	0.2	0.075	150	18	0.5	0.00061	87	0.0001	240.0000
22	TiO_2	TiO_2 modified with Ru(2,2′-bipyridyl-4,4′-dicarboxylic acid) 2(NCS)2	420	N. A.	NO	30.01	4.20E-07	0.11	0.083	300	0.00012	1000	1.22741	99	0.0123	0.0014
23	TiO_2	Cu doped titanium dioxide	365	110.7	SO2	64.06	3.65E-07	N. A.	0.00083	125	0.1008	120	0.31441	62	0.1195	121.4458
24	TiO_2	Cu doped titanium dioxide	365	110.7	NO	30.01	3.65E-07	N. A.	0.00083	125	0.1008	65.5	0.08040	43	0.0458	121.4458
25	$BiFeO_3$	Immobilized $BiFeO_3$ nanoparticles	365	55.1	NOx	30	3.65E-07	1.2	3	15	1.5	5	0.00614	35.83	0.0039	0.5000

3.7.6 Natural Organic Matter Decragation

Natural organic matter (NOM), a complex matrix of organic compounds primarily composed of a mixture of humic and fulvic substances, including anionic macromolecules if various molecular weights with both aromatic and aliphatic components, presents a serious risk to public health and complicates standard processing methods, making NOM a major threat to drinking water treatment [96].

Most natural waters have NOM levels between 0.1 and 20 mg/L, nonetheless, there has been a recent rise in its content in ambient water matrices, placing stress on nearby ecosystems and the current water treatment infrastructure. Numerous significant alterations in the climate are to blame for this rise on NOM concentration. The primary analytical methods for identifying and measuring natural organic matter (NOM) in water are shown in Table 3.2 [96].

Table 3.2 Primary methods for detecting and measuring natural organic matter (NOM) in water [96].

Method	Advantages	Disadvantages	Complexity of Method
Adsorption at 254 nm	– Ease of use – Very fast measurement – Cheap	– Measurement of unsaturated organics in water (not only NOM/humic acid) – High nitrate content in low dissolved organic carbon (DOC) waters may interfere the measurement	Low
COD	– Simple – Well known method	– Toxic treatment chemicals – Low accuracy – High minimum detection limit	
TOC	– Fast measurement – Tailorable modes of detection for specific experiments	– Expensive specialised equipment – Measurement of total organics in water (not only NOM/humic acid)	
Fluorescence spectroscopy	– No pre-treatment required – Gives information on specific NOM	– Only detects fluorescent NOM molecules – Sensitive to chemical environment, e.g., pH	
FTIR	– Good signal to noise ratio – Extensive libraries of humic substances to identify specific compound characteristics	– Can see large water band interference – Pre-treatment could alter chemical makeup of NOM	
HPLC	– Good separation of NOM compounds	– Requires expensive, high purity solvents, columns etc. – NOM can have unwanted interactions with the stationary phase	
GC-MS	– Accurate detection of all substances found in water	– Cost of reagents, columns, etc. – Difficulty in analysing and interpreting results	High

Due to its mostly unrealized potential for prospective environmental engineering applications, photocatalysis is a rapidly developing field of study within the field of AOPs. The use of semiconductors (such as TiO_2 and ZnO) as sensitizers for light-induced redox reactions is the foundation of ongoing research on photocatalytic NOM elimination [96].

3.7.7 Applications in Health

In 2019, the World Health Organization identified the top ten global health threats. These included a worldwide influenza pandemic, antimicrobial resistance, dangerous pathogens like Ebola, vaccine hesitancy, dengue fever, AIDS, and other infectious diseases, which together made up 60% of the list. Over the past few centuries, bacterial infections have emerged as a major threat to human life. Some of the most lethal bacteria include *Mycobacterium tuberculosis*, *Staphylococcus*, *Salmonella*, *Escherichia coli*, and *Bacillus anthracis*. These infections claim thousands of lives each year [97].

The use of antibiotics has become a common and successful antibacterial tactic since Fleming´s 1928 discovery. However, the overuse and prolonged use of conventional antibiotics have encouraged the growth of germs resistant to these drugs, endangering public health through a variety of pathways, including livestock, food, and water [97].

One of the most promising alternatives to antibiotics for treating bacterial infections and water contamination brought on by specific pathogens are photocatalytic antibacterials agents, which have no drug resistance or adverse effects because of their rapid and effective bactericidal efficacy. Photocatalysis has special benefits in the field of antibacterials, and its controllability is crucial. Zinc oxide (ZnO), titanium dioxide (TiO_2), copper sulfide (CuS), bismuth sulfide (Bi2S3), molybdenum sulfide (MoS_2), graphene carbon nitride (g-C_3N_4), and other inorganic semiconductor materials are examples of materials used in photocatalytic antibacterial strategies. Organic photocatalysts include antimicrobial peptides and polymerization induced luminescence (AIE) [97].

The reaction between bacteria and ROS, an intermediate product of the photocatalytic reaction process, which has higher activity, is known as the photocatalytic antibacterial process. ROS is primarily the result of an incomplete reduction reaction between light-excited electrons/holes and oxygen (O_2) or water [97].

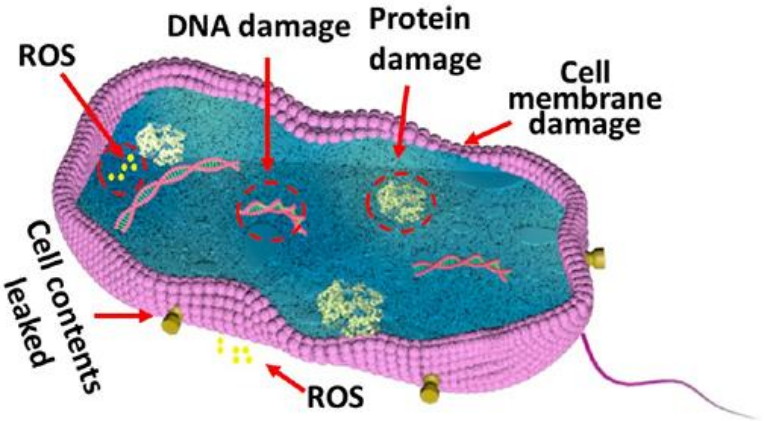

Fig. 3.7 Schematic of the photocatalytic antibacterial action [97].

3.7.8 Use of Photodynamic Therapy

Photodynamic therapy (PDT) was discovered more than a century ago by Oscar Raab, a medical student working with Prof. Hermann von Tappeiner. He noticed that paramecia incubated with a fluorescent dye and exposed to light died, while those kept in the dark were unaffected. Von Tappeiner was the first to coin the term "photodynamic reaction". Light's healing potential has been recognized since antiquity, with phototherapy dating back to approximately 3000 B.C [98].

PDT is a unique form of light therapy that relies on the interaction of three primary components: molecular oxygen, a light source, and a photosensitizer (PS) (Figure 3.8). Depending on the target location, the photosensitizer's absorption spectrum, and the necessary light dose, the three primary light source types utilized in PDT are lasers, light-emitting diodes, and lamps [98].

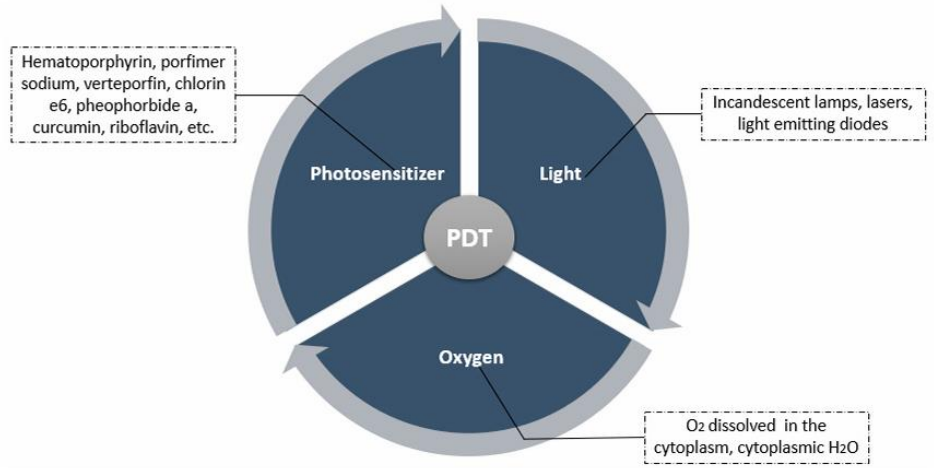

Fig. 3.8 Key elements of photodynamic treatment [98].

The in-situ oxygen molecules function as electron acceptors, and the non-toxic photosensitizing substances deposited at the target site are activated under the right light irradiation, allowing it to absorb and transfer electrons. As a result, harmful reactive oxygen species (ROS) are produced, which rupture the cell membrane and cause necrosis or apoptosis, which results in irreparable harm to microorganisms and target tissues [98].

PDT has become increasingly popular among different kinds of therapies because of the advantageous interaction between light, photosensitive substances (also known as photosensitizers), and oxygen. PDT has been used in several medical specialties over the past 40 years, including oncology, dermatology, urology, ophthalmology, and dentistry. It is effective in curing a variety of illnesses. The primary benefits of PDT that make it more promising than traditional treatment approaches like chemotherapy, radiation, and surgery are improves cosmetic results, fewer functional disruptions, good patient tolerance, fertility preservation, and reduce systemic toxicity [98].

Classic PSs impede the use of PDT, despite the fact that it is a promising and helpful therapy approach for many diseases. The most frequently cited disadvantages of conventional PDT are its low water solubility, shallow light penetration depth, and ineffective tumor targeting. Complex scheduling, the need for several treatments, post-treatment patient monitoring, and photosensitivity problems in the initial weeks following therapy are additional drawbacks. Combinatorial techniques with various therapeutic modalities show the prospect of overcoming PDT limitations (Figure 3.9). This allows for the exploitation of each treatment's benefits while counteracting its drawbacks [98].

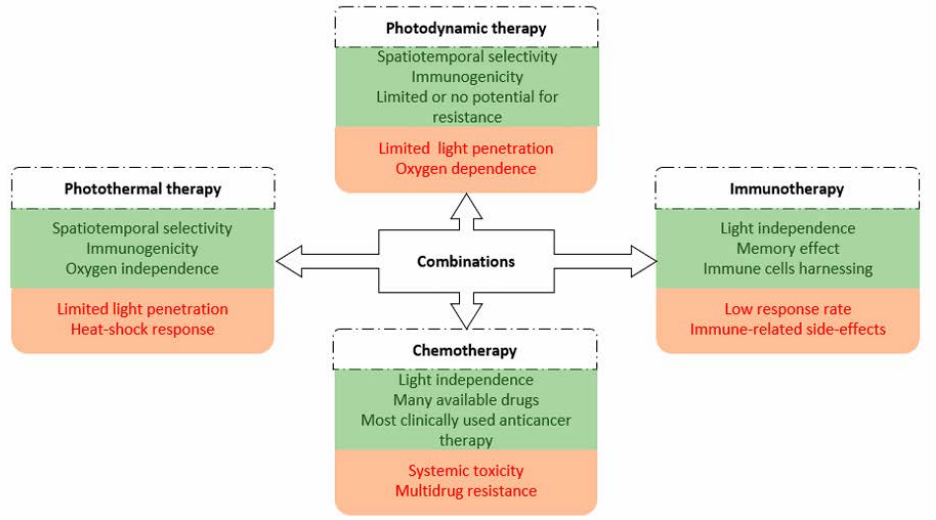

Fig. 3.9 Potential pairings of PDT with additional treatment approaches [98].

3.7.9 Uses in the Building Industry

The use of cementitious materials as catalyst supporting media has gained popularity in recent years. The primary tactic is to make use of urban building facades as media catalysts. A vast amount of surface area is available for photocatalytic reactions in the cementitious materials utilized in building facades. This approach has a strong chance of reducing urban pollutants while preserving the building's architectural appeal [99].

Moreover, by preventing the growth of germs by photocatalytic degradation, adding TiO_2 photocatalyst to cementitious materials may be able to maintain the sterility of the cement-based surface. Therefore, as seen in Figure 3.10, using cement-based materials as catalyst supporting media has the potential to convert cementitious materials into environmentally friendly goods including air-purifying pavement, self-cleaning external walls, and antibacterial concrete [99].

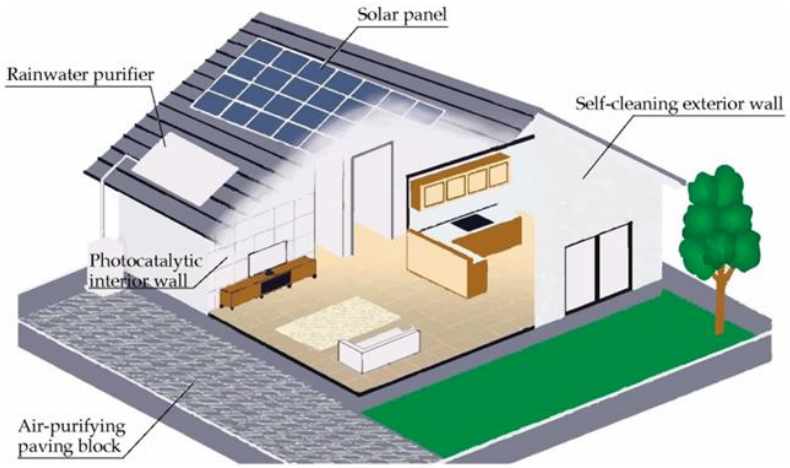

Fig.3.10 TiO_2-based solution for environmentally friendly construction [99].

Much effort is being made in the building sector to create novel building materials that incorporate TiO_2 photocatalyst. Construction materials with sophisticated properties, such self-cleaning, air purifying, and self-sterilizing surfaces, are now possible thanks to photocatalysis technology. Applications include antimicrobial tiles for hospital interiors, self-cleaning buildings facades, and photocatalytic concrete highways for air pollution removal. Additionally, as the use of photocatalytic building materials expands, tunneling and road infrastructure may be useful in reducing environmental pollution. Lastly, it can help manage the urban heat island effect in cities with high population densities. By subjecting the cement to external UV radiation, modern commercial technologies such as TXActive® and TioCem® photocatalytic cement, which contain TiO_2 particles, may efficiently remove a variety of pollutants, such as NOX, SOX, NH3, CO, and volatile organic compounds (Figure 3.11) [99].

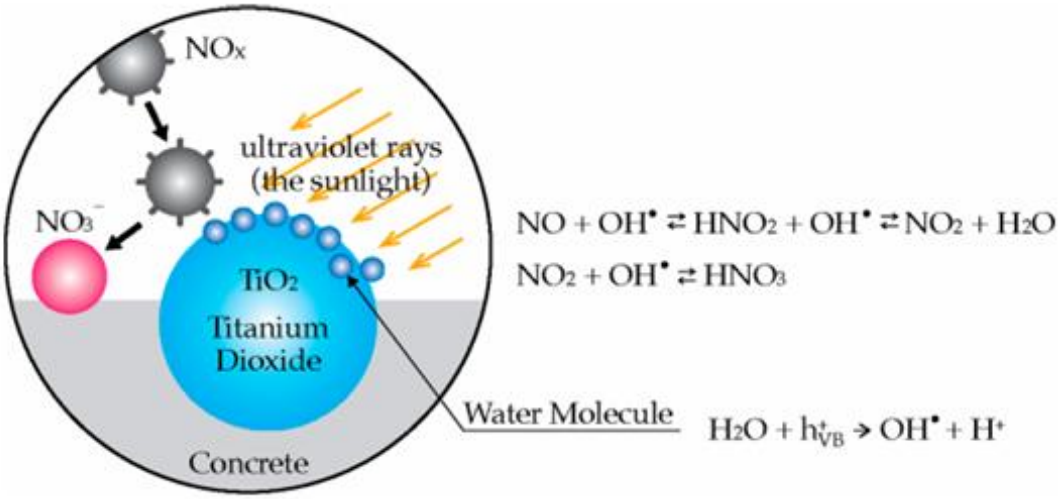

Fig.3.11 The steady-state process of photocatalytic oxidation of NOX [99].

Chapter 4

Hydrogen production through photocatalytic water splitting, Materials used in Photocatalysis and Rare Earth Elements

4.1 Introduction

The demand for energy has skyrocketed due to the world's population growth and rapid urbanization. The main cause of global warming is the enormous rise in CO2 and other greenhouse gases (GHG) in our atmosphere, which has been brought on by our heavy reliance on fossil fuels as our main energy source since the industrial revolution. Thus, it is essential for future energy sustainability and global security to decarbonize the energy supply by using clean, sustainable, and renewable energy [100].

The transition to a clean and ecologically friendly energy system will require resources for renewable energy (RE). The unpredictable and intermittent nature of these resources is the main barrier to reaching 100% RE. This necessitates technical adaptation, particularly with regard to balancing the varying supply and demand for energy. As renewable energy sources become more integrated into the current energy systems, large-scale energy storage devices will be needed to manage their unpredictability and intermittency [100].

The solution might lie in the ingenious idea of storing RE in a transportable, useable, and storable energy carrier like hydrogen. The concept of hydrogen-based energy storage systems, or HDESS, is therefore gaining traction as a cost-effective choice for extensive export, transportation, and RE restoration. Hydrogen-powered gadgets are driving the hydrogen economy, a 100% renewable energy sector [100].

4.2 Hydrogen assets and challenges

The most prevalent and basic element in the universe is hydrogen. Hydrogen's adaptability is one of its main qualities. It can be made from a variety of sources, including fossil fuels (like steam methane reforming) and renewable energy sources (like solar and wind energy). Because of its adaptability, hydrogen can suit some industrial needs while also aiding in the decarbonization process. The high energy density of hydrogen is another significant property. Hydrogen is a desirable fuel for automobiles, ships, and even airplanes since it has more energy per unit weight

than gasoline. When it burns, water vapor is emitted; no hazardous pollutants that promote climate change are created [101].

Furthermore, hydrogen can be used in a wide range of industrial applications due to its special chemical characteristics. For example, it is a perfect raw material for the synthesis of ammonia, a crucial component of fertilizers, due to its capacity to react with nitrogen at high temperatures. Furthermore, it is highly useful in the food and chemical industries for hydrogenation and metal refining due to its reactivity with other elements [101].

The potential benefits of hydrogen are undeniable, though, and nations and industries worldwide are investing resources in research and development, which is resulting in advancements in hydrogen production, storage, and utilization. However, the use of hydrogen is associated with several challenges, including the difficulty of transporting and storing hydrogen due to its low density at room temperature and the high cost of building the infrastructure for large-scale hydrogen production [101].

4.3 Hydrogen production through photocatalytic water splitting

4.3.1 The mechanism

Chemical energy (hydrogen) is produced from photonic energy, which originates from the higher-energy spectrum of solar light, specifically the ultraviolet and upper visible spectrum. Photonic energy, represented as hv, is proportional to the radiation frequency, where ν is the frequency and h is the Planck's constant. An electron-hole pair is created when a photon strikes the photocatalyst, and the electrical charge that results is used to dissociate water. A photocatalyst must have the right band gap and positioned valence bands (VBs) and conduction bands (CBs) for oxidation/reduction reactions in order to split water and produce hydrogen. Furthermore, choosing the right photocatalyst requires the quick creation and separation of electron ole pairs. Reactions involving photo-oxidation and photo-reduction can be expressed as [102]- [105]:

$$\text{Photoreduction: } 2H_2O+2e^- \xrightarrow{h\nu} H_2+2OH^- \quad (10)$$

$$\text{Photo-oxidation: } 2H_2O \xrightarrow{h\nu} O_2+4H^++4e^- \quad (11)$$

4.3.2 Critical Parameters for High-Efficiency Photocatalytic Water-Splitting

The basic idea behind photocatalytic water splitting is to create H2 and O2 from water by using particles in solution with incident sunlight. It can supply hydrogen in a clean, sustainable manner without causing greenhouse gas emissions or negatively impacting the atmosphere. Figure 4.1 shows some of the key elements influencing how well a photocatalytic hydrogen production process works [102]- [105].

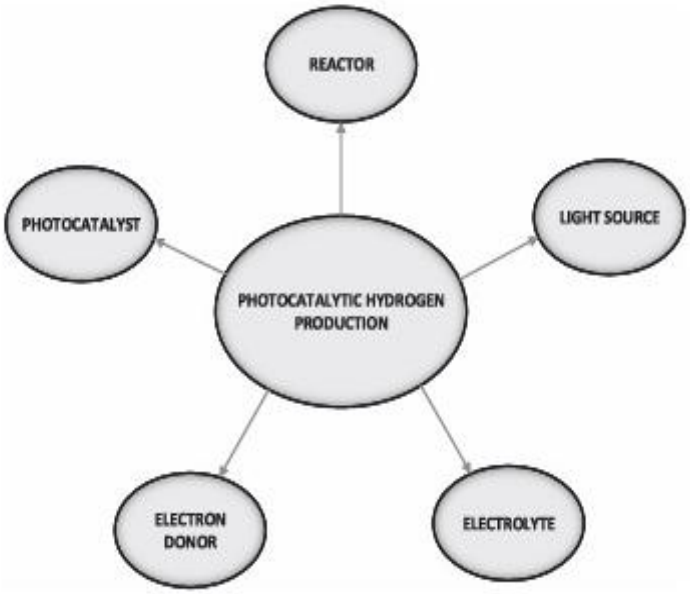

4.1 Essential Factors in Optimizing Photocatalytic Water-Splitting Efficiency [102].

4.3.3 Photocatalyst Characteristics

Certain materials exhibit excellent quantum efficiency among the several photocatalysts that have been investigated with UV light. Nevertheless, these current photocatalysts frequently exhibit inefficiency during the water splitting process. Having a suitable band gap to support the maximum amount of solar spectrum utilization, a suitable CB and valance band placement to drive oxidization and reduction reactions of overall water splitting, stability in the redox environment, low production and operation costs, recyclability, abundance, corrosion resistance, and suitability for large-scale production are all necessary for an efficient process. Figure 4.2 lists the photocatalyst requirements for effective hydrogen production [102]- [105].

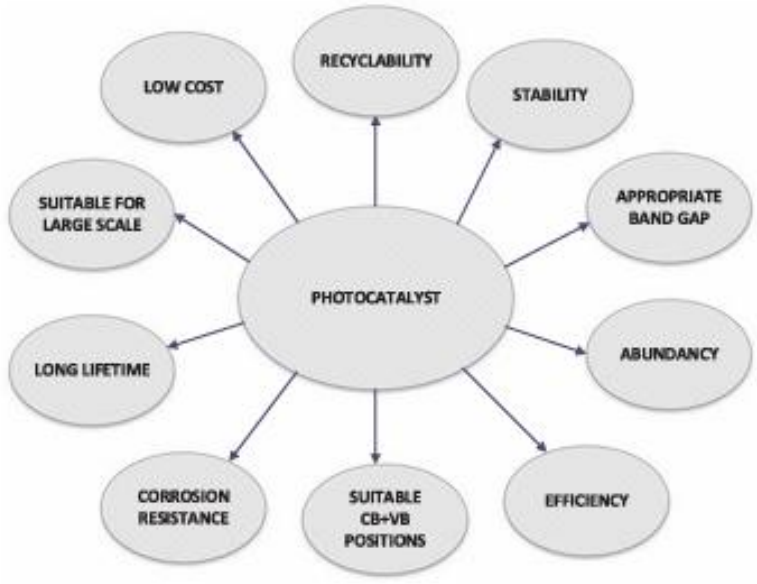

4.2 Core Features of Photocatalysts [102].

4.3.4 Materials suitable for Water-Splitting

A range of semiconductors have been discovered to be capable of HER, oxygen evolution reaction (OER), or water splitting by taking advantage of the characteristics of elements across the periodic table. The most researched photocatalyst for water splitting is TiO2. It is affordable, plentiful, stable, non-corrosive, and environmentally benign. However, because its band gap (3.2 eV) is in the UV region, it cannot use the visible light spectrum. The photocatalyst's active light spectrum region has a significant impact on how much solar energy is used. The solar conversion efficiency is just 2% up to 400 nm, which is comparable to the efficiencies seen in plants' photosynthetic systems. At 600 nm, the efficiency increases to 16%, and at 800 nm, it increases to 32% [106].

The most often utilized photocatalysts for water splitting are d^0 or d^{10} transition metal cations' oxides, sulphides, and nitrides. Photocatalysts such as CdSe, CdS, Ta_3N_5, TaON, C_3N_4, SiC, $BiVO_4$, WO_3, Cu_2O, Fe_2O_3, and others are among them. High charge recombination rates, poor charge transport, and low light harvesting limit the performance of metal oxides such as WO_3, $BiVO_4$, and Fe_2O_3. $BiVO_4$'s conduction band edge position renders it inappropriate for HER. Cu_2O is prone to self-reduction in aqueous solution, while having a potential 18% solar-to-fuel conversion efficiency. Likewise, CdS is prone to self-oxidation. Table 4.1 lists the photocatalytic activity of CdS-based and TiO_2-based photocatalysts [106].

Table 4.1 An overview of the water splitting photocatalytic activity of several photocatalysts [106].

Photocatalyst	Co-catalyst used	Photocatalyst amount	Reactant solution and sacrificial agents	Light source	Activity	AQY (%)	Stability (hours)
Polymer P7	Pt	25 mg	7.5 ml water, trimethylamine (TEoA) 7.5 ml, methanol 7.5 ml	300 W Xe Lamp with >420 nm cutoff filter	116 μmol h^{-1} g^{-1}	0.0225	65
TFPT-covalent organic framework	Pt	5 mg	1 ml TEoA, 9 ml water	300 W Xe Lamp with 420 nm < λ < 900 nm cutoff filter	1970 μmol h^{-1} g^{-1}	2.20	N/A
NiS/$Zn_{0.5}Cd_{0.5}$ S /RGO composite	RGO, NiS	50 mg	80 ml water, 0.35 M Na_2S, 0.25 M Na_2SO_3	–	375.7 μmol h^{-1}	31.10	12
NGO-QDs	–	1.2 g	200 ml aqueous solution, pH = 3	300 W Xe Lamp with 420 nm < λ < 800 nm cutoff filter	0.5 μmol h^{-1}	N/A	72
Hollow C_3N_4 nanosphere	3 wt % Pt	20 mg	100 ml aqueous solution, 10% TEoA	300 W Xe lamp	275 μmol h^{-1}	N/A	16
g-C_3N_4/carbon black/NiS	NiS	50 mg	15 ml TEoA, 85 ml distilled water	300 W Xe Lamp with > 420 nm cutoff filter	992 μmol h^{-1} g^{-1}	N/A	15
mpg-g-C_3N_4/CNT/NiS composites	NiS	50 mg	90 ml water, 10 ml TEoA	300 W Xe lamp	521 uμmol h^{-1} g^{-1}	N/A	N/A
3 wt % P3TH-g-C_3N_4 composite	1 wt % Pt	300 mg	600 ml aqueous solution, 0.25 M Na_2S, 0.25 M Na_2SO_3 M	300 W Xe Lamp with > 420 nm cutoff filter	560 μmol h^{-1}	2.90	N/A
Hydrogenated ZnO nanorods arrays	–	1.64 gm	100 ml aqueous solution, 0.1 M Na_2SO_3, 0.1 M Na_2SO_3	300 W Xe lamp	122,500 μmol h^{-1} g^{-1}	N/A	30
$Cu_{1.94}S$–$Zn_xCd_{1-x}S$	Pt	20 mg	50 ml DI, 0.1 Na_2S, 0.1 M Na_2SO_3	300 W Xe lamp with > 420 nm cutoff filter	13,533 μmol h^{-1} g^{-1}	26.40	N/A
CdS/ZnS core-shell	–	1 mg	20 ml aqueous solution	300 W Xe lamp with > 420 nm cutoff filter	239 μmol h^{-1} mg^{-1}	16.80	46
Si, Fe co doped TiO_2	–	400 mg	540 ml distilled water, 60 ml ethanol	500 W Xe lamp	320 μmol h^{-1} g^{-1}	N/A	N/A

4.3.5 The Reactors

Depending on the light source design, reactant and product hydrodynamics, and photocatalyst usage mode, photocatalytic processes can be conducted in a variety of reactor types. Among the reactors are parabolic trough reactors, moving beds, fluidized beds, and thin film reactor systems. The efficiency of this reactor will be calculated taking into account the QY and photochemical thermodynamic efficiency parameters. A recent study used CFD to predict the hydrodynamics and radiation absorption of a compound parabolic collector. The development of photocatalysts has received more attention than reactors [106].

4.3.6 The Electrolyte

For simplicity, electrolytes are assumed to consist only of deionized water, protons, hydroxide ions, and any additional salts, acids, or bases. The role of ionic species in reaction kinetics and thermodynamics, along with their effect on charge transport within the photoelectrochemical cell, is analyzed in relation to their influence on photocatalytic water-splitting efficiency. To clarify these functions and effects, four electrolyte properties were examined for their impact on the hydrogen evolution rate: (i) pH, (ii) dissolved oxygen, (iii) electrolyte conductivity, and (iv) electrolyte composition [107].

Since dissolved oxygen exerts minimal influence on the system, the decline in performance observed during photocatalytic pollutant degradation is likely attributed to surface site deactivation. In contrast, increased electrolyte conductivity enhances ion transport, thereby accelerating the water-splitting rate. It was found that above pH 13, the improved conductivity—resulting from the addition of extra base—was the primary factor driving the rise in photocurrent. Beyond this threshold, further increases in pH had negligible effect. Additionally, the nature of the cation species was shown to have little impact on the overall water-splitting rate. However, if the anion species' oxidation potential makes it thermodynamically preferable to water, it might lower the water splitting rate. The concept of seawater splitting is complicated by the anion oxidation problem [107].

4.4 Material used in photocatalysis

4.4.1 Introduction

Noble metals, transition metal, non-metals, and metalloids are various elemental groups based on their chemical & physical characteristics which can be used for fabrication of photocatalysts and may not be limited. Some examples of noble metals are platinum (Pt), palladium (Pd), ruthenium (Ru), and rhodium (Rh). Although nitrogen (N), clay, graphene, and carbon dots (CDs) are non-metals and metalloids, copper (Cu), zinc (Zn), and titanium (Ti) belong to transition metals. These materials will be discussed in the next section [108].

4.4.2 Transition metals

4.4.2.1 Copper (Cu)

While Cu typically has a lower Fermi level than semiconductors, electrons typically move from materials with a high Fermi level to those with a low Fermi level. Consequently, when the semiconductor and Cu are combined, the semiconductor's electrons will move to Cu until their Fermi levels match [109].

Cu is frequently utilized as a co-catalyst in reaction systems because of its high electronic conductivity, which enables it to swiftly transfer charge to the material's surface and start the reaction. Cu can also be utilized as a charge transfer channel to speed up electron migration between interfaces and as a bridge to join two distinct materials. It is frequently thought of as the reactive center due to its capacity to enrich electrons; its introduction can expand the active site; additionally, its unique adsorption to the substrate can enhance the material's photocatalytic activity and product selectivity [109].

By adding Cu, the materials' range of light absorption can be expanded. Cu's ability to react to near-infrared light (NIR) has drawn attention to its localized surface plasma resonance (LSPR). If the input photon's frequency matches the Cu particle's oscillation frequency under illumination, Cu will absorb the photon and use Landau damping to decay into electron-hole pairs. The photogenerated electrons and holes can be separated by transferring the hot electrons produced by Cu's LSPR effect to the semiconductor that is coupled to Cu via the interface. The holes left on Cu can perform the oxidation reaction, while the hot electrons that are produced can continue the reduction reaction in the photocatalytic reaction [109]. Figure 4.3 recapitulates the properties of Cu.

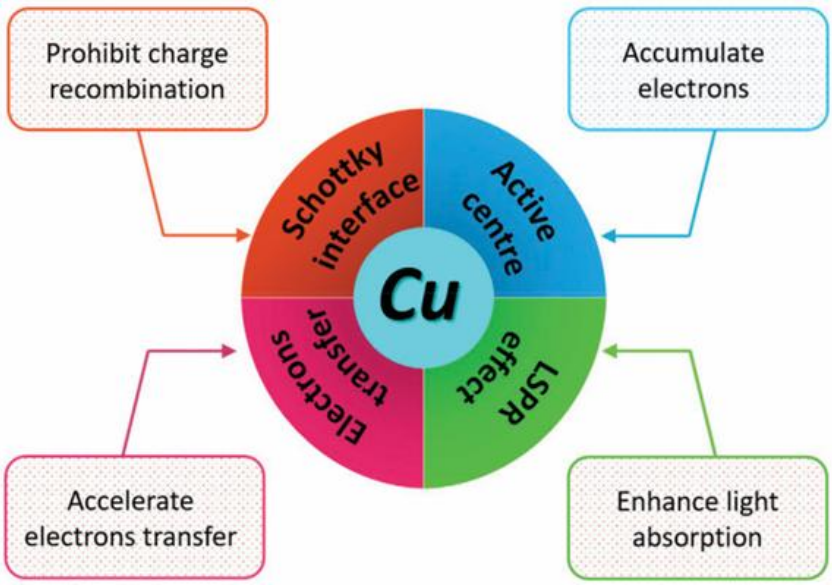

Fig. 4.3 Copper's functions in photocatalysis reactions [109].

4.4.2.2 Zinc (Zn)

The most important compound in which zinc takes part is ZnO. The semiconductor material zinc oxide (ZnO) has a high exciton binding energy of over 60 meV and a broad band gap, usually approximately 3.37 eV. Its properties are presented in table 4.2 [111].

Table 4.2 ZnO's structural and physical characteristics [111].

Property	Wurtzite ZnO	Sphalerite ZnO
Crystal system	Hexagonal	Cubic (Zinc Blende)
Coordination number	Tetrahedral (each Zn and O atom is coordinated with four atoms)	Tetrahedral
Lattice Parameters	a ≈ 3.25 Å, c ≈ 5.2 Å	a ≈ 4.62 Å
Stability	Thermodynamically stable at ambient conditions	Metastable; forms under specific conditions
Physical properties	Piezoelectric and pyroelectric	Centrosymmetric; lacks piezoelectricity
Electronic Bandgap	≈3.37 eV	Slightly similar (depends on preparation)
Application	Sensors, optoelectronic devices, catalysts	Rare; specialized conditions

Because of these characteristics, it can be used in a variety of fields, such as photocatalysis and optoelectronics. Its broad range of applications in airborne volatile organic compounds (VOC) breakdown, water disinfection, and organic pollutant degradation highlights its importance to the environment. Also, ZnO's promise as a renewable energy source is highlighted by its capacity to produce hydrogen through water splitting. Notwithstanding these benefits, issues including photocorrosion, stability issues, and low quantum efficiency still restrict its usefulness in practical applications. To overcome its inherent limitations, current developments have concentrated on increasing ZnO's visible light activity (VLA), which was first acknowledged for its effectiveness under ultraviolet (UV) light [111].

To improve ZnO's performance in these domains, they have concentrated on altering its structural and electrical properties. To change ZnO's electrical and magnetic characteristics, one method is to dope it with transition metals. For example, ZnO films' electrical and magnetoelectric transport characteristics have been demonstrated to be enhanced by titanium ion implantation, which may increase the films' applicability for electronic devices. The impact of chloride ion doping on ZnO nanostructures was investigated in another study. The study showed that different amounts of chloride ions can greatly increase the photocatalytic breakdown efficiency of methylene blue in both acidic and alkaline conditions, suggesting possible uses in environmental cleanup. Additionally, effective room-temperature techniques have been used to synthesize silver-doped ZnO nanoparticles. These nanoparticles are effective materials for antibacterial and environmental

cleanup applications because of their distinct structural and optical characteristics as well as their increased photocatalytic activity. Finally, it has been investigated how stacking order affects the optical and physical characteristics of Cu_2ZnSnS_4 absorber layers made from DC-sputtered oxygenated precursors. This study offers important insights into how material performance in solar applications might be affected by structural changes. The forms of ZnO and their properties are displayed in Table 4.3 [111].

Table 4.3 Synthesis and photocatalytic activity of ZnO photocatalyst [111].

ZnO Morphology	Synthesis Method	Target Contaminants	Removal Efficiency	Experimental Condition
Nanowires	Hydrothermal	Methylene Blue (MB)	86% after 180 min	UV irradiation
Nanowires	Hydrothermal	Methyl Orange (MO)	49% after 180 min	UV irradiation
Nanowires	Hydrothermal	Acid Red 14 (AR14)	93% after 180 min	UV irradiation
ZnO/Cu-DPA Composite	Co-precipitation	Methylene Blue (MB)	87% within 80 min	Visible light irradiation
ZnO Nanoparticles	Precipitation	Methylene Blue (MB)	96.5%	Direct sunlight irradiation
ZnO/PVP Nanoparticles	Sol-gel	Industrial dye wastewater	Significant degradation	UV irradiation
Porous ZnO Coral-like Nanoplates	Wet-chemical	Methylene Blue (MB)	Enhanced efficiency	UV irradiation
ZnO/Activated Carbon Composite	Co-precipitation	Acid Green 25 (AG25)	Faster degradation	UV irradiation
ZnO Nanoparticles	Green synthesis	Various organic dyes	Effective degradation	UV irradiation

4.4.2.3 Titanium (Ti)

It is essential to use self-sustaining and clean technologies while interacting with the scientific community. Titanium dioxide (TiO_2) is a member of a class of materials with enormous practical potential that, in every way, helps to address some of the new problems facing humanity. Because of its high photocatalytic activity, chemical and biological stability, insolubility in water and acidic and basic environments, corrosion resistance, nontoxicity, low cost, and availability when compared to oxide, sulfide, and other materials, it is the most widely used photocatalyst [112].

In the presence of TiO_2 as a photocatalyst, heterogeneous photocatalytic oxidation of organic compounds in an aqueous solution offers the potential for effective waste, drinking, surface, and groundwater treatment as well as the production of ultraclean water appropriate for the pharmaceutical industry and microelectronics. Many organic substances and their intermediates are fully mineralized. Degradation leads to carbon dioxide, water, nitrates, chalcogenides, phosphates, and other inorganic ions, depending on the parent compound's structure [112].

TiO_2's photocatalytic activity is mostly determined by its morphology and crystal structure. Consequently, crystallite size and specific surface area are crucial elements for TiO_2 photocatalytic activity. Compared to their 0D and 2D counterparts, 1D TiO2 nanostructures have drawn more interest because of their efficient electronic charge characteristics, larger surface area, and higher aspect ratio. TiO_2 is found in one rhombic form (brookite) and two tetragonal forms (rutile and anatase). While rutile and anatase are readily made, brookite is challenging to obtain in a lab setting. Although rutile is the stable phase in bulk, the anatase structure is typically preferred in solution-phase production techniques for TiO_2. Surface energy and precursor chemistry are the two primary causes of these findings. It has been discovered that anatase has a lower surface energy than rutile and brookite. At ambient temperature, rutile, anatase, and brookite TiO2 are estimated to have bandgap energies (also known as optical absorption edges) of 3.00, 3.21, and 3.13 eV, respectively. As the crystal growth temperature drops, the photon energy values of the rutile and anatase optical absorption edges rise. In general, bulk rutile and anatase bandgaps are regarded as indirect [112].

But despite all the benefits listed above, TiO_2 has certain disadvantages when it comes to real-world use. Only around 3–4% of the radiation from a nearby UV region of sunlight is used during the photocatalytic process because of the wide band gap. As a result, TiO_2 is essentially inactive in the presence of sunshine. This lessens the sun's suitability as the most cost-effective light source. With a normal UV flux of 20–30 Wm^{-2}, there are 0.2–0.3 mol photons $m^{-2}h^{-1}$ in the 300–400 nm region close to the Earth's surface [112].

By enhancing its photosensitivity and determining the relationship between its surface, interfacial, and microstructural features and the corresponding mechanisms essential to its photoelectric properties, recent experimental and theoretical studies have attempted to improve the optical properties of TiO_2. Element doping in conjunction with other semiconductors to create heterojunctions, the synthesis of nanostructures with specific morphologies, surface sensitization to improve optical characteristics using organic dyes, metal nanostructures or metal complexes, etc. are common techniques to improve the optical properties of TiO_2. One way to describe the doping approach is the intentional introduction of contaminants intoa substance that is semiconductor-like [112].

4.4.3 Noble Metals

4.4.3.1 Platinum (Pt)

Optimizing the atomic-scale structure of photocatalysts to enable the separation of electron-hole pairs for improved performance is a highly desirable yet difficult task. Currently, a highly effective photocatalyst is created by combining single Pt atoms on Pt_1/def-TiO_2 (adefective TiO_2) support [113].

Pt is thought to be the finest co-catalyst among different metals because of its low potential for H_2 evolution and appropriate Fermi level for trapping electrons. The sensible design of phase interfaces within this hetero structured photocatalyst is crucial for establishing charge transfer efficiency and ensuing reaction activity. In addition to acting as sites for proton reduction, Pt atoms can encourage nearby TiO_2 units to produce surface oxygen vacancies through a hydrogen spillover effect. This results in the creation of an atomic interface between the isolated Pt atom and the Ti^{3+} defect with the atomically distributed Pt-O-Ti^{3+} active center [113].

The presence of the Pt-O-Ti^{3+} atomic interface contributes to the increased transfer efficiency of the photogenerated electrons from Ti^{3+} defective sites to single Pt atoms, which makes it easier to separate electron–hole pairs and prevents their subsequent recombination, according to several photo-electrochemical characterizations and density functional theory (DFT) calculations. The Pt_1/def-TiO_2 catalyst has exceptional photo-electrochemical properties and record-level photocatalytic hydrogen production performance due to its unique Pt O-Ti^{3+} atomic interface construction (Figure 4.4). Its remarkably high turnover frequency (TOF) of 51423 h^{-1} is 591 times higher than that of the Pt nanoparticle supported TiO_2 catalyst (Pt NPs/f-TiO_2) and outperforms the majority of known photocatalysts [113].

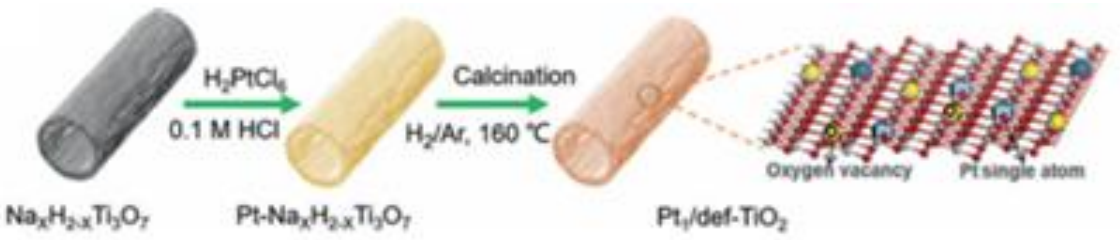

Fig.4.4 The Pt1/def-TiO_2 catalyst's preparation procedure [113].

However, the existing hetero-structured photocatalysts' restricted fraction of interfacial sites prevents further enhancement of photocatalytic activity. Furthermore, the application of these heterostructured photocatalysts is hampered by the low atom-utilization efficiency, high cost, and shortage of Pt [113].

4.4.3.2 Palladium (Pd)

A good noble metal for plasmonic photocatalysis is palladium. Table 4.4 displayed typical Pd enhanced photocatalyst instances. Pd NPs have been shown to increase photocatalytic activity in a variety of applications, such as water splitting, CO_2 reduction, organic pollutant breakdown in air and water, and many more [114].

When the electrons oscillate at the same frequency as radiation, free electrons may be produced on nanostructures. This effect has been used to improve photocatalysis triggered by

visible light. Palladium nanocubes were able to produce free electrons through the SPR effect and absorb photons of visible light [114].

One important metric for assessing a catalyst's performance is its chemical stability. High stability was demonstrated by the Pd NPs modified photocatalyst in the breakdown of organic contaminants [114].

Table 4.4 Typical instances of photocatalysts improved by Pd NPs [114].

Photocatalyst	Application	Photoactivity
Pd−TiO_2	Oxidation of benzene	$\theta_{TiO2} = 28.2\%$ $\theta_{Pd\text{-}TiO2} = 65.3\%$
	Reduction of CO_2	$n_{CH4,\ TiO2} = 0.075$ μmol/g/h $n_{CH4,\ Pd-TiO2} = 0.212$ μmol/g/h
	Degradation of Methylene Blue	$\theta_{TiO2} = 8\%$ $\theta_{Pd\text{-}TiO2} = 55\%$
	Oxidation of NO	$\theta_{TiO2} = 43.9\%$ $\theta_{Pd\text{-}TiO2} = 87.2\%$
Pd−ZnO	Degradation of RhB	$\theta_{ZnO} = 31\%$ $\theta_{Pd\text{-}ZnO} = 98\%$
Pd−C_3N_4	Reduction of Cr(VI)	$\theta_{C3N4} = 0\%$ $\theta_{Pd\text{-}C3N4} = 99.89\%$
	Hydrogen evolution	$n_{H2,C3N4} = 152.9$ μmol/g/h $n_{H2,Pd-C3N4} = 1208.6$ μmol/g/h
	Degradation of bisphenol	$\theta_{C3N4} = 6.0\%$ $\theta_{Pd\text{-}C3N4} = 93.9\%$
	Reduction of CO_2	$n_{CH4,C3N4} = 0.08$ μmol/g/h $n_{CH3OH,C3N4} = 0.39$ μmol/g/h $n_{CH4,Pd-C3N4} = 0.40$ μmol/g/h $n_{CH3OH,Pd-C3N4} = 3.17$ μmol/g/h
Pd−Bi_2WO_6	Degradation of phenol	$\theta_{Bi2WO6} = 60.0\%$ $\theta_{Pd\text{-}Bi2WO6} = 95.2\%$
Pd−Bi_2MoO_6	Degradation of phenol	$\theta_{Bi2MoO6} = 10\%$ $\theta_{Pd\text{-}Bi2MoO6} = 100\%$
Pd−BiOBr	Degradation of phenol	$\theta_{BiOBr} = 67\%$ $\theta_{Pd\text{-}BiOBr} = 100\%$
Pd−$BiVO_4$	Degradation of phenol	$\theta_{BiVO4} = 3.4\%$ $\theta_{Pd\text{-}BiVO4} = 100\%$

Only light photons with wavelengths less than 429 nm can initiate the photocatalytic process for pure BiOBr. Nearly all visible light photons can activate BiOBr for a photocatalytic reaction when Pd NPs are placed onto the surface. Additionally, the absorbance intensity increased with the loading amount of Pd NPs. It showed that Pd NPs held great promises for increasing the solar spectrum's use. It was discovered that Pd NPs could absorb light with wave lengths between 200 and 1000 nm [114].

Although TiO_2 is the most popular and commercially available photocatalyst, its use under solar light is limited by its wide band gap, which allows only UV light to be used as its light source. Nevertheless, loading palladium nanoparticles onto the surface of TiO_2 may be a useful technique to increase its visible light-driven photocatalytic activity. The photocatalytic activity in the oxidation of NO was significantly enhanced by Pd NPs-modified TiO_2, and it was 72% greater than that of P25. To evenly distribute the Pd nanoparticles across the TiO_2 nanotubular surface, a straightforward incipient wetness impregnation technique has also been used. The photocatalytic activity of TiO_2 nanotubes in the breakdown of organic contaminants was significantly enhanced under simulated solar light following treatment with Pd NPs. Comparable outcomes were also documented, demonstrating that Pd NPs work well as a co-catalyst to increase TiO_2's visible light-driven photocatalytic activity [114].

Another photocatalyst that does not react to visible light is ZnO. It's treated with Pd show enhanced photocatalytic activity. Because the work function of palladium and the Fermi level of ZnO differ, Pd NPs may operate as a carrier of photogenerated electrons from the conduction band of ZnO when they are placed onto the photocatalyst. Furthermore, the SPR effect may cause palladium nanoparticles on the surface to absorb light photons and move excited plasmonic-state electrons to ZnO's conduction band. The separation of photogenerated charge carriers is made easier by the electron transfer between Pd and ZnO, which raises ZnO's photocatalytic activity [114].

In contrast, the best photocatalytic activity in the elimination of organic pollutants from water was demonstrated by the Pd NPs modified peanut-shaped $BiVO_4$ (Pd-$BiVO_4$). The photocatalytic activity of pure $BiVO_4$ was low when considering the ratios of concentration to removal of total organic compounds (TOC). $BiVO_4$'s photocatalytic activity in the breakdown of phenol under visible light was greatly enhanced by the surface modification of Pd NPs, and it was even on par with TiO_2 under UV light [114].

4.4.3.3 Ruthenium (Ru)

Hydrogen peroxide (H_2O_2) is a significant green oxidant that is used extensively in chemical synthesis, pulp production, wastewater treatment, and disinfection. Adopting the clean/environmentally friendly photocatalysis technology is therefore crucial for producing value-added compounds and H_2O_2 simultaneously by effectively utilizing both photo-generated electrons and holes in redox reactions [115].

In situ hot injections are used for designing and creating Ruthenium (Ru) atom-incorporated CdS quantum dots (QDs) employing oleylamine as the stabilizer and thioacetamide (TAA), cadmium chloride (CdCl2), and ruthenium (III) chloride (RuCl3) as the precursors. When compared to CdS QDs (Ru0), Ru (0.1 weight percent) included CdS QDs (Ru0.1) show the highest activity of H2O2 evolution (8.78 mmol g^{-1} h^{-1}) with the maximum enhancement factor of ≈1372%. Additionally, Ru0.1's typical benzaldehyde (BAD) evolution rate (11.70 mmol g^{-1} h^{-1}) is approximately 168% greater than Ru0's (6.96 mmol g^{-1} h^{-1}) [115].

High oxidation state (+3) Ru atoms can both significantly attract photogenerated electrons moving from the bulk to the Ru0.1 surface as a whole and, evidently, increase the number of photogenerated holes moving to the surface by limiting their electron recombination. The majority of photogenerated electrons on the surface can be easily captured by oxygen (O_2), a strong electron scavenger, in ≈0.1 μs, according to in situ transient state SPV spectroscopy. The remaining photogenerated holes are roughly ten times higher than those of Ru0. Furthermore, in situ TAS shows that under practical circumstances, Ru0.1 can still hold onto roughly 16% of the photo-

generated electrons at about 3100 ps following light excitation, but Ru0 can only hold onto about 8% of the photo-generated electrons simultaneously [115].

4.4.3.4 Silver (Ag)

While it can be controlled in terms of size, shape, temperature, and irradiation intensity, silver, a common plasmonic metal. In the included heterogeneous systems, metallic Ag enables morphological surface alteration, localized spatial charge separation, and quick charge separation and trapping, all of which significantly improve photocatalytic performance. Metallic Ag plays two main roles in improving photocatalysis: the LSPR effect and the Schottky effect [116].

The LSPR effect, which is triggered by visible light, can produce additional electrons and holes to take part in photocatalysis. By creating a Schottky junction or Ohmic contact inside the metal–semiconductor structure, Ag is able to effectively separate charges between the semiconductor and Ag thanks to the appropriate work function. Ag's numerous functions as an electron trapper, visible light response inducer, and hot carrier provider efficiently permit a wide photoactive spectrum region and quick charging while impeding the recombination process [116].

Numerous Ag-based photocatalysts were investigated for a range of uses, including CO_2 reduction, antibacterial application, water splitting, pollutant removal, etc., as shown in Figure 4.5.The low selectivity towards liquid fuels like alcohol and other hydrocarbons in the photocatalytic CO_2 reduction process on Ag-based photocatalysts, the slow oxygen evolution kinetics during water splitting, how to control equitably Ag^+ release over an extended period of time, and the low charge separation efficiency during pollutant degradation are all critical issues that still need appropriate solutions [116].

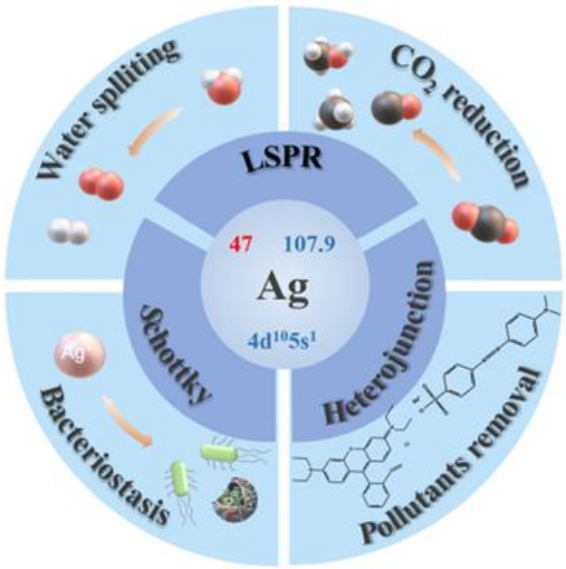

Fig.4.5 Ag-based photocatalysts (gray: hydrogen atom, black: carbon atom, pink: oxygen atom) and their photocatalytic uses [116].

4.4.3.5 Rhodium (Rh)

One of the metals in the platinum group is rhodium (Rh). Since no acid or combination of acids, including aqua regia, can attack it, it is more noble than platinum. A commercial process based on rhodium plating has existed since the early twentieth century. It belongs to the platinum group of metals, which makes it incredibly resistant to corrosion. Rh deposits are rare and found in trace amounts, that's why it is prohibitively expensive to purchase [117].

Rh is electrodeposited for functional or aesthetic purposes. The procedure of electrodeposition is thought to be a simple, economical, and efficient way to create a noble metal coating. By dramatically reducing the amount of cathode material on the substrate during coating, pulse current electrodeposition (PC) aims to increase coating quality while saving a substantial amount of money and time [117].

Rhodium can also be used to flash plate precious stone mounts and settings to increase their brilliance. The most common contact surface for reed switch contacts is still rhodium deposit due to its acceptable electrical contact resistance values and resistance to abrasion and arcing [117].

When doped with rhodium, $BaTiO_3$, a potentially environmentally friendly photocatalyst, can destroy the color methylene blue by 96%. Rh-doped $SrTiO_3$ nanostructure with Rh preserved in the photoactive +3 oxidation state. When exposed to visible light, this shows efficient methyl or ange breakdown [117].

The breakdown of organic pollutants was enhanced by the conversion of inactive Rh & Sb doped TiO_2 nanorods into an active composite photocatalyst. When exposed to visible light, rhodium (IV)-doped titania shows photocatalytic activity toward the oxidation of organic materials. The Rh complex's covalent bond with modified TiO_2 is responsible for the photocatalyst's increased stability. TiO_2 modified with rhodium is utilized in methyl orange breakdown and esterification reactions. Rhodium and antimony-coated rutile TiO_2 nanorods that are visible-light active are utilized to break down organic contaminants [117].

4.4.4 Non-metals and metalloids

4.4.4.1 Nitrogen (N)

Research has demonstrated that by decreasing the TiO2 band gap, nitrogen doping enhances the material's photocatalytic properties. This was accomplished because the addition of nitrogen reduces the TiO2 band gap by generating an intermediate band gap. More electrons will be excited to the conduction band because of absorbed visible light when the band gap narrows. The generated holes and the excited electron in the conduction band conducted a redox reaction in which the OH- ions and oxygen molecules, respectively, scavenged the electron and hole [118].

By creating a single electron-trapped oxygen vacancy site in the form of Ti-O-N, nitrogen added to the TiO2 crystal structure will decrease the recombination of photon-generated electron-hole pairs. Nitrogen doping of TiO2 preserved its UV light activity while enhancing wider absorption in the visible spectrum. They pointed out that nitrogen doping lowers electron-hole recombination in addition to changing the crystal structure. When nitrogen is added to the TiO2 crystal lattice, the transition from anatase to rutile structure is prevented, allowing the annealing temperature to rise. The doping parameters, such as electrolyte concentration, reaction voltage, and reaction time, have a significant impact on the photoelectrochemical characteristics of N-doped TiO2 nanotubes [118].

The nitrogen doping of TiO2 in both wet and dry methods. Titanium nitride (TiN) powder is oxidized in flowing oxygen gas or nitrified with ammonia gas passing over titanium dioxide power in the dry process. The rutile phase N-doped TiO2 is the product of the oxidation process, whereas the anatase TiO2 doped with nitrogen is produced by treating anatase TiO2 for three hours at 600 degrees Celsius in ammonia/argon gas. The wet process is made using techniques such as sol-gel, in which titanium trichloride (TiCl3) or titanium sulfate (Ti (SO4)2) solution is mixed with ammonia solution (NH4OH) [118].

Numerous techniques, such as hydrothermal, sol-gel, ball milling, ion implantation, titanium nitrate oxidation, chemical vapor deposition, etc., have been used to add nitrogen to the TiO2 crystal structure. Nitrogen dioxide, tert-butylamine, ammonia, hydrazine, urea, triethylamine, and thiourea are examples of nitrogen sources. When triethylamine is used as a nitrogen precursor, the maximum photocatalytic activity is seen [118].

4.4.4.2 Clay

Clays are essential in many fields due to their outstanding physiochemical characteristics. These include robust surface reactivity, biocompatibility, swelling properties, cation-exchange capacity, and good adsorption capacity. Layered (like smectites) and fibrous (like sepiolite) clays are considered attractive materials because of their demonstrated effectiveness as a semiconductor substrate for the catalytic degradation of several organic contaminants. The characteristics of clay materials could be characterized by either cationic or anionic clays (e.g., stacked double hydroxides). One or more Si-O tetrahedral sheets and one Al–O (Mg–O) octahedral sheet make up the layers of aluminosilicate that are frequently found in clay minerals (Figure 4.6) [119].

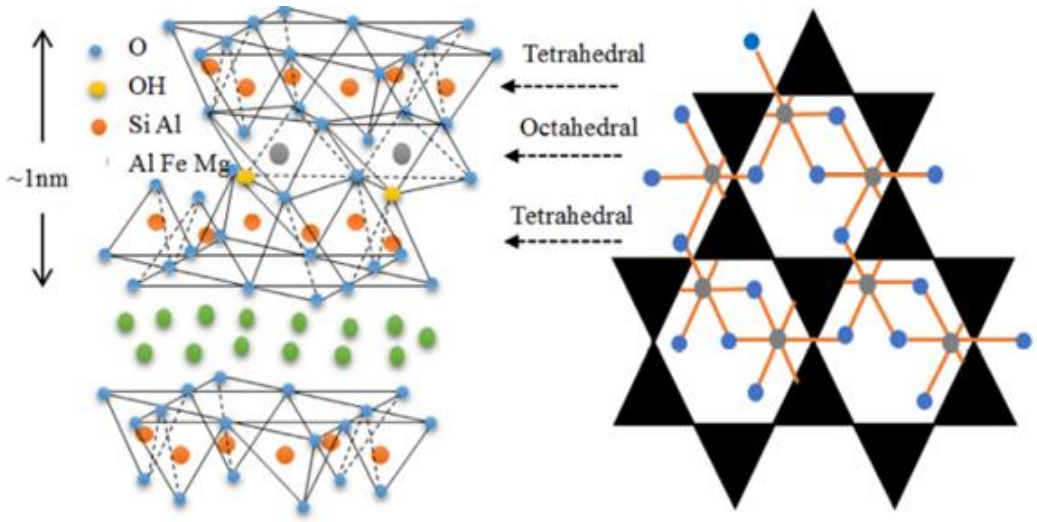

Fig.4.6 Several parts of a simple clay construction [119].

Heterogeneous photocatalysts have been generated more frequently using clay minerals. The following clay minerals have been used as supports montmorillonite, bentonite, kaolinite, hectorite, halloysite, and LDH. To create TiO2/clay nanocomposites, TiO2 is impregnated onto the clay's surface or between its layers. A lower charge recombination rate in TiO2/clay nanocomposites is responsible for increased photocatalytic activity [119].

Clay minerals have been extensively studied as support for many types of photocatalysts in recent years. When photocatalyst nanoparticles are distributed across clay mineral surfaces, more active surface sites are created and the aggregation of photocatalyst particles is decreased, increasing the photocatalytic activity of the catalysts. Furthermore, certain clay impurities, like iron, can improve the material's optical qualities and adjust its photo response activity [119].

Additionally, the main photocatalyst and clay must make surface contact in wastewater treatment. Clay with a large surface area, like two-dimensional or sheet-structure clay like montmorillonite, may have more surface interaction with the main photocatalyst than one-dimensional or pillar-loke-structure clay like attapulgite and sepiolite, which would improve the separation of the main photocatalyst's electron and hole [119].

4.4.4.3 Graphene

Research on artificial photocatalysis is currently focused on graphene (GR), a single-layer carbon sheet with a hexagonal packed lattice structure that has demonstrated promise in enhancing surface reactions, light absorption, and electron transfer kinetics [120].

Today, multifunctional GR-based photocatalysts, including GR-semiconductors, GR-metal, and GR-organics, are widely used in carbon dioxide (CO2) reduction, environmental purification, selective organic transformation, photocatalytic water splitting, and fixing of nitrogen (N2), to offer a practical and sustainable solution to the issues of rising energy demands and environmental

crises. The applications are compiled in Table 4.5. Ideal GR has been viewed as a promising cocatalyst to increase the conversion efficiency of solar energy in artificial photosynthesis systems because of its distinctive and intriguing characteristics, which include a 2D flat structure, a high theoretical specific surface area, superior optical transmittance, excellent electron conductivity, and good chemical stability. Furthermore, GR can also function as a macromolecular photosensitizer to produce photoelectrons on its own in certain particular photocatalytic systems [120].

Table 4.5. An overview of the recent photocatalytic uses of GR-based hybrids [120].

Entry	Composite photocatalyst	Light source	Reaction type	Reaction conditions
1	TNTAs@rGO/MoS_2 [a]	300 W Xe lamp, 320–780 nm	H_2 evolution	vacuum, methanol (10 vol%) or lactic acid (10 vol%)
2	Ni_2P-FGR [b]	300 W Xe lamp, ≥ 420 nm	H_2 evolution	vacuum, TEOA [c] (10 vol%), Eosin Y
3	CdS-EGR [d] CdS-rGO	300 W Xe lamp, ≥ 420 nm	H_2 evolution	vacuum, lactic acid (10 vol%)
4	$CH_3NH_3PbI_3$/rGO	300 W Xe lamp, ≥ 420 nm	H_2 evolution	HI solution
5	Fe_2O_3/rGO/PCN [e]	300 W Xe lamp, ≥ 420 nm	overall water splitting	H_2O, H_2PtCl_6
6	graphene/carbon nitride	[1]300 W Xe lamp, ≥ 420 nm [2]LED solar simulator	[1]H_2 evolution [2]photooxidation of 1,4-DHP [f]	[1]N_2, TEOA (10 vol%), H_2PtCl_6 [2]10^{-4} mol/L 1,4-DHP
7	rGO-CoO_x/$BiVO_4$-Pt-metal sulfides [g]	300 W Xe lamp, ≥ 420 nm	overall water splitting CO_2 reduction to CO	Ar gas flow, H_2O CO_2 gas flow, H_2O
8	$CsPbBr_3$ QD/GO [h]	100 W Xe lamp, AM 1.5 G	CO_2 reduction to CO	CO_2, ethyl acetate
9	nanographene-rhenium complex	100 W tungsten lamp, ≥ 490 nm	CO_2 reduction to CO	CO_2, tetrahydrofuran, TEOA
10	NH_2-rGO/Al-PMOF [i]	125 W medium-pressure mercury lamp	CO_2 reduction to formate	CO_2, TEOA/acetonitrile (*v*:*v* = 1:5)
11	hypercrosslinked polymer-TiO_2-GR	300 W Xe lamp, ≥ 420 nm	CO_2 reduction to CH_4 and CO	CO_2, H_2O
12	*N*-doped GR/CdS	350 W Xe lamp, ≥ 420 nm	CO_2 reduction to CO and CH_4	CO_2, H_2O
13	α-Fe_2O_3/amine-rGO/$CsPbBr_3$	150 W Xe lamp, ≥ 420 nm or AM 1.5 G	CO_2 reduction to CH_4 and CO	CO_2, H_2O
14	$CsPbBr_3$/USGO/α-Fe_2O_3 [j]	300 W Xe lamp, ≥ 400 nm	CO_2 reduction to CO	CO_2, acetonitrile/H_2O (*v*:*v* = 200:1)
15	Cs_4PbBr_6/rGO	300 W Xe lamp, ≥ 400 nm	CO_2 reduction to CO	CO_2, ethyl acetate/H_2O (*v*:*v* = 1000:1)
16	ZnPc/GR/$BiVO_4$ [k]	300 W Xe lamp, ≥ 420 nm	CO_2 reduction to CH_4 and CO	CO_2, H_2O
17	TaON@GR	300 W Xe lamp, ≥ 420 nm	CO_2 reduction to CH_4	CO_2, H_2O
18	transition metal hydroxide-GR [l]	300 W Xe lamp, ≥ 420 nm	CO_2 reduction to CO	CO_2, TEOA, acetonitrile/H_2O (*v*:*v* = 3:2), $[Ru(bpy)_3]Cl_2 \cdot 6H_2O$
19	Co-metal-organic layers@GR	Blue LED, λ = 450 nm	CO_2 reduction to CO	CO_2, TEOA, acetonitrile/H_2O (*v*:*v* = 4:1), $[Ru(phen)_3](PF_6)_2$
20	single Co atoms/GR	300 W Xe lamp, ≥ 420 nm	CO_2 reduction to CO	CO_2, acetonitrile/TEOA/H_2O (*v*:*v*:*v* = 3:1:1), $[Ru(bpy)_3]Cl_2 \cdot 6H_2O$

Nevertheless, the existing GR-based hybrids' photocatalytic performance remains inadequate. Researchers have developed a variety of optimization strategies to achieve preferable photoconversion efficiency, including chemical doping, dimensionality optimization, reducing the defect density of GR, depositing cocatalysts, and optimizing interfacial parameters. These strategies are crucial for the future design and fabrication of high-performance GR-based hybrids. Thus, before talking about the synthesis of GR-based composites oriented by the various roles of GR in photocatalysis, the optimization methodologies of multifunctional GR-based hybrids are briefly described [120].

4.4.4.4 Carbon dots (CDs)

When light is absorbed by CDs, charge carriers can be photogenerated. Additionally, organic molecules, including organic colors, can adsorb onto the highly functionalized surface of the CDs. Because the reaction occurs on the surface of the CDs and less energy is lost as a result of charge recombination (which might happen because of the small band gap that CDs present), this encourages the photocatalytic reaction. It is therefore not surprising that CDs have been used in photocatalytic applications, given their characteristics. The nanoparticles have been employed as spectral converters, electron mediators, photosensitizers, and, lastly, as a single photocatalyst. To date, their primary applications have been in the areas of photocatalytic organic compound degradation, photoreduction, and hydrogen production through water splitting [121].

With a sp2 conjugated amorphous or nanocrystalline core, CDs exhibit a spherical or quasi-spherical shape. Depending on the synthesis, their typical size ranges from 1 to 10 nm (Figure 4.6). Although the surface of CDs may contain oxygenated functional groups (such as -OH, -COOH, and CHO), the majority of the core is made up of sp2 carbon or graphene/graphene oxide sheets joined by sp3 carbon atoms. A number of functional groups, including alcohols, amines, and carboxylic acids, may be present on the surface of CDs. These groups help the CDs become more soluble in water and enable them to go through further functionalization processes by serving as a binding site for other molecules when necessary. This leads to the complex internal and exterior structure of CDs, whose composition is heavily influenced by the precursors and synthetic conditions. This is especially true given that the core type of the CDs can also be modified throughout the synthesis process [121].

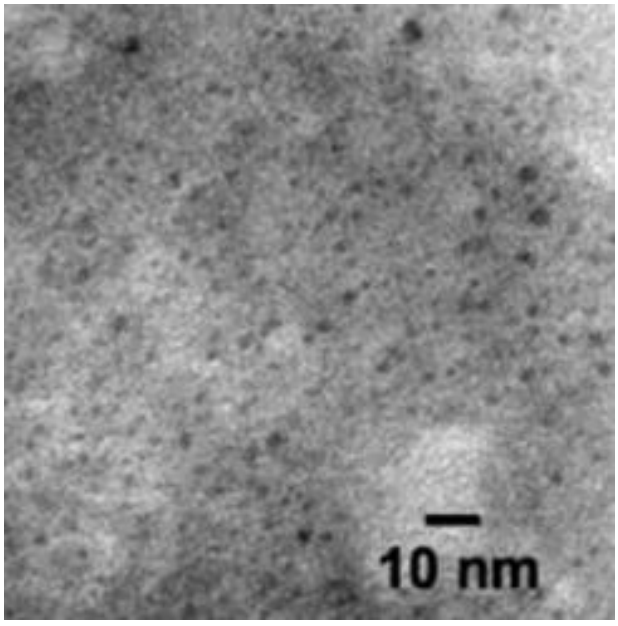

Fig. 4.7 TEM picture of CDs at 10 nm [121].

Top-down and bottom-up techniques are the two categories into which CD synthesis can be separated based on the method selected. Breaking down macroscopic carbon-based materials (such graphite or activated carbon) into smaller nanosized particles, or CDs, is the foundation of top-down synthesis techniques. Techniques including arc discharge, laser ablation, chemical and electrochemical oxidation, and ultrasonic synthesis can be used to accomplish this. The bottom-up method, on the other hand, is predicated on creating CDs from molecular constituents like citric acid. Thermal breakdown, hydrothermal therapy, template-based methods, microwave treatment, and plasma treatment are among methods that can be used for this. CDs can be made in almost any setting without the need for costly and time-consuming processes because of their low cost and relative ease of preparation in some cases [121].

Numerous favorable characteristics of CDs, including high photoluminescence (PL), broadband optical absorption, a large photoresponsive region, excellent chemical and photo-stability, good water solubility, biocompatibility, and low toxicity, are among the factors driving interest in them. Additionally, CDs with up conversion PL (UCPL) can be made. This technology is helpful for photocatalytic nanocomposites because it can transform lower-energy, higher-wavelength radiation into higher-energy, lower-wavelength radiation [121].

4.5 Rare Earth Elements

4.5.1 Atomic Properties

Yttrium (Y), scandium (Sc), and the fifteen metallic elements in the lanthanide series are among the seventeen chemical elements that make up the rare earth elements (REEs), according to the International Union of Pure and Applied Chemistry (IUPAC). The only one of them that is not found in nature is promethium (Pm). Although scandium only demonstrates this similarity in aqueous solutions, yttrium and scandium are both categorized as REEs because of their similar geochemical behavior to lanthanides. While cerium (Ce) can take on a tetravalent state, and europium (Eu) can also occur in a divalent state, these metals are mainly found in a trivalent oxidation state. In general, as more electrons are introduced to the outer shell, atomic radii rise with atomic number. However, a mechanism called lanthanide contraction causes atomic radii to decrease as atomic number increases in REEs. This happens because the electrons in the "f" orbitals are drawn inward, decreasing the atomic radius, because they are unable to adequately protect other electrons from the nucleus' attraction. Because of this special characteristic, REEs can display a variety of chemical reactivities [122].

4.5.2 LREEs and HREES

Light rare earth elements (LREEs) and heavy rare earth elements (HREEs) are the two subgroups into which rare earth elements (REEs) are usually separated (Figure 4.7). Electrons from gadolinium (Gd, atomic number 64) to lutetium (Lu, atomic number 71) and yttrium (Y) are HREEs, whereas elements

from lanthanum (La, atomic number 57) to europium (Eu, atomic number 63) are LREEs. Except for scandium (Sc), which does not fall within either group, these two classes of REEs are typically found in the same mineral formations. In general, there are more LREEs than HREEs in nature [122].

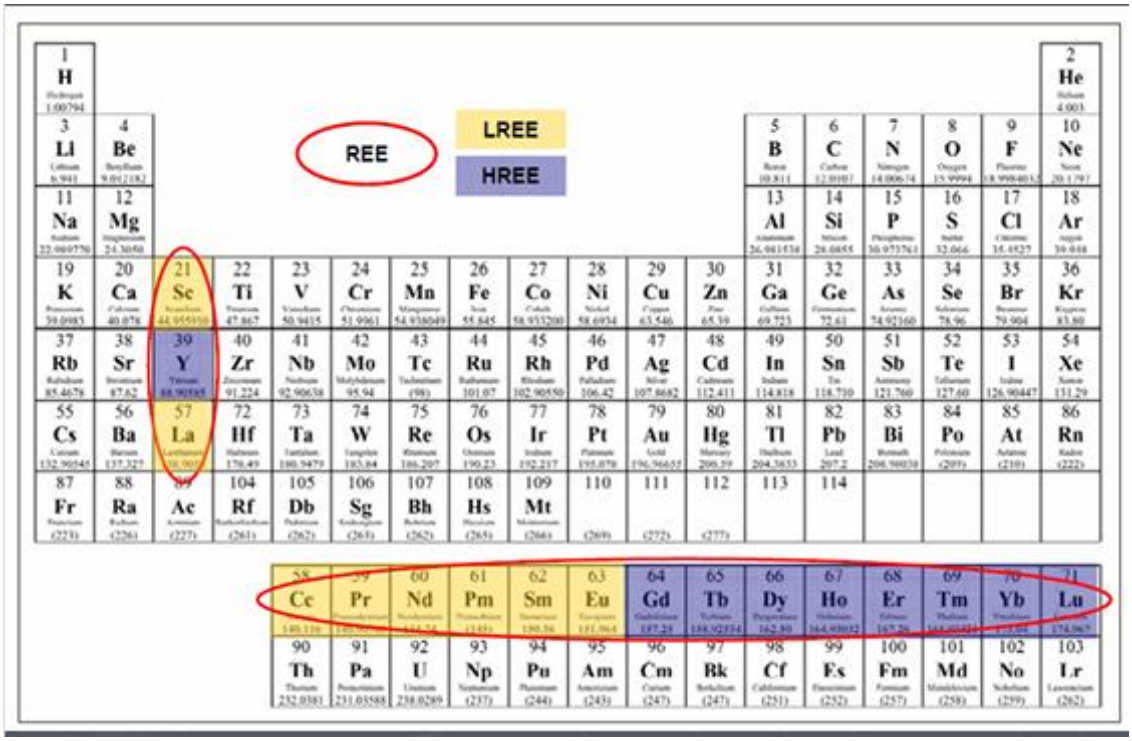

Fig. 4.8 Periodic table of the elements, showing their division into LREEs and HREEs [122].

4.5.3 Global Extraction

4.5.3.1 Introduction

REE deposits and associated resources are comparatively numerous in the earth's crust and were created during geological time in a variety of geographical locations and deposit types. However, they are rarely concentrated on concentrations of mineable ore, in contrast to a number of other deposits. Alkaline/peralkaline igneous systems and carbonatite are commonly linked to economically significant REE deposits. Hydrothermal aqueous fluids can cause the mobilization, transport, and deposition of REE ores in intraplate tectonic settings, which can result in the formation of deposit-scale alteration zones [123].

Carbonatites and alkaline rocks, like the massive Bayan Obo REE deposit in China and possible REE deposits like Bear Lodge, Wyoming in the US, are common hosts for hydrothermal REE-bearing calcite. The other main sources of carbonatite deposits include Araxa in Brazil, Mount Weld in Australia, and Mountain Pass in the United States. A summary of some of the major REE deposits and their locations around the world is given in Table 4.6. Although REE deposits from a variety of other settings are also recognized, the most prolific resources in Europe are carbonatites and alkaline igneous rocks. Long acknowledged as possible REE deposits in India are the Amba Dongar carbonatite complex and a carbonatite REE deposit in Kamthai, Barmer district, Rajasthan [123].

Table 4.6 The global distribution of REE resources [123].

Deposit	*Location*	*Type*	*Main REE*	*REE mineral(s)*
Bayan Obo	China	Carbonatite/hydrothermal	La, Ce, Nd	Bastnasite, parisite, monazite
Mountain Pass	USA	Carbonatite	LREE	Bastnasite
Mount Weld	Australia	Laterite/carbonatite	LREE	Apatite, monazite, synchysite, churchite
Illimaussaq	Denmark	Peralkaline igneous	La, Ce, Nd, HREE	Eudialyte, steenstrupine
Pilanesberg	South Africa	Peralkaline igneous	Ce, La	Eudialyte
Steenkampskraal	South Africa	Vein	La, Ce, Nd	Monazite, apatite
Hoidas Lake	Canada	Vein	La, Ce, Pr, Nd	Apatite, allanite
Thor Lake	Canada	Alkaline igneous	La, Ce, Pr, Nd, HREE	Bastnasite
Strange Lake and Misery Lake	Canada	Alkaline igneous/ hydrothermal	La, Ce, Nd, HREE	Gadolinite, bastnasite
Nolans Bore	Australia	Vein	La, Ce, Nd	Apatite, allanite
Norra Karr	Sweden	Peralkaline igneous	La, Ce, Nd, HREE	Eudialyte
Khibina and Lovenzero	Russia	Peralkaline igneous	LREE+Y, minor HREE	Eudialyte, apatite
Nkwombwa Hill	Zambia	Carbonatite	LREE	Monazite, bastnasite
Kagankunde	Malawi	Carbonatite	LREE	Monazite-Ce, bastnasite-Ce
Tundulu	Malawi	Carbonatite	LREE	Synchesite, parisite, bastnasite
Songwe	Malawi	Carbonatite	LREE, Nd	Synchesite, apatite
Chinese ion adsorption deposits	China	Soils	La, Nd, HREE	Clay minerals
Maoniuping	China	Carbonatite	LREE	Bastnasite
Dong Pao	Vietnam	Carbonatite	LREE	Bastnasite, parisite
Amba Dongar	India	Carbonatite	LREE	Bastnasite
Kamthai, Rajasthan	India	Carbonatite	LREE	Bastanasite-La, bastanasite-Ce, synchysite, carbocernaite, cerianite, ancylite, parisite

Weathering and sedimentary transport are two processes that create secondary deposits like placers and ion adsorption deposits. India has the largest and richest placer deposits of heavy minerals that contain rare earth elements (REEs) along its 7517-kilometer coastline. These resources can be further categorized according to their mineralogy, form of occurrence, and genetic relationships. Different types of REE resources are shown in Figure 4.8 [123].

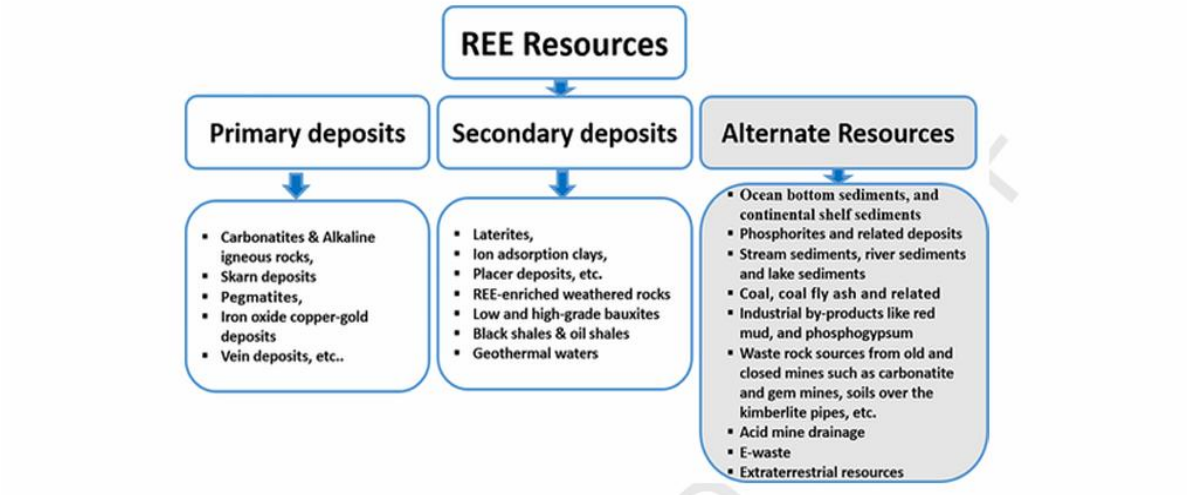

Fig. 4.9 An example of the various kinds of REE resources [123].

4.5.3.2 Primary Deposits

Primary REE deposits are frequently found in vain and skarn deposits, pegmatites, carbonatites, alkaline igneous rocks, and iron oxide copper-gold deposits. The most significant REE resources among these carbonatites are peralkaline silicate rocks with noticeable REE concentrations. For many years, these REE reserves in igneous rocks have been crucial in supplying the industrial need. Furthermore, based on the origin, magma evolution, and rock types that host mineralization, these igneous mineral deposits can be categorized into five different groups: (i) carbonatites; (ii) peralkaline silica undersaturated rocks; (iii) peralkaline granites and pegmatites; (iv) pegmatites associated with sub- to meta-luminous granites; and (v) Fe oxide–phosphate deposits. Globally, skarn deposits of rare earth elements (REEs) are crucial for sustainable economic growth. These elements are abundant in apatite crystals found in Fe oxide–phosphate deposits [124].

4.5.3.3 Secondary Deposits

Laterites, ion adsorption clays, low- and high-grade bauxites, and placer deposits are a few of the significant secondary sources of rare earth elements. More than 95% of the world's HREE requirement is met by ion-adsorption deposits, which are created when primary deposits within weathering crusts are eroded and weathered. Various secondary deposits, ranging in composition from aluminous bauxites to hematite, goethite, and titanium sands, as well as REE, can be formed by intense lateritic weathering of bedrocks in tropical or sub-tropical climates [124].

An important source of essential REE is ionic clays, which are created when REE minerals weather naturally and the released REE ions are adsorbed on the clay surface. The best mining method for these ion-adsorption clay deposits is in situ leaching. REE ions are mostly adsorbed on clay minerals, and weathering of REE-rich granites is the primary cause of ion-adsorption REE deposits. One of the main sources of REE in the world today is regolith-hosted REE deposits from regions with significant REE resources [124].

Around Meizhou City in Guangdong Province, China, there are numerous regolith-hosted REE deposits, with the greatest REE range of 1162 μg/g. It was discovered that the REE concentrations in the regolith-hosted REE deposits in the central Andes coastal region of Chile might reach 2000 μg/g. Allanite, sillimanite, garnet, rutile, zircon, monazite, and ilmenite are among the heavy minerals that are economically concentrated in beach sands, which are the result of weathering, fragmentation, and degradation. Some of these minerals, especially monazite and allanite, are rich in REE. For these precious metals, black shales can also be regarded as a supplementary resource. The Safaga-Qussier section of Egypt's black shales have an average REE enrichment of 255.3–325.3 μg/g. China's black shale region, where the average REE concentration

is about 245 μg/g. Paleoproterozoic black shales from Eastern India's Singhbhum mobile band contain up to 372 μg/g. Prior to considering black shale deposits as an alternate source of REE, more research on black shale formations was conducted globally, in addition to the industry standard of ~300 g/g cut-off grade for mining. Black shales have an average global REE content of 134.19. oil shale samples in Tongchuan City, Southern Ordos Basin, China, showed moderately high amounts of REE (105–195 g/g, with an average concentration of 151 g/g). This necessitates additional research to determine the REEpotential of these rocks. The aforementioned value is much lower than the 1000 g/g (ash base) cut-off grade for REE deposits hosted by coal. In actuality, determining the cut-off value for the economic recovery of REE depends on the sizes of various deposits, the total REE concentrations, and the specific REE compositions [124].

Important supplies of precious metals and minerals may be found in geothermal fluids. Geothermal waters have an approximate total REE concentration of 0.17 ng/mL. Discovered that a high temperature (T >60 C) promoted the release of the more readily soluble REE from rocks into the water in the mineral and thermal waters of the Polish Lowlands. Geothermal water in the Ganzi–Litang fault region of western Sichuan, China, with total REE concentrations between 0.059 and 0.547 ng/mL. The lithology of the reservoir is linked to the REE levels in geothermal waters, which are greatly impacted by pH, HCO3, Na+, and Mn minerals. Even though there is not much REE in geothermal waters, if you consider how common geothermal waters are in locations like Iceland, this source can be one of the more promising ones for REE if you have an effective extraction method. Since geothermal brine can be a financially viable mineral resource, considerable efforts have recently been undertaken to develop technology for the extraction of rare earth elements (REE) from geothermal brine. Right now, it only appears to be possible to extract REE from geothermal brine when combined with other byproducts like silica and lithium [124].

4.5.3.4 Alternative Deposits

Global demand and requirements cannot currently be met by the primary and secondary REE resources that have been identified. Over the past ten years, there has been a lot of interest in finding and creating alternate resources for REE. In order to satisfy the expanding demand globally, numerous research are conducted to identify possible alternative resources. Strong analytical methods are being used to comprehend the potential of different alternative REE resources in the future. These methods include inductively coupled plasma mass spectrometry (ICP-MS), inductively coupled plasma optical emission spectrometry (ICP-AES), scanning electron microscopy with energy dispersive X-ray spectroscopy (SEM-EDX), X-ray fluorescence spectrometry (XRF), X-ray diffractometry (XRD), and integrated mineral analysis (IMA) [124].

Continental shelf sediments and ocean bottom deposits are among the most promising of these resources. Extensive sedimentary basins formed through continental rifting provide favorable

environments for REE accumulation. These rifting processes enhance subsidence and reduce basal heat flow, thereby expanding the depth of hydrothermal circulation and promoting the formation of massive deposits of elements such as copper, lead, zinc, nickel, and REE [124].

Phosphorites and their associated formations also represent major potential reservoirs. Phosphate ores are generally classified according to their origin as either sedimentary or igneous. Approximately 80% of global phosphate ores are of marine sedimentary origin, around 17% are linked to volcanic activity, and the remaining fraction occurs in residual sedimentary or guano-type deposits [124].

Fluvial, lacustrine, and stream sediments offer another important source of REE enrichment. Through the physical and chemical weathering of REE-bearing source rocks, erosion and transport processes enable the continuous accumulation of these elements in downstream deposits. For example, sediments of the Yellow River exhibit a progressive increase in REE concentration from upstream regions to the estuary and adjacent bay [124].

Coal and its combustion by-products, such as fly ash and bottom ash, have also gained recognition as promising alternative resources. Coal is a highly complex geological material containing approximately 200 minerals and about 73 elements, including REE, which occur in multiple forms—ranging from inorganic and organic associations to intimately bound phases. Key mineral hosts include carbonate, silico-phosphate, crandallite-group minerals, and apatite. A detailed understanding of these modes of occurrence is essential for efficient recovery [124].

Industrial by-products such as low-grade bauxite, red mud, phosphogypsum, gem mining residues, and metallurgical slags further expand the range of potential REE sources. Both low-grade and high-grade bauxites—particularly those located in the basal sections of karst-type deposits—are regarded as significant prospective resources, as demonstrated by numerous studies of Mediterranean bauxite formations [124].

Finally, waste rock and tailings from closed and abandoned mines represent an attractive secondary source of REE. Mining operations worldwide generate more than 100 billion tons of solid waste annually, and these materials offer considerable potential because they have already been extracted and partially processed, reducing the costs associated with accessing and concentrating the elements [124].

4.5.4 The geopolitical significance of critical rare earth resources

Variations in rare earth prices (REP) significantly influence the global economy and national strategies. Rare earth reserves and their extraction are distributed very unevenly, primarily concentrated in a limited number of countries like China, Vietnam, Myanmar, and Brazil. As per the U.S. Geological Survey in 2021, China's rare earth mine output reached 140,000 tons in 2020, representing over half of the worldwide total production. China has emerged as the leading

producer, consumer, and exporter of rare earth elements globally. Consequently, rare earth is distinct from other conventional commodities and resources due to its extensive applications and limited availability, enhancing its geopolitical significance, implying that rare earth is regarded as a negotiating tool in political agreements [125].

Because there is no standardized global market for trading REEs and because China has reportedly used—or could use—these materials as a diplomatic instrument, some political analysts consider its near-monopoly a potential risk to regional security [126]. Geopolitical risk (GPR) is commonly applied to energy and resource dynamics. GPR assesses the probability of wars, terrorist activities, and geopolitical tensions using information from 11 leading global newspapers. Elevated GPR can trigger panic among countries, resulting in increased demand for rare earth elements due to their extensive applications in energy and defense security. The rise in demand leads to a surge in the REP. For example, a price increase took place in the REP when the export of rare earths to Japan was postponed due to a territorial conflict in September 2010 [125]. Figure 4.9 shows the diagrammatic change from 2012 until 2022 between rare earth price, geopolitical risk and global economic activities.

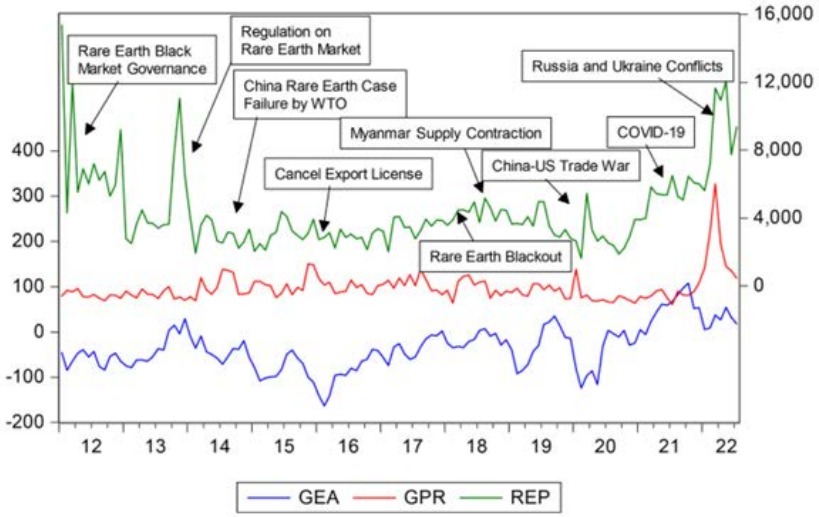

Fig 4.10 The patterns of REP, GPR, and GEA.REP refers to the right axis; GPR and GEA refer to the left axis [125].

Rare earth elements (REEs) drew significant attention in 2011 following a diplomatic dispute between China and Japan. When China opted to limit REE exports, prices skyrocketed to record levels. In the 1990s, Deng Xiaoping, who was China's leader at that time, notably stated, "The Middle East has oil; China possesses rare earth," emphasizing China's perception of REEs as critical strategic assets. Prior to China's ascendance, the United States was at the forefront of REE production and distribution but ultimately relinquished its top status, probably because of regulations regarding the management of radioactive substances. Following the withdrawal of Western industries in the 1980s, China dedicated many years to exploring and developing untapped regions, resulting in the establishment of the largest REE mine globally in the northern part of the country [126].

Our focus is on China and Japan because Japan ranks among the world's top importers of rare earth elements (REEs), while China is one of the leading exporters. Data from the Japan Oil Gas and Metals National Corporation (JOGMEC) shows that in 2017, China exported a total of 51,190 gross metric tons of rare earth metals and REE compounds. During the same year, Japan imported 12,461 metric tons (based on metal content) of these rare earth metals and compounds from China [126].

However, others believe that China's 2011 REE export restrictions were mainly driven by domestic priorities, such as conserving resources, protecting the environment, and fostering high-tech and downstream industries. Since expanding REE production, whether mining or refining, is difficult, expensive, and often environmentally damaging, the factors influencing REE imports and exports are closely watched by many industries around the world [126].

Rare earth elements serve as a crucial resource, extensively utilized in contemporary economic endeavors. The sectors that utilize rare earths create new energy vehicles, permanent magnet motors, and equipment for wind power production. Thus, REP assesses the extent of renewable energy usage. Specifically, REP alterations adversely impact the stock market performance of renewable energy indices. Consequently, the matter of REP is crucial for the government, investors, and companies related to resources to evaluate risk and devise appropriate policies and initiatives [125].

The rapid expansion in the REP has been observed, with geopolitical events happening regularly, including the U.S. election, Brexit, and the U.S.–China trade conflict. Moreover, the increase in the REP during the Russia-Ukraine conflict offered further compelling proof. Consequently, we can deduce that REP will rise during significant geopolitical events [125].

The continuous trade embargo between China and the U.S. places extra pressure on the renewable energy industry and rare earth sector. Significantly, the COVID-19 pandemic has heightened this concern as businesses are eager to diversify their supply chains beyond China. In particular, the pandemic has seldom influenced the upstream sector of rare earth, as the effect of the outbreak in the production areas is relatively limited. Nonetheless, the requests for downstream manufacturing of rare earth elements experience significant disruption during an epidemic, impacting sectors like new energy vehicles and the energy-efficient appliance industry, resulting in adverse feedback on the REP. For example, a reduction in Chinese automobile manufacturing during the first half of 2022 contributed to falling prices. From January to June, vehicle production fell by 2.1% year-over-year, as government data revealed, attributed to supply chain issues stemming from COVID-19 lockdowns in Shanghai. Additionally, consumer demand was declining because of the economic downturn caused by the pandemic. Consequently, the economic cycle appears to influence rare earth demand and price variability [125].

4.5.5 The recycling of rare earth elements

Recycling and reusing metals are essential in an economy that uses few resources. Products with rare earth elements (REEs) nearing the end of their life cycle should ideally be preprocessed to produce recycled materials high in REEs. These materials can then be processed further to produce rare earth compounds, making it easier to reuse them in later production cycles. Disassembly, physical separation, and size reduction are all parts of preprocessing. Due to differences in element type, metal content, and composition, choosing the right technique can be difficult when recovering metals and other REEs from electronic trash. It is essential to reduce pollution while increasing the recovery process's technical efficiency using a material-centered approach. Nevertheless, there are disadvantages to the preprocessing processes used today, such as the loss of important components like shredding dust. Thus, it is essential to optimize the pre-treatment phase to stop the loss of REEs during recovery. Energy recovery and the elimination of hazardous components also require the integration of pre-treatment procedures with chemical and other physical techniques [127].

When materials containing rare earth elements (REEs) are no longer economically viable for industrial use, they are considered waste and become secondary RE resources, such as electronic waste (e-waste), mine tailings, red mud, and phosphogypsum. Extracting REEs from these secondary resources presents a promising solution to address challenges linked to RE mining and processing, such as the removal of radioactive substances, energy demands, and resource availability. Recycling can be classified into two types: closed-loop and open-loop. In closed-loop recycling, the recovered RE alloys are reused for similar purposes, though it faces challenges in terms of collection, sorting, separation of components, and processing. In open-loop recycling, the recovered REEs from RE alloys are repurposed for different applications [122].

There are many obstacles to developing scalable and long-lasting benefits in circular economic business models (CEBMs). Closed-loop manufacturing, material reuse, extending product life, and developing creative recycling methods to extract materials' intrinsic value are the main focuses of CEBMs. Upcycling and downcycling are two types of closed-loop cycles. Materials that have reached the end of their useful lives are recycled to create higher-value products in up-cycling and lower-value products in down-cycling. Closed-loop cycles serve as the foundation for recycling models, which provide chances to maximize inputs, cultivate effective components, and understand the dynamic effects of changing CEBMs. Upcycling makes a substantial contribution to the sociotechnical system's sustainability [127].

Notwithstanding the difficulties, some rare materials have significant potential for recycling and provide financial advantages. However, there are still many environmental issues associated with the costly and complex extraction and separation of REEs. The mining and beneficiation of REEs raise significant environmental concerns, especially given their frequent correlation with

uranium and thorium. To stop radioactive elements from spreading into the environment, strict control procedures are necessary. The evaluation of REE recycling's efficacy and potential, as well as secondary sources and production waste, will continue to be a priority, requiring ongoing research for various REEs in various circumstances. This ongoing focus is essential for assessing REEs' total environmental impact and their role in promoting "clean energy" [127].

By 2040, the demand for rare-earth elements (REEs) is expected to increase by up to seven times. Recycling has difficulties gathering and disassembling items that include rare earth elements (REEs), but it can avoid many of the difficulties associated with starting new mining operations. Both challenges and benefits result from the significant differences in the amounts and proportions of rare earth elements (REEs) and related compounds found in recycled sources compared to natural ores. The "REE balancing problem" that is widespread in natural deposits is avoided since produced goods only contain the precise REEs required, even though REE concentrations in trash are often low. As opposed to processing the complete lanthanide group, this implies that fewer REEs need to be separated. Furthermore, recovering common metals like copper, tin, and zinc or expensive metals like gold, silver, and platinum from electronic waste can help offset the costs of recycling [128].

The United States Geological Survey (USGS) estimated that 240,000 tonnes of rare earth elements (REEs) were produced globally in 2020. Permanent magnets, which account for around 80% of the total economic value of REEs, are made from about 25% of this quantity, mostly neodymium, praseodymium, dysprosium, and terbium. By 2025, there will be 6.9 million electric cars (EVs) in the U.S. alone, up from 1.4 million in 2020. This demand could represent about 10% of the global REE supply utilized in magnet manufacture, since an average EV motor or generator needs 2 to 5 kg of magnets, with about 1 kg of REEs included [128].

Neodymium (Nd) and other rare earth elements (REEs) are predicted to be in high demand worldwide, meaning that recycling will be crucial to supplying these vital metals in addition to increased primary production. Currently, relatively little REEs are recycled from industrial waste or end-of-life consumer products, primarily due to the fact that it is not profitable. Ineffective or nonexistent collecting infrastructure, the high cost of disassembling products to extract the elements, and the lack of reasonably priced recovery methods for recycling materials are some of the obstacles to recycling. Furthermore, the concentrations of REEs in many possible recycling sources are quite low, and the amounts that are accessible are frequently insufficient to warrant the expenditure of money on recycling infrastructure [128].

However, due to the anticipated gap between supply and demand, incentives for recycling rare earth elements (REE) are expected to grow. Consequently, significant efforts have recently focused on developing new methods specifically designed to recover REEs from end-of-life (EOL) products or secondary sources. The most promising materials for recovery are those that can yield substantial

amounts of critical rare earths because of their high concentration, large quantity, or ideally both, along with cost-efficient collection and pre-processing. Examples of such materials include permanent magnets from hard disk drives (HDDs), actuators like the low-profile speakers found in TVs and mobile devices, and compact motors or generators, such as traction motors used in electric and hybrid vehicles. Additionally, industrial waste—such as machining debris (swarfs), manufacturing breakages of magnets, and large quantities of spent catalysts—also represent potential sources for recovery [128].

Mineral acids are most commonly used to extract rare earth elements (REEs) into the aqueous phase. Using acids including sulfuric, hydrochloric, and nitric acid, numerous research has shown how REEs may be leached from sources such as permanent magnets, fluorescent phosphors, catalysts, and different REE-containing wastes. In order to make the recovery of rare earth elements (REEs) commercially viable, the researchers began with mixed scrap materials and combined the recovery of REEs from the ferromagnetic section with the processing of the non-magnetic fraction to extract both base and precious metals. A novel electrochemical technique that included an extraction column for effective separation was used to recover base metals like copper, tin, zinc, and lead in a selective manner. The residues from electrochemical leaching were subsequently used to recover precious metals, such as palladium, gold, and silver. Because it used less electricity and chemical input than conventional pyrometallurgical and hydrometallurgical processes, this approach not only recovered a larger percentage of the total metals but also performed better environmentally. Biologically generated leaching agents have been proposed by some scientists as an alternative to mineral acids. This method lowers the costs associated with high energy consumption, reagents, and capital investment while also reducing many of the environmental problems associated with the corrosive chemicals commonly utilized in conventional hydrometallurgy [128].

4.5.6 Future Visions

Mineral resources are crucial to the development of sustainable energy technologies, as many of them are intrinsically dependent on rare earth elements (REEs), copper, lithium, nickel, cobalt, and other essential minerals. Because of their special optical and electromagnetic characteristics, REEs are essential for clean energy technologies such as heat pumps, solar panels, wind turbines, electric car batteries, and hydrogen electrolyzers. [129].

The demand for rare earth elements (REE) has increased significantly from 75,500 tonnes (t) of REO in 2000 to 123,100 (t) REO in 2016. This is because the uses of REE have evolved from rare earth metal used in lighter flints to high purity separated rare earth metals used in advanced electronics, lighting, power generation, and military applications [130].

As the different applications have varied, the types of REE products used have also changed. The use of elements like Eu, terbium (Tb), and more recently, Lu, in lighting, the use of La in

specialty glass goods, and the creation of REE permanent magnet alloys have all historically demonstrated this, as has the rise in the usage of Sm, Nd, and dysprosium (Dy) [130].

The U.S. Department of Energy prioritizes REEs in its domestic supply chain when developing energy transition policies, the European Union established the European Raw Materials Alliance, and Australia classified the REEs market as a critical mineral market and created the "2023–2030 Critical Minerals Strategy" to support the industry's expansion. According to the European Commission, key raw materials are those for which, in comparison to the majority of other raw materials, there is a substantial risk of supply disruption and its associated economic impact. According to Japan, key minerals are those that have significant industrial demand, both now and in the future, driven by technological advancements, but are challenging to mine economically or technically [129].

Dysprosium, terbium, praseodymium, and neodymium are critical REEs, according to lists of critical materials from different nations and the great importance of REEs to clean energy technology. They are vital to the manufacturing of permanent magnet generators, which are necessary for renewable energy technologies to be efficient and competitive in the market. There will be a situation where supply cannot keep up with demand for essential rare earth elements (REEs), which is necessary for the development of sustainable energy technology [129].

The rise of hybrid electric vehicles (HEVs) and full electric vehicles (EVs) is predicted to be the most disruptive technology for the consumption of REE over the next ten years. This is expected to result in significant changes to the types and quantities of raw materials that the automotive industry consumes. Due to the development of HEV and EV models by almost all of the major automakers, production of these vehicles is expected to rise from 2.3 million units in 2016 to over 10.1 million units in 2026. Compared to HEV models, EV models have significantly lower operating expenses throughout the course of their lifetimes, and they are expected to expand at the fastest rates until 2026. The demand for neodymium-iron-boron (NdFeB) magnets is expected to rise sharply as a result of this production expansion [130].

The demand for neodymium, dysprosium, and praseodymium in China's electric vehicle market in 2030 is expected to be 3.90 to 15.90 thousand tons, 1.60 to 6.30 thousand tons, and 0.70 to 3.00 thousand tons, respectively, under pessimistic, natural, and optimistic scenarios. Under a quick development scenario, the overall demand for praseodymium and neodymium in China's wind power sector will reach 37.00 thousand tons in 2040, excluding technical advancements. The combined demand for terbium in wind power and electric vehicle development in 2030 will be 0.52,000 tons under a net-zero emissions scenario in 2050 [129].

In 2022, China produced 210,000 tons of rare earth elements, which accounted for 70% of global production. The country produced 6.10 thousand tons of dysprosium, 1.10 thousand

kilograms of terbium, 8.90 thousand tons of praseodymium, and 30.20 thousand tons of neodymium. The demand for neodymium and dysprosium in China's electric vehicle market in 2030, under the most pessimistic scenario, has already surpassed the present level of domestic extraction if the future supply capacity of essential REEs is calculated based on China's current output. Similarly, under the rapid development scenario for 2040, the demand for praseodymium and neodymium in China's wind power sector surpasses the amount of domestic extraction. A more severe scenario of supply not meeting demand will arise in the future with regard to the supply of REEs for the worldwide wind power and electric car market [129].

4.5.7 REE Challenges

There are numerous potential applications in digital and green technologies, and the recent increase in the search for rare earth element (REE) deposits presents a number of technological, financial, and geopolitical difficulties [130].

Better knowledge of the mineralogy of REE deposits and related research to develop effective and environmentally acceptable processing techniques may be the more pressing challenge, particularly for those minerals and deposit types that have never been mined before. Throughout the 1980s, 1990s, and 2000s, very little research on REE ore processing was conducted outside of China. Since then, a lot of effort has been made, including updating reference works and publishing several reviews [130].

Every new project requires thorough mineralogy, customized processing flow sheets, and geometallurgy studies since, even for carbonatites that are presently mined, the mineralogy of the REE differs from carbonatite to carbonatite. Processing deposits linked to alkaline igneous rocks is extremely difficult due to mineralogy’s complexity. Although the granitic and syenitic magmatic-hydrothermal deposits, like Strange Lake, would be able to yield sizable amounts of Nd and Dy without having an excess of La and Ce, their complicated mineralogy actually makes them much less desirable for REE beneficiation. The REE may be found in a very broad variety of minerals in these rock types, such as fergusonite, zircon, apatite, and allanite, for which there is currently no known processing pathway; research into the creation of processing techniques is still in its infancy. Processing techniques for ion adsorption deposits are rather straightforward and include either heap leaching or in situ leaching of the clays using a chemical cation exchange agent, usually ammonium sulfate. The problem is that no commercial processing has been carried out outside of China, where the usage of ammonium sulfate and ground clearance have seriously harmed the environment [130].

An appealing method of quickly bringing new supplies online, possibly even switch-on, switch-off supplies that could respond swiftly to demand fluctuations—is the extraction of rare

earth elements (REE) as byproducts from already-existing mines. Getting the primary commodity's miners to change their processing pathways in order to create REE appears to be the difficult part of this situation. The extra money is frequently insufficient to promote the recovery of rare earth elements (REE) from waste products or to force modifications to long-standing procedures. It is necessary to have both creative business models and innovative procedures. Globally, placers are mined for elements like zirconium and titanium, and occasionally, REE may be a byproduct. However, several nations currently avoid this because of radiation concerns [130].

It is difficult for all mining operations to obtain the required permits, including the less obvious social license to operate, but it is especially difficult for REE producers if their ores contain naturally occurring radioactive minerals and will generate radioactive waste. The typical mining issues of water use, waste and wastewater management, dust, noise, excessive traffic, and social considerations are among the other environmental issues. Although they could be harmful in extremely high concentrations, the REEs themselves are not thought to be poisonous; nothing is known about how harmful the individual elements are. Although responsible sourcing is not currently a significant concern in the manufacturing of REEs, the necessary social and environmental requirements are only going to rise [130].

Lastly, the cost of mining, processing minerals, dissolving, and separating the rare earth elements (REE) to create particular rare earth metals are usually included in the major capital expenditure estimates. Since there is hardly any supply chain to sell into outside of China, it is challenging to establish a lower cost development to make an ore concentrate or intermediate product. With the exception of China, very few processors will take a mixed REE product and perform toll separation. In a situation where REE prices are low, building a supply chain will be difficult if no government is willing to adopt an interventionist approach. The ability to create domestic high-tech markets without having to pay exorbitant rates for REE raw materials from China is another reason why REE is important, in addition to the modest amounts used in military applications. The development of the complete value chain, from mining through processing and separation to end uses, is the main obstacle to the supply of REEs outside of China [130].

Chapter 5

Conclusions

The present work has provided a comprehensive exploration of catalytic and photocatalytic processes, with a particular emphasis on their applications in energy conversion, storage, and hydrogen production. By examining the fundamental principles of catalysis and the design of advanced catalytic devices, the basis and practical applications of photocatalysis, as well as the specific role of photocatalytic water splitting for hydrogen production, this study highlights the central role of materials science in addressing urgent global energy challenges. Furthermore, the investigation into the use of rare earth elements within photocatalytic systems underscores the delicate balance between scientific innovation, material availability, and environmental responsibility.

Catalysis lies at the heart of modern chemical and energy industries. As discussed in Chapter 2, catalysts not only enhance the efficiency of chemical reactions but also enable processes that would otherwise be energetically or kinetically unfavorable. The development of catalytic devices for energy conversion and storage represents one of the most critical technological frontiers, bridging chemistry, materials science, and engineering. Devices such as fuel cells, batteries, and supercapacitors increasingly rely on advanced catalytic materials to improve energy efficiency, durability, and cost-effectiveness.

The findings of this chapter demonstrate that significant progress has been achieved in tailoring catalytic surfaces, nanostructures, and hybrid materials to improve reaction selectivity and conversion rates. Importantly, the intersection between catalysis and renewable energy systems shows that these advances are not merely incremental but transformative, offering pathways toward a low-carbon economy. However, despite notable achievements, challenges remain in terms of scalability, cost reduction, and long-term stability, especially when considering real-world deployment.

Chapter 3 provided an overview of photocatalysis, a field that merges photochemistry with catalysis to utilize light—particularly solar radiation—as a sustainable energy input. The fundamental principles of photocatalysis, including photon absorption, electron-hole generation, and charge transfer processes, were carefully examined. These mechanisms serve as the foundation for a wide

variety of applications, from environmental remediation (such as pollutant degradation and wastewater treatment) to renewable energy conversion.

The versatility of photocatalysis lies in its capacity to harness a clean and abundant energy source—sunlight—while directly driving chemical transformations. Advances in semiconductor design, heterojunction engineering, and surface modification have expanded the operational efficiency of photocatalysts, making them increasingly viable for practical use. The reviewed applications underscore that photocatalysis is not only a promising research field but also a strategic technology for sustainable development. Nevertheless, the intrinsic limitations of photocatalytic processes, such as low quantum efficiency, rapid recombination of charge carriers, and limited spectral response, highlight the importance of continued material innovation.

The final substantive chapter addressed one of the most urgent applications of photocatalysis: hydrogen production through water splitting. As emphasized in Chapter 4, hydrogen is widely recognized as a clean energy carrier, with the potential to decarbonize sectors ranging from industry to transportation. Photocatalytic water splitting represents a direct and elegant approach to generating hydrogen, using only water and solar energy. This reaction epitomizes the broader goals of renewable energy research—transforming inexhaustible resources into clean fuels with minimal environmental impact.

The performance of photocatalysts for water splitting is strongly influenced by the choice of materials. Traditional semiconductors such as TiO_2 have been extensively studied, yet their limitations in visible light absorption necessitate the development of novel materials. Here, rare earth elements (REEs) have proven valuable. Their unique electronic structures, optical properties, and capacity to modify band gaps render them critical in designing efficient photocatalysts. Rare earth-doped materials have demonstrated enhanced light absorption, improved charge separation, and greater photocatalytic stability.

At the same time, reliance on rare earth elements introduces a new dimension of complexity. While REEs offer remarkable advantages in photocatalysis, their extraction and supply are associated with geopolitical, environmental, and economic challenges. This duality underlines the importance of developing recycling strategies, exploring alternative materials, and optimizing REE utilization to ensure that their deployment in photocatalysis remains sustainable.

Taken together, the chapters demonstrate a clear narrative: catalysis and photocatalysis are indispensable pillars of the transition toward sustainable energy systems. Catalytic devices support efficient energy conversion and storage; photocatalysis extends the frontiers of renewable energy utilization; and photocatalytic water splitting offers a direct pathway to a hydrogen economy. Across these domains, the strategic incorporation of rare earth elements enhances material performance but also necessitates careful resource management.

Looking forward, several perspectives emerge:

1. Material Innovation: The continued discovery and design of novel catalytic and photocatalytic materials will remain essential. This includes not only rare earth-based systems but also earth-abundant alternatives, nanostructured composites, and advanced heterostructures.
2. Integration into Devices: Laboratory-scale demonstrations must evolve into scalable, robust, and economically viable devices. Bridging the gap between fundamental science and industrial application will require multidisciplinary collaboration.
3. Sustainability Considerations: Energy technologies cannot be evaluated solely on efficiency metrics. Environmental impacts, resource availability, and lifecycle sustainability must be integral to future developments, particularly concerning rare earth elements.
4. Hydrogen Economy: Photocatalytic hydrogen production remains one of the most ambitious yet promising research directions. Overcoming efficiency bottlenecks, ensuring material stability, and integrating hydrogen generation with storage and distribution networks will be critical to realizing its potential.
5. Policy and Collaboration: Finally, the advancement of these technologies is not purely a scientific challenge but also a societal one. International cooperation, supportive policies, and investment in research infrastructure will be necessary to accelerate progress and ensure equitable access to clean energy innovations.

In conclusion, this work affirms that catalysis and photocatalysis represent key enabling technologies for the sustainable energy transition. By coupling fundamental insights with innovative material design and practical applications, these fields can contribute significantly to addressing the pressing global challenges of climate change, resource scarcity, and environmental degradation. The promise of hydrogen production through photocatalysis exemplifies the transformative potential of this research, offering a vision of a clean, renewable, and resilient energy future. At the same time, the consideration of rare earth elements highlights that technological progress must be accompanied by responsible stewardship of natural resources.

Thus, the findings presented here not only reinforce the scientific and technological significance of catalysis and photocatalysis but also call for a holistic approach—one that unites innovation, sustainability, and international collaboration in the pursuit of a greener world.

REFRENCES

1. J. Kim, F. Jaumotte, A. J. Panton, G. Schwerhoff. Energy security and the green transition. Energy Policy 198,114409, **2025**.
2. S. R. Golroudbary, I. Makarava, A. Kraslawski, E. Repo. Global environmental cost of using rare earth elements in green energy technologies. Science of the Total Environment 832,155022,**2022**.
3. E. Roduner. Understanding catalysis. Chem. Soc. Rev. 43, 8226-8239,**2014**.
4. Polshettiwar V., & Asefa T. (Eds.). (2013). NANOCATALYSIS Synthesis and Applications. John Wiley & Sons. https://onlinelibrary.wiley.com/doi/pdf/10.1002/9781118609811
5. P. Munnik, P. E. de Jongh, K. P. de Jong. Recent Developments in the Synthesis of Supported Catalysts. Chem.Rev 115, 6687−6718, **2015**.
6. F. Hess, B. M. Smarsly, H.Over. Catalytic Stability Studies Employing Dedicated Model Catalysts. Accounts of Chemical Research 53,380-389, **2020**.
7. C. Vogt, B. M. Weckhuysen. The concept of active sites in heterogeneous catalysis. Nature Reviews Chemistry 6, 89-111, **2022**.
8. C. Wang, Z. Wang, S. Mao, Z. Chen, Y. Wang. Coordination environment of active sites and their effect on catalytic performance of heterogeneous catalysts. Chinese Journal of Catalysis 43, 928–955 , **2022**.
9. M.J. Ndolomingo, N. Bingwa, R. Meijboom. Review of supported metal nanoparticles: synthesis methodologies, advantages and application as catalysts. Journal of Materials Science 55, 6195–6241, **2020**.
10. H. Chen, X. Liang, Y. Liu, X. Ai, T. Asefa, X. Zou. Active Site Engineering in Porous Electrocatalysts. Advanced Materials 32(44), 2002435, **2020**.
11. B. Cornils, W. A. Herrmann. Concepts in homogeneous catalysis: the industrial view. Journal of Catalysis 216,23–31, **2003**.
12. D.J. Cole-Hamilton, R.P. Tooze (Eds.).(2006). Catalyst Separation, Recovery and Recycling. Springer. 10.1007/1-4020-4087-3
13. W.A. Herrmann, B. Cornils. Organometallic Homogeneous Catalysis-Quo vadis? Chem. Int. Engl. 36, 1048-1067, **1997**.
14. V.L. Arcus, A.J. Mulholland. Temperature, Dynamics, and Enzyme-Catalyzed Reaction Rates. Annu. Rev. Biophys 49,163–80, **2020**.
15. S. J. Benkovic, S. Hammes-Schiffer. A Perspective on Enzyme Catalysis. Science 301, **2003**.
16. S. Wu, R. Snajdrova, J.C. Moore, K. Baldenius, U.T. Bornscheuer. Biocatalysis: Enzymatic Synthesis for Industrial Applications. Chem. Int. 60, 88–119, **2021**.
17. J. C. Slater. BAND THEORY. Chem. Solids Pergamon 8, 21-25, **1959**.

18. M. Zhang, K. Zhang, X. Ai, X. Liang, Q. Zhang, H. Chen, X. Zou. Theory-guided electrocatalyst engineering: From mechanism analysis to structural design. Chinese Journal of Catalysis 43, 2987–3018,**2022**.
19. M.R. Tarasevich, O.V. Korchagin. Electrocatalysis and pH (a Review). Russian Journal of Electrochemistry 49, No. 7, 600–618, **2013**.
20. L. Yuan, X. Sui, C. Liu, Y. Zhuo, Q. Li, H. Pan, Z. Wang. Electrocatalysis Mechanism and Structure–Activity Relationship of Atomically Dispersed Metal-Nitrogen Carbon Catalysts for Electrocatalytic Reactions. Small Methods, 7, 2201524,**2023**.
21. D. Medvedev, V. Maragou, E. Pikalova, A. Demin, P. Tsiakaras. Novel composite solid state electrolytes on the base of $BaCeO_3$ and CeO_2 for intermediate temperature electrochemical devices. Journal of power sources 221,217-227,**2013**.
22. A.M. Bagher, M.M.A. Vahid, M. Mohsen. Types of Solar Cells and Application. American Journal of Optics and Photonics 3 (5), 94-113, **2015**.
23. S. Wang, S.P. Jiang. Prospects of fuel cell technologies. National Science Review 4, 161–163, **2017**.
24. R. Wu, P. Tsiakaras, P.K. Shen. Facile synthesis of bimetallic Pt-Pd symmetry-broken concave nanocubes and their enhanced activity toward oxygen reduction reaction. Applied Catalysis B: Environmental 251, 49-56, **2019.**
25. S.L. Douvartzides, F.A. Coutelieris, P.E. Tsiakaras. On the systematic optimization of ethanol fed SOFC-based electricity generating systems in terms of energy and exergy. Journal of Power Sources 114 (2), 203-212, **2003**.
26. E. Gorbova, V. Maragou, D. Medvedev, A. Demin, P. Tsiakaras. Influence of sintering additives of transition metals on the properties of gadolinium-doped barium cerate. Solid State Ionics 179 (21-26), 887-890, **2008**.
27. D. Liu, A. Barbar, T. Najam, M.S. Javed, J. Shen, P. Tsiakaras, X. Cai. Single noble metal atoms doped 2D materials for catalysis. Applied Catalysis B: Environmental 297, 120389, **2021**.
28. C. Molochas, P. Tsiakaras. Carbon Monoxide Tolerant Pt-Based Electrocatalysts for H2-PEMFC Applications: Current Progress and Challenges. Catalysts 11 (9), 1127, **2021**.
29. J. Lyagaeva, G. Vdovin, L. Hakimova, D. Medvedev, A. Demin, P. Tsiakaras. BaCe0. 5Zr0. 3Y0. 2–xYbxO3–δ proton-conducting electrolytes for intermediate-temperature solid oxide fuel cells. Electrochimica Acta 251, 554-561, **2017**.
30. Y. Liu, B. Huang, X. Chen, Z. Tian, X. Zhang, P. Tsiakaras, P.K. Shen. Electrocatalytic production of ammonia: biomimetic electrode–electrolyte design for efficient electrocatalytic nitrogen fixation under ambient conditions. Applied Catalysis B: Environmental 271, 118919**, 2020**.

31. C.G. Vayenas, S. Bebelis, I.V. Yentekakis, P. Tsiakaras, H. Karasali. Non-faradaic electrochemical modification of catalytic activity reversible promotion of platinum metals catalysts. Platinum Metals Rev 34 (3), 122, **1990**.
32. Y. Wang, C. He, A. Brouzgou, Y. Liang, R. Fu, D. Wu, P. Tsiakaras, S. Song. A facile soft-template synthesis of ordered mesoporous carbon/tungsten carbide composites with high surface area for methanol electrooxidation. Journal of power sources 200, 8-13, **2012**.
33. A. Brouzgou, S. Song, P. Tsiakaras. Carbon-supported PdSn and Pd_3Sn_2 anodes for glucose electrooxidation in alkaline media. Applied Catalysis B: Environmental 158, 209-216, **2014**.
34. K. Wang, Y. Wang, Z. Liang, Y. Liang, D. Wu, S. Song, P. Tsiakaras. Ordered mesoporous tungsten carbide/carbon composites promoted Pt catalyst with high activity and stability for methanol electrooxidation. Applied Catalysis B: Environmental 147, 518-525, **2014**.
35. G.M. Andreadis, A.K.M Podias, P.E. Tsiakaras. The effect of the parasitic current on the direct ethanol PEM fuel cell operation. Journal of Power Sources 181 (2), 214-227, **2008**.
36. G. Andreadis, S. Song, P. Tsiakaras. Direct ethanol fuel cell anode simulation model, Journal of Power Sources 157 (2), 657-665, **2006**.
37. A. Tan, Y. Wang, Z. Fu, P. Tsiakaras, Z. Liang. Highly effective oxygen reduction reaction electrocatalysis: Nitrogen-doped hierarchically mesoporous carbon derived from interpenetrated nonporous metal-organic frameworks. Applied Catalysis B: Environmental 218, 260-266, **2017**.
38. P. Tsiakaras, C. Athanasiou, G. Marnellos, M. Stoukides, J.E. ten Elshof, H.J.M. Bouwmeester. Methane activation on a $La_{0.6}Sr_{0.4}Co_{0.8}Fe_{0.2}O_3$ perovskite: Catalytic and electrocatalytic results. Applied catalysis A: General 169 (2), 249-261,**1998**.
39. P. Tsiakaras, C.G. Vayenas. Oxidative coupling of CH_4 on Ag catalyst-electrodes deposited on ZrO_2 (8 mol% Y_2O_3). Journal of Catalysis 144 (1), 333-347, **1993**.
40. G.M. Andreadis, A.K.M. Podias, P.E. Tsiakaras. The effect of the parasitic current on the direct ethanol PEM fuel cell operation. Journal of Power Sources 181 (2), 214-227, **2008**.
41. A. Tan, Y. Wang, Z. Fu, P. Tsiakaras, Z. Liang. Highly effective oxygen reduction reaction electrocatalysis: Nitrogen-doped hierarchically mesoporous carbon derived from interpenetrated nonporous metal-organic frameworks. Applied Catalysis B: Environmental 218, 260-266, **2017**.
42. J. Lyagaeva, D. Medvedev, A. Demin, P. Tsiakaras. Insights on thermal and transport features of $BaCe_{0.8-x}Zr_xY_{0.2}O_{3-\delta}$ proton-conducting materials. Journal of Power Sources 278, 436-444, **2015**.
43. Y. Wang, C. He, A. Brouzgou, Y. Liang, R. Fu, D. Wu, P. Tsiakaras, S. A facile soft-template synthesis of ordered mesoporous carbon/tungsten carbide composites with high surface area for methanol electrooxidation. Journal of Power Sources 200, 8-13, **2012**.

44. E. Gorbova, V. Maragou, D. Medvedev, A. Demin, P. Tsiakaras. Influence of sintering additives of transition metals on the properties of gadolinium-doped bariumcerate. Solid State Ionics 179 (21-26),887-890, **2008**.
45. F.A. Coutelieris, S. Douvartzides, P. Tsiakaras. The importance of the fuel choice on the efficiency of a solid oxide fuel cell system. Journal of Power Sources 123 (2), 200-205, **2003**.
46. S. Song, V. Maragou, P. Tsiakaras. How far are direct alcohol fuel cells from our energy future?. J. Fuel Cell Sci. Technol. 4 (2), 203-209, **2007**.
47. T.H. Nguyen, A. Fraiwan, S. Choi. Paper-based batteries: A review. Biosensors and Bioelectronics 54, 640–649,**2014.**
48. C. Zou, L. Zhang, X. Hu, Z. Wang, T. Wik, M. Pecht. A review of fractional-order techniques applied to lithium-ion batteries, lead-acid batteries, and supercapacitors. Journal of Power Sources 390, 286-296, **2018**.
49. J. Lach, K. Wróbel, J. Wróbel, P. Podsadni, A. Czerwiński. Applications of carbon in lead-acid batteries: a review. Journal of Solid State Electrochemistry 23, 693–705,**2019**.
50. J. Baranwal, B. Barse, G. Gatto, G. Broncova, A. Kumar. Electrochemical Sensors and Their Applications: A Review. Chemosensors 10(9), 363, **2022**.
51. L.A. Dunyushkina, A.A. Pankratov, V.P. Gorelov, A. Brouzgou, P. Tsiakaras. Deposition and Characterization of Y-doped $CaZrO_3$ Electrolyte Film on a Porous $SrTi_{0.8}Fe_{0.2}O_{3-d}$ Substrate. Electrochimica Acta 141, 202, 39-46, **2016**.
52. A. Kalyakin, G. Fadeyev, A. Demin, E. Gorbova, A. Brouzgou, A. Volkov, P. Tsiakaras. Application of Solid oxide proton-conducting electrolytes for amperometric analysis of hydrogen in H_2+N_2+H_2O gas mixtures. Electrochimica Acta 141, 120-125, **2014**.
53. G. Fadeyev, A. Kalyakin, A. Demin, A. Volkov, A. Brouzgou, P. Tsiakaras. Electrodes for solid electrolyte sensors for the measurements of CO and H_2 content in air. International Journal of Hydrogen Energy 38(30), 13484-13490, **2013**.
54. G. Balkourani, T. Damartzis, A. Brouzgou, P. Tsiakaras. Cost Effective Synthesis of Graphene Nanomaterials for Non-Enzymatic Electrochemical Sensors for Glucose: A Comprehensive Review. Sensors 22, 355, **2022**.
55. E. Gorbova, F. Tzorbatzoglou, C. Molochas, D. Chloros, A. Demin, P. Tsiakaras. Fundamentals and Principles of Solid-State Electrochemical Sensors for High Temperature Gas Detection. Catalysts 12, 1, **2022**.
56. A Kalyakin, A. Demin, E. Gorbova, A. Volkov, P. Tsiakaras. Combined amperometric-potentiometric oxygen sensor. Sensors and Actuators B: Chemical 313, 127999, **2020**.
57. A. Demin, E. Gorbova, A. Brouzgou, A. Volkov, P. Tsiakaras. Sensors based on solid oxide electrolytes. Solid Oxide-Based Electrochemical Devices, 167-215, **2020**.

58. A. Kalyakin, A. Volkov, A. Demin, E. Gorbova, P. Tsiakaras. Determination of nitrous oxide concentration using a solid-electrolyte amperometric sensor. Sensors and Actuators B: Chemical 297, 126750, **2019**.
59. A. Volkov, E. Gorbova, A. Vylkov, D. Medvedev, A. Demin, P. Tsiakaras. Design and applications of potentiometric sensors based on proton-conducting ceramic materials. A brief review. Sensors and Actuators B: Chemical 244, 1004-1015, **2017**.
60. A. Kalyakin, A. Volkov, J. Lyagaeva, D. Medvedev, A. Demin, P. Tsiakaras. Combined amperometric and potentiometric hydrogen sensors based on $BaCe_{0.7}Zr_{0.1}Y_{0.2}O_{3-\delta}$ proton-conducting ceramic. Sensors and Actuators B: Chemical 231, 175-182, **2016**.
61. A. Kalyakin, J. Lyagaeva, D. Medvedev, A. Volkov, A. Demin, P. Tsiakaras. Characterization of proton-conducting electrolyte based on $La_{0.9}Sr_{0.1}YO_{3-\delta}$ and its application in a hydrogen amperometric sensor. Sensors and Actuators B: Chemical 225, 446-452, **2016**.
62. G. Fadeyev, A. Kalyakin, E. Gorbova, A. Brouzgou, A. Demin, A. Volkov, P. Tsiakaras. A simple and low-cost amperometric sensor for measuring H_2, CO, and CH_4. Sensors and Actuators B: Chemical 221, 879-883, **2015**.
63. G. Fadeyev, A. Kalakin, A. Demin, A. Volkov, A. Brouzgou, P. Tsiakaras. Electrodes for solid electrolyte sensors for the measurement of CO and H_2 content in air. International journal of hydrogen energy 38, 13484-13490, **2013**.
64. G. Balkourani, A. Brouzgou, M. Archonti, N. Papandrianos, S. Song, P. Tsiakaras. Emerging materials for the electrochemical detection of COVID-19. Journal of Electroanalytical Chemistry 893, 115289, **2021**.
65. A. Brouzgou, E. Gorbova, Y. Wang, S. Jing, A. Seretis, Z. Liang, P. Tsiakaras. Nitrogen-doped 3D hierarchical ordered mesoporous carbon supported palladium electrocatalyst for the simultaneous detection of ascorbic acid, dopamine, and glucose. Ionics 25, 6061-6070, **2019**.
66. X. Yuan, D. Yuan, F. Zeng, W. Zou, F. Tzorbatzoglou, P. Tsiakaras, Y. Wang. Preparation of graphitic mesoporous carbon for the simultaneous detection of hydroquinone and catechol. Applied Catalysis B: Environmental 129, 367-374, **2013**.
67. V.A. Martinez Lopez, H. Ziar, J.W. Haverkort, M. Zeman, O. Isabella. Dynamic operation of water electrolyzers: A review for applications in photovoltaic systems integration. Renewable and Sustainable Energy Reviews 182, 113407, **2023**.
68. Q. Xu, G. Qian, S. Yin, C. Yu, W. Chen, T. Yu, L. Luo, Y. Xia, P. Tsiakaras. Design and synthesis of highly performing bifunctional Ni-NiO-MoNi hybrid catalysts for enhanced urea oxidation and hydrogen evolution reactions. ACS Sustainable Chemistry & Engineering 8 (18), 7174-7181, **2020**.

69. L. Yan, B. Zhang, J. Zhu, Y. Li, P. Tsiakaras, P.K. Shen. Electronic modulation of cobalt phosphide nanosheet arrays via copper doping for highly efficient neutral-pH overall water splitting. Applied Catalysis B: Environmental 265, 118555, **2020**.
70. L. Zhang, J. Lu, S. Yin, L. Luo, S. Jing, A. Brouzgou, J. Chen, P.K. Shen, P. Tsiakaras. One-pot synthesized boron-doped RhFe alloy with enhanced catalytic performance for hydrogen evolution reaction. Applied Catalysis B: Environmental 230, 58-64, **2018**.
71. G. Long, K. Wan, M. Liu, Z. Liang, J. Piao, P. Tsiakaras. Active sites and mechanism on nitrogen-doped carbon catalyst for hydrogen evolution reaction. Journal of Catalysis 348, 151-159, **2017**.
72. C. Yu, F. Xu, L. Luo, H.S. Abbo, S.J.J. Titinchi, P.K. Shen, P. Tsiakaras, S. Yin. Bimetallic Ni–Co phosphide nanosheets self-supported on nickel foam as high-performance electrocatalyst for hydrogen evolution reaction. Electrochimica Acta 317, 191-198, **2019**.
73. B. Long, H. Yang, M. Li, M.S. Balogun, W. Mai, G. Ouyang, Y. Tong, Panagiotis Tsiakaras. Shuqin Song, Interface charges redistribution enhanced monolithic etched copper foam-based Cu2O layer/TiO2 nanodots heterojunction with high hydrogen evolution electrocatalytic activity. Applied Catalysis B: Environmental 243, 365-372, **2019**.
74. J. Lu, Z. Tang, L. Luo, S. Yin, P.K. Shen, P. Tsiakaras. Worm-like S-doped RhNi alloys as highly efficient electrocatalysts for hydrogen evolution reaction. Applied Catalysis B: Environmental 255, 117737, **2019**.
75. S. Jing, D. Wang, S. Yin, J. Lu, P.K. Shen, P. Tsiakaras. P-doped CNTs encapsulated nickel hybrids with flower-like structure as efficient catalysts for hydrogen evolution reaction. Electrochimica acta 298, 142-149, **2019**.
76. P. Xu, L. Qiu, L. Wei, Y. Liu, D. Yuan, Y. Wang, P. Tsiakaras. Efficient overall water splitting over Mn doped Ni2P microflowers grown on nickel foam. Catalysis Today 355, 815-821, **2020**.
77. C. Yu, J. Lu, L. Luo, F. Xu, P.K. Shen, P. Tsiakaras, S. Yin. Bifunctional catalysts for overall water splitting: CoNi oxyhydroxide nanosheets electrodeposited on titanium sheets. Electrochimica Acta 301, 449-45, **2019**.
78. L. Yan, B Zhang, J. Zhu, Y. Li, P Tsiakaras, P.K. Shen. Electronic modulation of cobalt phosphide nanosheet arrays via copper doping for highly efficient neutral-pH overall water splitting. Applied Catalysis B: Environmental 265, 118555, **2020**.
79. B. Zhang, J. Shan, W. Wang, P. Tsiakaras, Y. Li. Oxygen Vacancy and Core–Shell Heterojunction Engineering of Anemone-Like CoP@ CoOOH Bifunctional Electrocatalyst for Efficient Overall Water Splitting. Small, 2106012, **2022**.
80. A. Saad, Y. Gao, K.A. Owusu, W. Liu, Y. Wu, A. Ramiere, H. Guo, P. Tsiakaras. Ternary Mo2NiB2 as a Superior Bifunctional Electrocatalyst for Overall Water Splitting. Small 18 (6), 2104303, **2022**.

81. L. Yan, B. Zhang, J. Zhu, Y. Li, P. Tsiakaras, P.K. Shen. Electronic modulation of cobalt phosphide nanosheet arrays via copper doping for highly efficient neutral-pH overall water splitting. Applied Catalysis B: Environmental 265, 11855, **2020**.
82. F. Sordello, P. Calza, C. Minero, S. Malato, M. Minella. More than One Century of History for Photocatalysis, from Past, Present and Future Perspectives. Catalysts 12, 1572,**2022**.
83. Muhammad B.T., Muhammad S. R., Muhammad S., Muhammad F. M. (Eds.). (2022). New Insights in Photocatalysis for Environmental Applications. Springer. https://doi.org/10.1007/978-981-19-2116-2
84. A. Chakravorty, S. Roy. A review of photocatalysis, basic principles, processes, and materials. Sustainable Chemistry for the Environment 8, 100155, **2024**.
85. A.O. Ibhadon, P. Fitzpatrick. Heterogeneous Photocatalysis: Recent Advances and Applications. Catalysts 3, 189-218, **2013**.
86. M.J. Muñoz-Batista, R. Luque. Heterogeneous Photocatalysis. ChemEngineering 5(2),26, **2021**.
87. F. Parrino, G. Palmisano. Highlights on Recent Developments of Heterogeneous and Homogeneous Photocatalysis. Molecules 26,23, **2021**.
88. Piet W.N.M. van Leeuwen. (2004). Homogeneous Catalysis: Understanding the Art. Kluwer Academic Publishers. ISBN 1-4020-2000-7
89. H. Hennig. Homogeneous photocatalysis by transition metal complexes. Coordination Chemistry Reviews 182, 101-123, **1999**.
90. S. Zhu, D. Wang. Photocatalysis: Basic Principles, Diverse Forms of Implementations and Emerging Scientific Opportunities. Energy Mater 7, 1700841,**2017**.
91. F. Zhang, X. Wang, H. Liu, C. Liu, Y. Wan, Y. Long, Z. Cai. Recent Advances and Applications of Semiconductor Photocatalytic Technology. Appl. Sci. 9,2489, **2019**.
92. G. Ren, H. Han, Y. Wang, S. Liu, J. Zhao, X. Meng, Z. Li. Recent Advances of Photocatalytic Application in Water Treatment: A Review. Nanomaterials 11, 1804,**2021**.
93. A. Farhan, M. Zulfiqar, Samiah, E. U. Rashid, S. Nawaz, H.M.N. Iqbal, T. Jesionowski, M. Bilal, J. Zdarta. Removal of Toxic Metals from Water by Nanocomposites through Advanced Remediation Processes and Photocatalytic Oxidation. Current Pollution Reports 9, 338–358, **2023**.
94. A.A. Okab, Z.H. Jabbar, B.H. Graimed, A.I. Alwared, S.H. Ammar, M.A. Hussein. A comprehensive review highlights the photocatalytic heterojunctions and their superiority in the photo-destruction of organic pollutants in industrial wastewater. Inorganic Chemistry Communications 158, 111503, **2023**.
95. A. Talaiekhozani, S. Rezania, K. Kim, R. Sanaye, A.M. Amani. Recent advances in photocatalytic removal of organic and inorganic pollutants in air. Journal of Cleaner Production 278, 123895, **2021**.

96. D.C.A. Gowland, N. Robertson, E. Chatzisymeon. Photocatalytic Oxidation of Natural Organic Matter in Water. Water 13, 288,**2021**.
97. Z. Zhou, B. Li, X. Liu, Z. Li, S. Zhu, Y. Lian, S. Wu. Recent Progress in Photocatalytic Antibacterial. ACS Appl. Bio Mater 4, 3909-3936, **2021**.
98. A.G. Niculescu, A.M. Grumezescu. Photodynamic Therapy—An Up-to-Date Review. Appl. Sci. 11, 3626,**2021**.
99. A.H. Hamdany, A. Satyanaga, D. Zhang, Y. Kim, J. Kim. Photocatalytic Cementitious Material for Eco-Efficient Construction—A Systematic Literature Review. Appl. Sci. 12, 8741,**2022**.
100. F. Dawood, M. Anda, G.M. Shafiullah. Hydrogen production for energy: An overview. International journal of hydrogen energy 45, 3847-3869,**2020**.
101. A.A. Levikhin, A.A. Boryaev. Physical properties and thermodynamic characteristics of hydrogen. Heliyon 10, e36414,**2024**.
102. C. Acar, I. Dincer, G.F. Naterer. Review of photocatalytic water-splitting methods for sustainable hydrogen production. Int. J. Energy Res. 40,1449–1473, **2016**.
103. X. Dong, T. Hao, Y. Xue, Y. Du, J. Zhao, F. Meng, X. Zhong, P. Tsiakaras. Enhanced photocatalytic hydrogen evolution activity: cross linking density and π linker modulation of pyrene and triazine based conjugated porous polymers. Fuel 400, 135764, **2025**.
104. S. Jing, Q. Xu, H Wang, P. Kannan, H. Liang, A. Brouzgou, R. Wang, P. Tsiakaras. Improved photocatalytic production of hydrogen peroxide over graphitic carbon nitride doped with potassium salts. Journal of Colloid And Interface Science 695, 137675, **2023**.
105. H. Liang, Q. Xu, R. Cheng, S. Jing, F. Chen, P. Tsiakaras. Triggering n→π* electronic transitions by thiazole modified graphitic carbon nitride for enhanced photocatalytic hydrogen peroxide production and Rhodamine B degradation. Carbon 244, 120603, **2025**.
106. R.D. Tentu, S. Basu. Photocatalytic water splitting for hydrogen production. Current Opinion in Electrochemistry 5, 56–62, **2017**.
107. S. Crawford, E. Thimsen, P. Biswas. Impact of Different Electrolytes on Photocatalytic Water Splitting. Journal of The Electrochemical Society 156 (5), 346-351,**2009**.
108. W.S. Koe, J.W. Lee, W.C. Chong, Y.L. Pang, L.C. Sim. An overview of photocatalytic degradation: photocatalysts, mechanisms, and development of photocatalytic membrane. Environmental Science and Pollution Research 27, 2522–2565, **2020**.
109. X. Zhu, J. Xiong, Z. Wang, R. Chen, G. Cheng, Y. Wu. Metallic Copper-Containing Composite Photocatalysts: Fundamental, Materials Design, and Photoredox Applications. Small Methods 6, 2101001,**2022**.

110. A. Baig, M. Siddique, S. Panchal. A Review of Visible-Light-Active Zinc Oxide Photocatalysts for Environmental Application. Catalysts 15, 100,**2025**.
111. A. Baig, M. Siddique, S. Panchal. A Review of Visible-Light-Active Zinc Oxide Photocatalysts for Environmental Application. Catalysts 15, 100, **2025**.
112. S.J. Armaković, M.M. Savanović, S. Armaković. Titanium Dioxide as the Most Used Photocatalyst for Water Purification: An Overview. Catalysts 13, 26, **2023**.
113. Y. Chen, S. Ji, W. Sun, Y. Lei, Q. Wang, A. Li, W. Chen, G. Zhou, Z. Zhang, Y. Wang, L. Zheng, Q. Zhang, L. Gu, X. Han, D. Wang, Y. Li. Engineering the Atomic Interface with Single Platinum Atoms for Enhanced Photocatalytic Hydrogen Production. Angew. Chem. 132, 1311–1317, **2020**.
114. Z. Li, X. Meng. Recent development on palladium enhanced photocatalytic activity: A review. Journal of Alloys and Compounds 830, 154669, **2020**.
115. A. Talebian-Kiakalaieh, M. Guo, E.M. Hashem, B. Xia, Y. Jiang, C. Chuah, Y. Tang, P. Kwong, J. Ran, S. Qiao. In Situ Characterizations Revealing Ruthenium-Atom-Induced Raise of Photocatalytic Performance. Adv. Energy Mater 13, 2301594, **2023**.
116. Y. Zhang, J. Liu, Y.S. Kang, X.L. Zhang. Silver based photocatalysts in emerging applications. Nanoscale 14,11909–11922,**2022**.
117. B.K. Devendra, B.M Praveen., V.S. Tripathi, G. Nagaraju, B.M. Prasanna, M. Shashank. Development of rhodium coatings by electrodeposition for photocatalytic dye degradation. Vacuum 205, 111460, **2022**.
118. G.E. Orizu, P.E. Ugwuoke, P. U. Asogwa, S. U. Offiah. A review on the inference of doping TiO2 with metals/non-metals to improve its photocatalytic activities. IOP Conf. Series: Earth and Environmental Science 1178, 012008, **2023**.
119. C. Chuaicham, J. Trakulmututa, K. Shu, S. Shenoy, A. Srikhaow, L. Zhang, S. Mohan, K. Sekar, K. Sasaki. Recent Clay-Based Photocatalysts for Wastewater Treatment. Separations 10, 77, **2023**.
120. Y. Li, Z. Tang, Y. Xu. Multifunctional graphene-based composite photocatalysts oriented by multifaced roles of graphene in photocatalysis. Chinese Journal of Catalysis 43, 708–730, **2022**.
121. R.M.S. Sendão, J.C.G. Esteves da Silva, L. Pinto da Silva. Applications of Fluorescent Carbon Dots as Photocatalysts: A Review. Catalysts 13, 179, **2023**.
122. N. Dushyantha, N. Batapolaa, I.M.S.K. Ilankoon, S. Rohitha, R. Premasiri, B. Abeysinghe, N. Ratnayake, K. Dissanayake. The story of rare earth elements (REEs): Occurrences, global distribution, genesis, geology, mineralogy and global production. Ore Geology Reviews 122, 103521,**2020**.

123. V. Balaram. Rare earth elements, resources, applications, extraction technologies, chemical characterization, and global trade– A comprehensive review. CSIR-National Geopysical Research Institute Hyderabad ,500007, **2023**.

124. V. Balaram. Potential Future Alternative Resources for Rare Earth Elements: Opportunities and Challenges. Minerals 13, 425, **2023**.

125. Z. Li, Q. Meng, L. Zhang, O. Lobont, Y. Shen. How do rare earth prices respond to economic and geopolitical factors? Resources Policy 85, 103853, **2023**.

126. J.H. Fan, A. Omura, E. Roca. Geopolitics and rare earth metals. European Journal of Political Economy 78, 102356,**2023**.

127. D.A. Gkika, M. Chalaris, G.Z. Kyzas. Review of Methods for Obtaining Rare Earth Elements from Recycling and Their Impact on the Environment and Human Health. Processes, 12, 1235, **2024**.

128. Y. Fujita, S.K. McCall, D. Ginosar. Recycling rare earths: Perspectives and recent advances. MRS Bulletin 47 (4), **2022**.

129. H. Ding, J. Ge. Towards clean energy technologies: Assessing the supply potential of critical rare earth elements in China. The Extractive Industries and Society 22, 101603, **2025**.

130. K.M. Goodenough, F. Wall, D. Merriman. The Rare Earth Elements: Demand, Global Resources, and Challenges for Resourcing Future Generations. Natural Resources Research 27(2), **2018**.